Novel Approaches to the Design of Phased Array Antennas

By

Danial Ehyaie

A dissertation submitted in partial fulfillment
of the requirement for the degree of
Doctor of Philosophy
(Electrical Engineering)
in The University of Michigan
2011

Doctoral Committee

Professor Amir Mortazawi, Chair
Professor Mahta Moghaddam
Professor Kamal Sarabandi
Associate Professor Jerome P. Lynch

To the most beloved people in my life,

My parents: Reza *and* Minoo

My sister and brother: Nona *and* Dana

My grandmother and uncle: Zarrintaj *and* Mehran

TABLE OF CONTENTS

List of Figures

List of Tables

ABSTRACT

This dissertation presents three new approaches to the design of phased array antennas in order to reduce their complexity. The first approach is based on extended resonance technique which, unlike conventional phased array designs, achieves power dividing and phase shifting tasks within a single circuit. A new extended resonance circuit is developed here that increases the maximum achievable scan angle by three times compared to the extended resonance phased array demonstrated previously. In order to expand the size of phased array, a new modular approach is used enabling a scalable design of extended resonance phased array for the first time. By applying heterodyne-mixing concept, a modular 24 GHz phased array has been demonstrated.

The second approach presented in this dissertation is based on a bi-directional feeding method. A new phased array is designed based on this approach which demands less phase shift from phase shifters compared to any of common phased arrays. The new bi-directional phased array allows for beam steering using only a single control voltage. A general design procedure for a bidirectional N-element phased array feed network is presented for the first time which allows applying this approach to phased arrays with any number of antenna elements. Furthermore, a new, compact phase shifter is designed and

utilized in the phased array. A 2.4 GHz bi-directional phased array has been designed and fabricated.

Finally, the third approach described in the dissertation allows the phase progression across the antenna elements to be controlled by using a single phase shifter. Therefore, the number of phase shifters required in the phased array is substantially reduced compared to conventional phased array designs which require a separate phase shifter per each antenna element. A variable phase shift is achieved in this approach by vector summation of signals. The amplitude ratios of these vectors are adjusted to provide a linear phase progression. This approach is much simpler than the traditional Cartesian phase shifting scheme. A 2 GHz phased array designed based on this approach has been fabricated and tested.

Chapter 1

Introduction

Phased array antenna is a multiple-antenna system in which the radiation pattern can be reinforced in a particular direction and suppressed in undesired directions. The direction of phased array radiation can be electronically steered obviating the need for any mechanical rotation. These unique capabilities have found phased arrays a broad range of applications since the advent of this technology.

Phased arrays have been traditionally used in military applications for several decades. Recent growth in civilian radar-based sensors and communication systems has drawn increasing interest in utilizing phased array technology for commercial applications. Many applications that can potentially benefit from phased arrays will be discussed in this chapter.

Despite the broad range of potential phased array applications, phased array technology has not been widely deployed in the commercial arena. The high cost and complexity of phased arrays is the primary impediment to their deployment in any large-scale commercial application. Thus, a substantial reduction in the cost and complexity of

1

phased array systems will facilitate their much wider use. In order to deploy phased arrays in a wide range of applications, ongoing efforts are underway to develop new architectures that allow complexity of phased array to be reduced. In addition to conventional designs of phased arrays, various approaches proposed to realize phased arrays with reduced complexity are discussed in this chapter. Finally, an overview of thesis presenting several new approaches to design phased arrays is given at the end of the chapter.

1.1   Background

Enhancing antenna directivity in order to improve long-range communication has been subject of extensive research since the time of Marconi's paper entitled "Directive Antenna" [1]. The first demonstration of directive wireless communication which can be considered as the origin of phased array technology was shown by Karl Ferdinand Braun. He won the Nobel Prize for demonstrating enhanced transmission of radio waves in one direction [2]. Up to 1920s, fixed beam antennas were primarily used to meet the demands for increased gain. For instance, Beverage [3] invented so-called "wave antenna" or "Beverage" antenna in order to increase the gain above that of dipoles and other simple elements. The Beverage antenna was basically a long horizontal wire of about one wavelength mounted over earth, and loaded with appropriate resistances.

Many forms of directive antenna array with high gain and resolution had been developed by mid 1930s [4]. However, in addition to increasing directivity, there was another issue which had not been addressed. The problem lied in the fact the received signal did not arrive from one elevation angle, but from waves which arrive at different
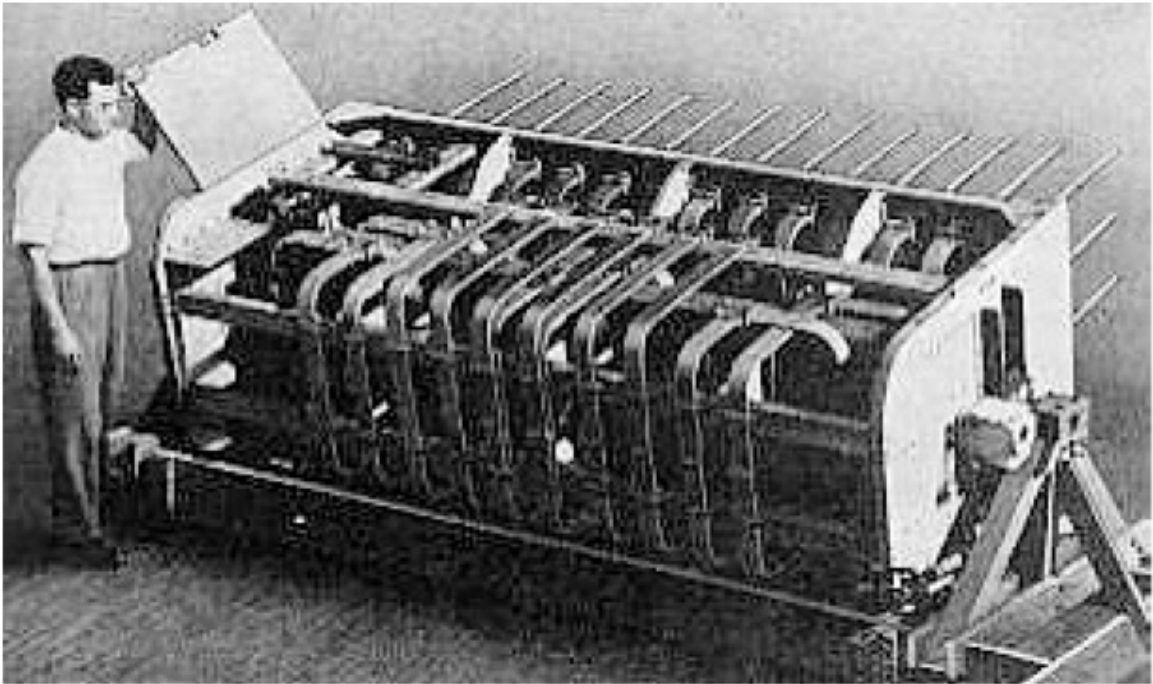
Fig. 1.1. Multiple unit steerable antenna array developed by Friis and Feldman for short range reception [4]

vertical angles that could change with time. Therefore, the signal would arrive outside of the angular range of the narrow band antenna much of the time.

In order to track the receive signal as its directions changes, a multiple unit steerable antenna was developed in 1937 by Friis and Feldman for short wave reception (Fig. 1). Basically they used mechanical phase shifters to provide the required phase progression across the antenna array. This early demonstration of electromechanical scanning certainly opened the door to many years of technology development in order to realize fully electronic scanning systems.

Although scanning antenna arrays had been developed for various electronic communications applications, radar system was the first application for which phased array was broadly used for the first time. Radars demanded extremely rapidly scanning beams, wide band performance, the ability to adapt the beam patterns to avoid jammers and clutter which could be addressed by phased array antennas. Friis and Lewis [5] developed an electromechanical phased array for radar application using rotary phase shifter developed by Fox [6]. The array was center-fed and used extra fixed line lengths to equalize phase across the array with all phase shifters set to zero. The phase shifters were ganged together and scanned the beam continuously with inter-element progression of 3600°/s. During World War II, phased arrays were integrated into the radar systems by another Nobel Prize winner, Luis Alvarez, to aid in the landing of airplanes in England [7].

Application of phased array technology later extended beyond military arena and brought another Nobel Prize for its users, Antony Hewish and Martin Ryle, who had adapted phased arrays for radio astronomy applications [8]. Nowadays, beside the established and sophisticated military applications, phased arrays are used for a wide range of commercial applications as well. Some of these applications are discussed in the next section.

1.2   Emerging applications of Phased array antennas

Phased arrays have been traditionally used for military radar applications for many decades. Radar systems either based on transmitting continuous wave or pulsed signal, emit a signal at a particular direction and collect the reflected signal in order to

Fig. 1.2. The Sea based X-band radar is a combination of the world's largest phased array radar carried aboard a mobile, ocean going semi-submersible platform

process, extract the information and identify the object. Phased array radars allow a warship to use one radar system for surface detection and tracking, air detection and tracking (finding aircraft and missiles) and missile uplink capabilities [9]. The electronic beam steering of the phased array radar is orders of magnitude faster than the traditional radars based on mechanical rotation. The largest phased array in the world is a $900 million dollar radar operated by US Missile Defense Agency. (Fig. 1.2)

Another important application that can take the advantage of phased arrays is automotive collision avoidance radar or adaptive cruise control technology [10]. As
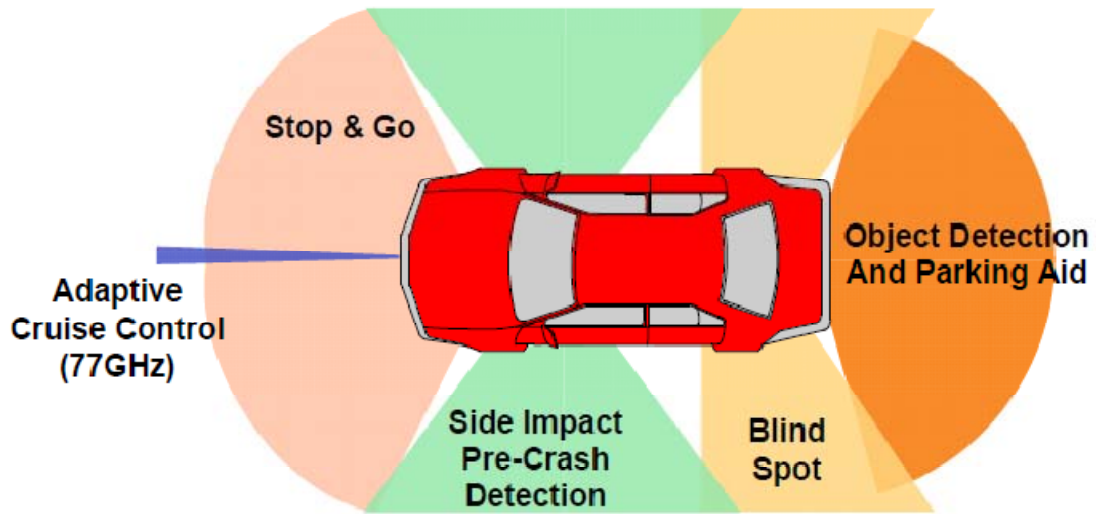
Fig. 1.3. Using radar sensors in the car can provide the driver with several driving-aid functions

shown in Fig 1.3, using radar sensors in the car can provide the driver with several driving-aid functions such as automatic cruise control (ACC), parking aid, blind spot detection, and side collision warning [11]. High resolution radar systems having powerful signal processors capable of advanced image processing can further enable object classification, roadside detection, and prediction of the lane course, therefore enabling intelligent interpretation of traffic scenes [12]. Finally, autonomous driving can be realized by combining short-range radar, global positioning techniques, and wireless communications. Every minute, on average, car accidents take life of at least one person [13]. This results in more than 42,000 deaths and 3,000,000 injuries a year in the United States alone. The financial damages caused by car accidents can be as high as 1–3 percent of the world's gross domestic product every year. For the United States, this exceeds $200 billion a year. Collision avoidance radars can reduce these staggering numbers by

monitoring an automobile's motion and its surroundings in order to warn and prevent car accidents by activating the breaks in threatening situations. The current collision avoidance radars can cost as high as $1,500 to $3,000. Due to their high cost, the radar is an option only on luxury models, such as the Mercedes S-class and Jaguar XKE. Developing low cost phased-arrays operating at frequency bands allocated by Federal Communications Commission (FCC) that can be deployed in ordinary cars is currently subject of extensive research.

It is believed that the emerging gigabit wireless personal communication systems at 60 GHz will be the first product with a large commercial market in the mm-wave frequency band. Phased arrays can play a significant role in success of these systems (Fig. 1.4). Spatial selectivity of phased array beams can increase the channel capacity of the gigabit wireless personal communication systems to achieve data-rates that have not been possible before [14-18]. Furthermore, phased arrays can facilitate the deployment of these systems by significantly reducing their power consumption through more efficient power management. In the United States, the emerging gigabit 60 GHz communication systems are allowed to transmit up to 39 dBm equivalent-isotropically-radiated power. Such high power levels are very challenging to generate using the low cost commercial integrated circuit technologies. Exploiting phased arrays in these systems can alleviate this problem by providing beam forming and increasing the radiation gain in a desired direction [14, 17, 18]. This will obviate the need for prohibitively large output power levels from millimeter-wave power amplifiers. Finally, by using phased arrays, more reliable and robust communication links can be achieved through mitigating the problem of multipath fading and co-channel interference and by suppressing the signals emanating
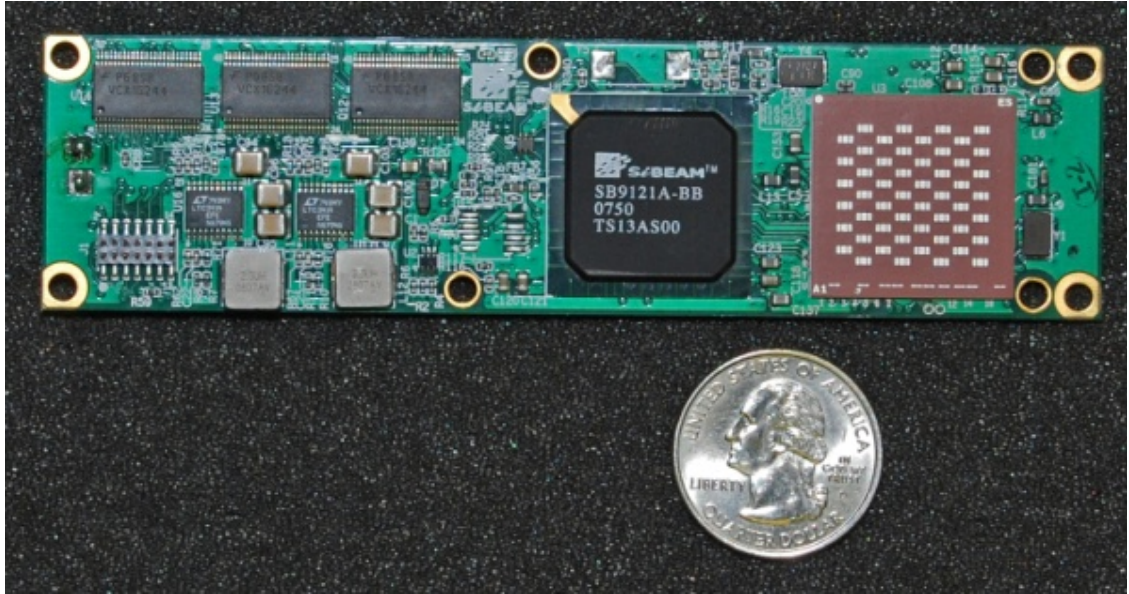
Fig. 1.4. SiBEAM 60 GHz phased array transceiver for wireless video-area network

from undesirable directions. The integrated circuit technologies now show a promising performance at mm-wave frequencies. Low cost, high integration density of the existing technologies allows for a system-on-chip implementation of mm-wave systems, and is expected to provide an unprecedented opportunity for application of phased array technology in the next generation of communication systems.

Phased arrays are widely used in base stations to enhance the signal coverage in a particular area while minimizing interference to other areas [19]. Satellite TV systems available in the current commercial market also employ phased arrays. Compared to traditional parabolic dish systems, phased array based broadcasting-reception links have the advantages of being more robust in inclement weather, having smaller profile and lower weight that allows them to be more easily mounted on walls and roofs. Moreover,

Fig. 1.5. HAARP is a research station directed by the Air Force Research Laboratory's Space Vehicles Directorate in Gokona, Alaska to gather data about the atmosphere

the adaptive beamforming allows mobile objects such as planes and vehicles to have access to satellite programs [20].

Biomedical applications are among the emerging applications that can take the advantage of phased-array [21-23]. For instance, phased array has been used in microwave imaging to detect early stage breast cancer [24-26]. In this method, a wideband impulses are emitted by an antenna array placed at the breast surface. The receiver uses beam-forming to focus the backscattered signal from the malignant tumor and compensate for the frequency dependent propagation effect. The malignant tumor

and breast tissue causes a dielectric discontinuity that affects the signal reflection. The microwave imaging can provide much higher detection probability than X-rays or ultrasound as the relevant contrast is an order of magnitude higher for microwave. The cost of microwave imaging is also much lower than other current alternatives such as magnetic resonance imaging (MRI) and is less harmful to the patients than X-ray.

1.3 Phased Array Principle

The block diagram of an N-element phased array is shown in Fig. 1.6. *"N"* identical antennas are equally spaced by a distance "d" along an axis. For simplicity, we discuss only the receiver case, while similar concepts are held for transmitter as well due to the reciprocity concepts. Separate variable time delays are incorporated at each signal path to control the phases of the signals before combining all the signals together at the output. A plane-wave beam is assumed to be incident upon the antenna array at an angle of θ to the normal direction. Because of the spacing between the antennas, the beam will experience a time delay equal to Eqn. 1.1 in reaching successive antennas.

$$\Delta\tau = \frac{2\pi d \, sin(\theta)}{\lambda}$$

(1.1)

Here, λ is the wavelength of the signals.

Hence, if the incident beam is a sinusoid at frequency ω with amplitude of A, the signals received by each of the antennas can be written as Eqn. 1.2.

$$S_i = Ae^{-jn\Delta\tau}$$

(1.2
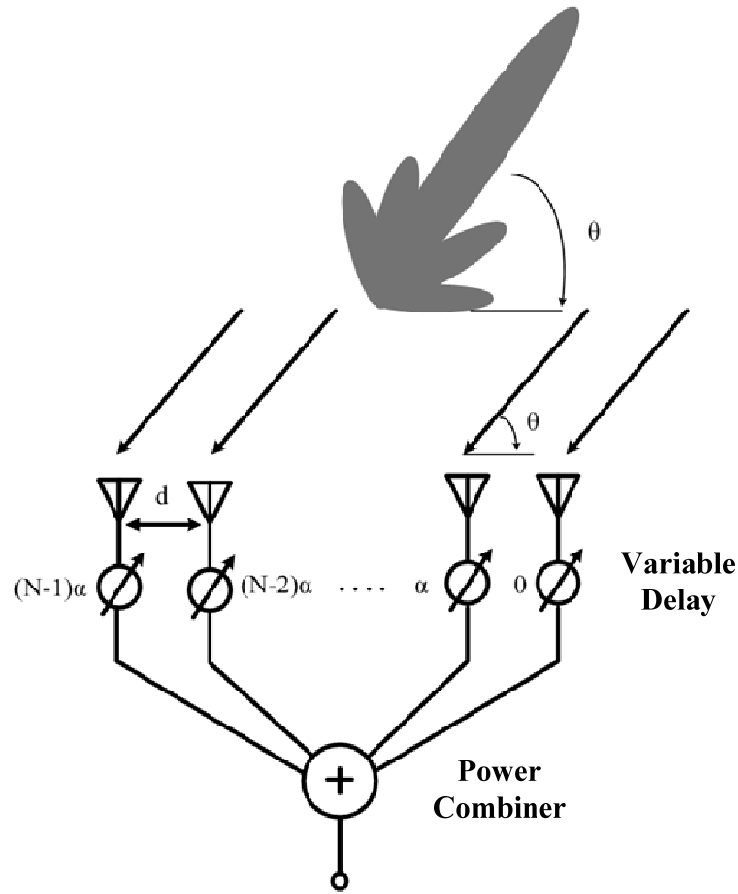
Fig. 1.6. Block diagram of N-element phased array

The plane wave incident at an angle upon the phased array experiences a linear delay progression at the successive antenna elements. Therefore, the variable delay circuits must be set to a similar but with reverse delay progression to compensate for the delay of the signal arrived at the antenna elements. In linear arrays, variable time delays are designed to provide uniform phase progression across the array. Therefore, the signal in each channel at the output of the variable delay block can be written as Eqn. 1.3.

11

$$S'_i = Ae^{-jn\Delta\tau}e^{-jn\alpha} \tag{1.3}$$

In this equation, α denotes the difference in phase shift provided by two successive variable time delay blocks. Therefore, array factor which is equal to the sum of all the signals normalized to the signal at one path can be written as Eqn. 1.4.

$$F = \sum_{n=1}^{N} e^{-jn(\Delta\tau-\alpha)} \tag{1.4}$$

According to Eqn. 1.4, the peak of the array factor occurs at an incident angle which can be determined by Eqn. 1.5.

$$\frac{2\pi d}{\lambda} sin(\theta) = \alpha \quad \text{Or} \quad \theta = arcsin(\frac{\alpha}{2\pi d}) \tag{1.5}$$

At this incident angle, which is called scan angle, the linear delay progression experienced by the wave arriving at the successive antennas is perfectly compensated with the time delays incorporated at each path resulting in all the signals being coherently combined at the output of the receive array. The array factor can also be shown as Eqn. 1.6.

$$F = \frac{sin^2[\frac{N}{2}(\frac{2\pi d}{\lambda}sin(\theta_{in})-\alpha)]}{sin^2[\frac{2\pi d}{2\lambda}sin(\theta_{in})-\alpha]} \tag{1.6}$$

At the scan angle "θ", the array factor has a maximum value of N^2. For other angles of incident, the array factor will be lower than this value indicating spatial

selectivity of phased array. In addition to the spatial filtering, one of the main capabilities of phased array is that the peak gain of the array, according to Eqn. 1.5, can be controlled by electronically tuning the variable time delays eliminating the need for any mechanical rotation of antenna array.

It should be also noted that the benefits of using phased array is increased as the number of elements in the phased array is increased. As mentioned before, the maximum value of array factor N^2 is directly proportional to the number of array elements. Furthermore, the beam width of the array can be decreased by increasing the number of array elements in order to enhance the spatial selectivity of phased array.

1.4 Advantages of using phased array

1.4.1 Spatial filtering

A major advantage of incorporating phased array into communication systems is its capability of spatial filtering. Phased arrays are able to suppress the signals emanating from undesired directions; even if omnidirectional rating elements are used. In general, the ultimate radiation/reception pattern of a phased array is determined by multiplying the received pattern of a single antenna element by the array factor, assuming identical
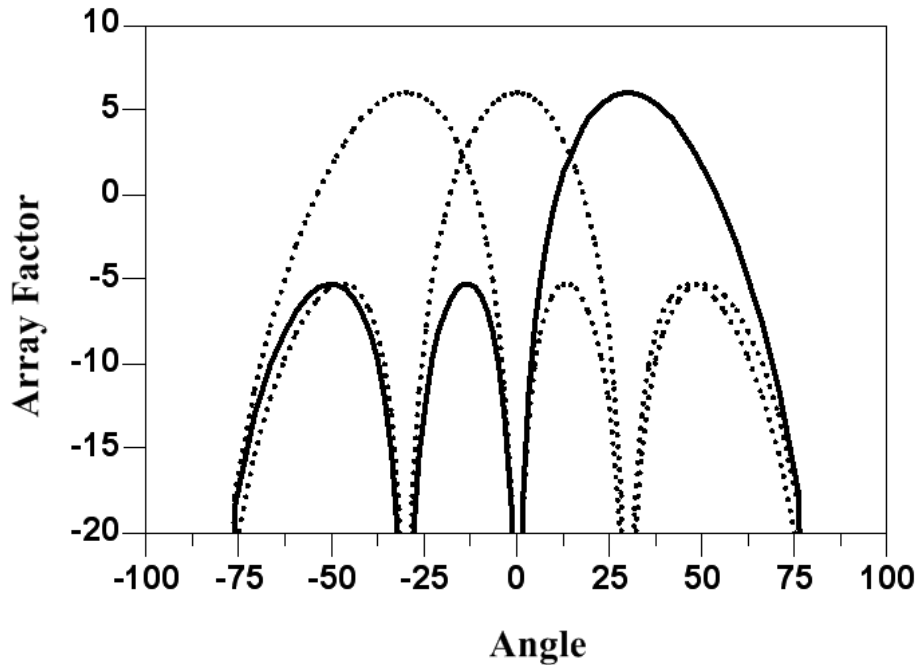
Fig. 1.7. Array factor for a linear 4-element phased array

antenna elements are used across the entire array. In order to demonstrate the spatial

filtering capability of phased arrays, the array factor for a linear 4-element phased array is

shown in Fig. 1.7 assuming all the antenna elements are identical and placed $\lambda/2$ apart,

where λ is the wavelength. As can be seen, the array radiates/receives signals with a

beamwidth 26 degrees centered at 30 degrees while the undesired signals emanating from

other angles are significantly attenuated. As mentioned before, the ultimate radiation/

reception pattern of a phased array is determined by multiplication of a pattern of each

individual antenna with the array factor. Therefore, by different arrangement of antenna

elements, various radiation/reception patterns can be achieved to fulfill the required

spatial filtering. For instance, array factors for linear 4-elemet phased array having

14
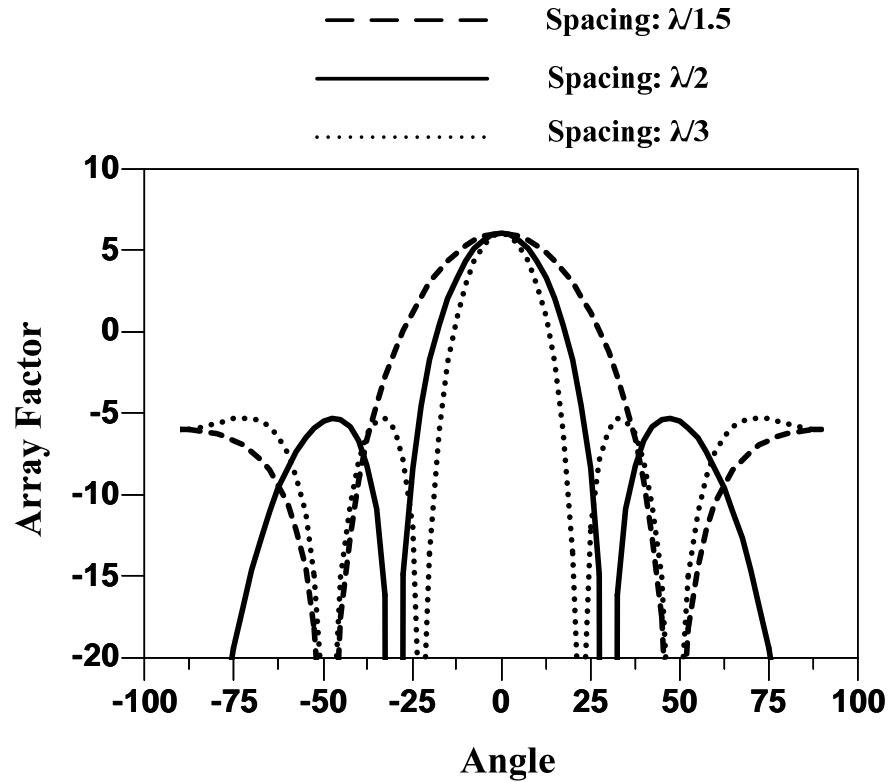
Fig. 1.8. Array factor for 4-elemenet array with different antenna spacings

different spacings, $\lambda/1.5$, $\lambda/2$ and $\lambda/3$ are compared in Fig. 1.8. As can be seen, by increasing the spacing between the antenna elements the beamwidth of the array radiation pattern decreases. However, increasing the spacing can cause in increase of side lobe level and emergence of grating lobes. Furthermore, in phased-array systems the amplitude excitation of the array elements can be tapered to lower the side lobe levels or to adjust the null positions at directions where the strong interfering signals are emanating from [27].

It should be noted that antenna elements can be placed in two dimensions as well to create spatial filtering in azimuth and elevation. Furthermore, the arrangement of the

15

antenna elements and their feeds can be changed in conjunction with the associated circuitry to allow for the multiple beams to be created and steered independently.

Spatial filtering of phased arrays not only allows for suppressing the interfering signals emanating from undesired sources, but, it also can alleviate the problem of fading and multi-channel interference [28]. Fading is caused when the signal travels along multiple paths before arriving at the receive antenna. Therefore, although all of these signals have been emanated from a single transmitter, the phases of these signals arriving at the receive antenna are different and can even cancel out each other. Therefore, it is desired to receive the signal from a specific path while suppressing the others propagating along other directions. Spatial filtering of phased array can be exploited to alleviate this problem.

1.4.2 Gain boosting in transmit phased array

In general, the maximum distance that reliable communication between a transmitting and receiving system can occur is determined by the maximum power transmitted in the direction of receiver. For a given receiver sensitivity, the power transmitted in the direction of receiver can significantly affect the maximum range of communication. In radars, also, the maximum transmit power determines the maximum range that radar would be able to detect a target with a given radar cross section.

$$P_{array} = N \sum P_{path}$$
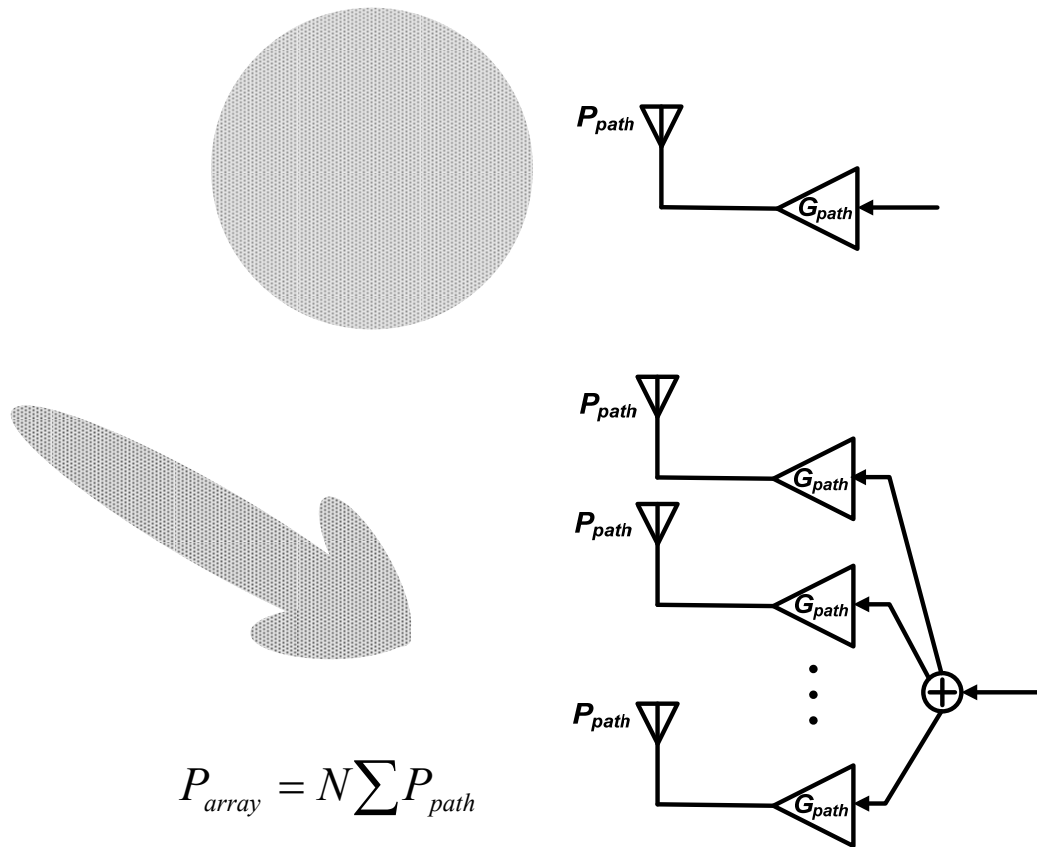
Fig. 1.9. Phased array transmitter can boost the gain in a desired direction

By implementing transmitter antennas using phased arrays one can boost the transmit power level in a desired direction while the total power transmitted remains the same. Therefore, compared to omnidirectional transmitter, phased array transmitter are capable of communicating over longer distance for a given receiver sensitivity (Fig. 1.9). An omnidirectional transmitter radiates electromagnetic power in all directions, and only a small fraction reaches the intended receiver. Not only is a major fraction of this power wasted, but it also causes interference for other users. With ever-increasing wireless applications and the rapid growth of number of wireless users, data-rates currently
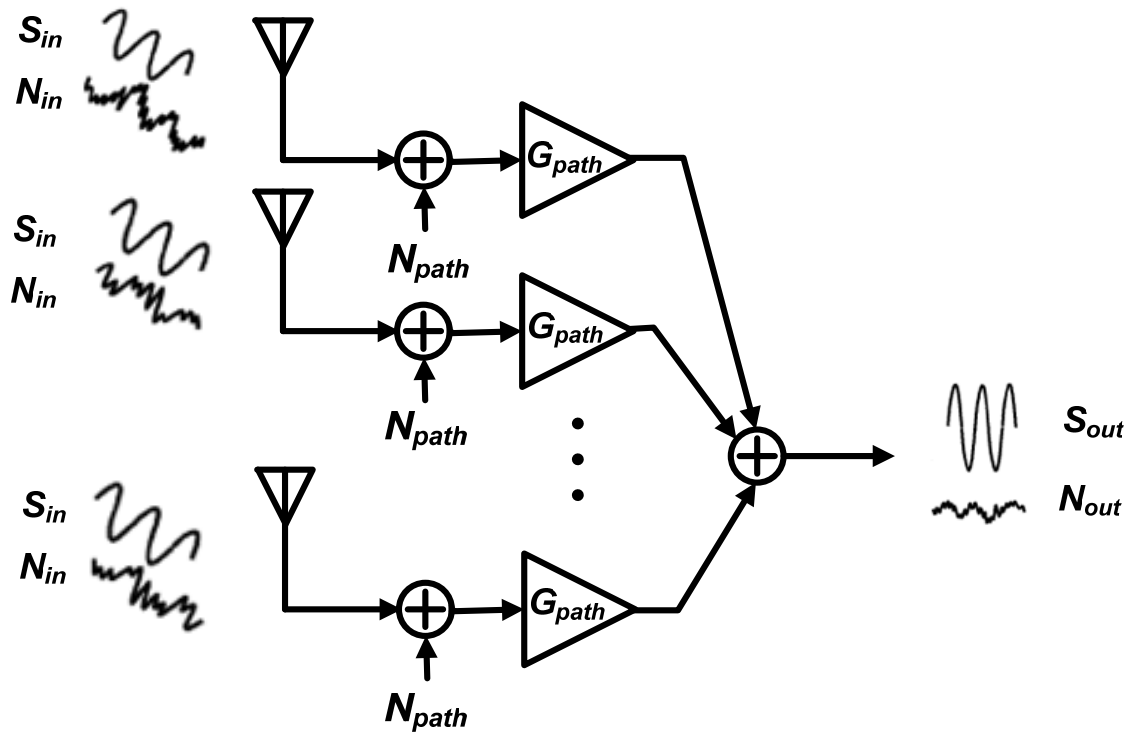
Fig. 1.10. Phased array receiver can improve the noise performance of the system

achievable in available wireless communication networks are in general limited by the interference rather than noise. An increase in transmit power for all users to increase the achievable range and data rate increases the interference level as well and therefore does not provide any benefit to the system overall capacity.

1.4.3 Sensitivity improvement in receive phased array

Sensitivity of a receiver can be directly obtained from the signal to noise ratio at the output of the receiver's front end. In general, a signal to noise ratio above a certain level is required to detect the signal with a target error probability in mind. The minimum signal to noise ratio possible would determine the minimum detectable signal at the

antenna element. Therefore, the noise figure of the receive systems is improved and the overall sensitivity of receive systems is enhanced. Having the noise figure $NF_{channel}$ and minimum acceptable signal to noise ratio at the output SNR_{out}, the signal to noise ratio at the input of a single path receiver is given in Eqn. 1.7.

$$SNR_{In}(dB) = SNR_{out}(dB) + NF_{channel} \tag{1.7}$$

In a receiver based on using phased array, the signals at the output of phased array are combined coherently for transmit signal coming from the desired direction. Assuming the current from the antenna elements are combined coherently, the current at the output will be N times larger than the current at each individual antenna; therefore, the signal power level at the output will be N^2 times larger than the received signal.

$$S_{out} = N^2 S_{in} \tag{1.8}$$

Here, n is the number of antenna elements

The noise contributed by the receive channels are not coherent, therefore, at the output of the phased array, the power of noise from different channels are combined. Output noise level, therefore, will be N times larger than the noise contribution of each channel N. As a result, the noise figure of the entire system can be calculated as shown in Eqn. 1.9.

$$NF_{array} = \frac{nP_N}{n^2 P_S} = n\frac{P_N}{P_S} = \frac{NF_{channel}}{N} \tag{1.9}$$

Therefore, the minimum acceptable SNR at the input of phased array can be shown as Eqn. 1.10. Assuming the noise performance of the channels remains the same as when used alone.

$$SNR_{In}(dB) = SNR_{out}(dB) + \frac{NF_{channel}}{N}$$ (1.10)

Thus, compared to the output SNR of a single-path receiver, the output SNR of the array is improved. This improvement can be more significant if number of antenna elements is increased. In general, the improvement in sensitivity of receiver by using phased array is given in Eqn. 1.11. For instance, a 16-path phased-array can improve receiver sensitivity by 12dB.

$$Sensitivity_{array}(dB) - Sensitivity_{channel}(dB) = 10\,log_{10}^{N}$$ (1.11)

1.5   Phased Array Architecture

1.5.1 Phased Arrays based on feed network design

Phased arrays are usually composed of a feed network and a number of phase shifters. Feed networks are used to distribute the output signal of the transmitter to the radiation elements and phase shifters control the phase of the signals at each radiating element to form a beam at the desired direction. There are almost as many ways to feed arrays as there are arrays in existence. In general, array feed networks can be classified into three basic categories: constrained feed, space feed and semi constrained feed which is a hybrid of the constrained and the space feeds [29]. In a space feed network, the array
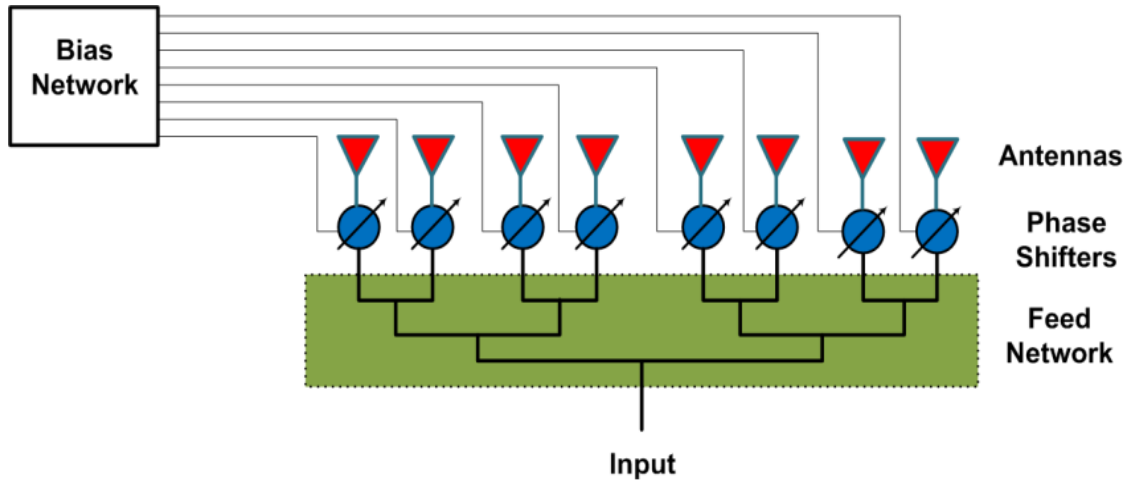
Fig. 1.11. General diagram of parallel fed phased array

is usually illuminated by a separate feed horn located at an appropriate distance from the array [30]. Due to the free space existing between the feed and radiating elements, this type of feed network is not a good candidate for planar arrays. The constrained feed, which is usually the simplest method of feeding an array, generally consists of a network which takes the power from a source and distributes it to the antenna elements with a feed line and passive devices. The constrained feed itself can be categorized into two basic types: parallel feeds and series feeds [31]. The architectures based on these two types of feed network are the most common approach to design phased arrays.

1.5.1.1 Parallel-fed Arrays

In parallel feed networks, which are often called corporate feeds, the input signal is divided in a corporate tree network to all the antenna elements as shown in Fig. 1.11. These networks typically employ only power dividers [32]. Therefore their performance critically depends on the architecture of the power splitter/combiner used. 2^N number of
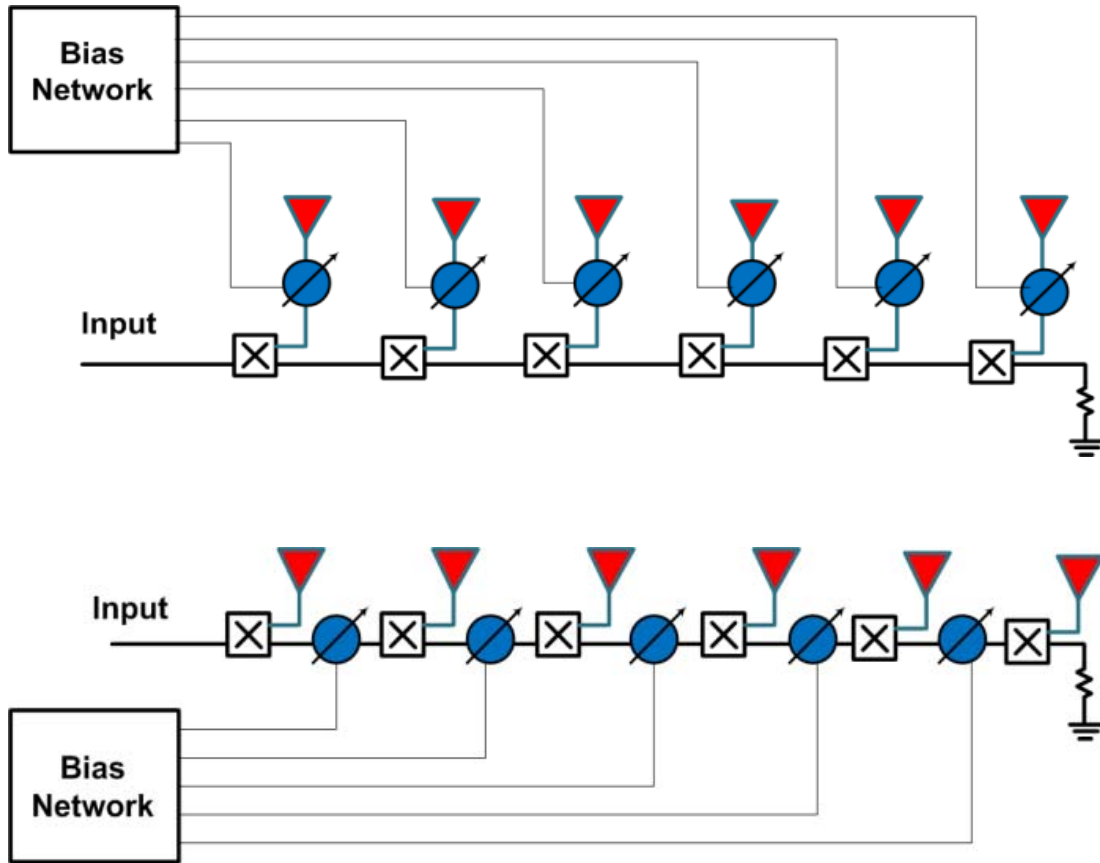
Fig. 1.12. General diagram of series fed phased array

radiation elements is preferred for these types of arrays, where N is the number antennas in the phased array.

1.5.1.2 Series-fed Arrays

In a series-fed array the input signal, fed from one end of the feed network, is coupled serially to the antenna elements as shown in Fig. 1.12. The compact feed network of series-fed antenna arrays is one of the main advantages that make them more attractive than their parallel-fed counterparts. Beside compactness, the small size of

series-fed arrays results in less insertion and radiation losses by the feed network [33]. The cumulative nature of the phase shift in series arrays also relaxes the design constraints on the phase tuning range of the phase shifters. In an N-element series-fed array, the required amount of phased shift is smaller than parallel fed arrays by a factor of *(N-1)*. However, the cumulative nature of phase shift through the feed network results in an increased beam squint versus frequency [34], which is one of the main limitations in series-fed designs. The loss through the phase shifters is also cumulative in series fed arrays which can be an issue in the design of arrays with a large number of array elements.

1.5.2   Phased array based on phase shift stage

Phase shifters can be placed at any stage of phased array. Based on the stage in which phase shifting is performed, phased arrays can be categorized into four district types: RF-phase shifting, LO-phase shifting, IF-phase shifting and digital phased arrays. In the following sections, each of these types of phase arrays is discussed.

1.5.2.1 RF phase shifting

Fig 1.13 displays the general architecture of phased arrays using RF phase shifting. In this architecture, the signals at the antenna elements are phase-shifted and combined in the RF domain. The combined signal is then down converted to baseband using heterodyne or homodyne mixing.

Designing phased arrays using RF phase-shifting has been traditionally more common compared to the other architectures. Since this technique requires only a single
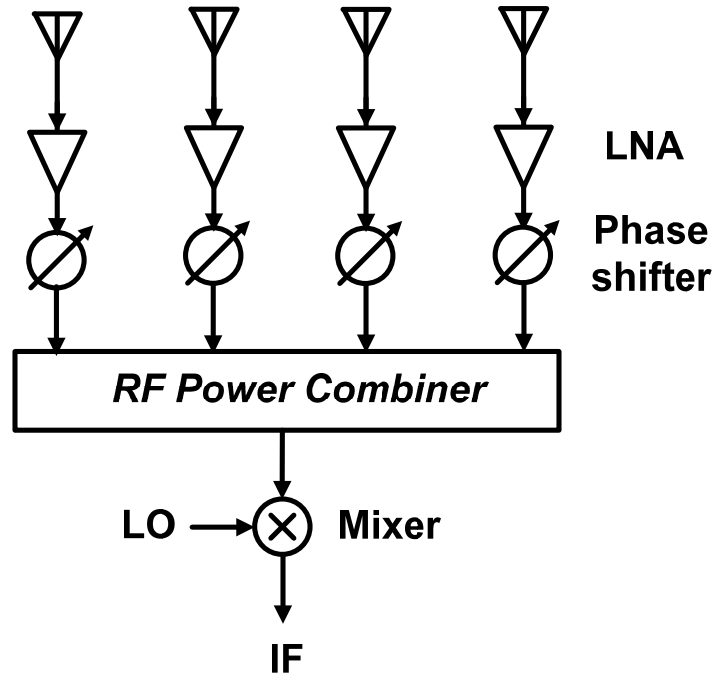
Fig. 1.13. General diagram of RF phase shifting phased array

mixer and there is no need of LO signal distribution, it usually results in the most compact architecture among other phase array designs [35-38]. Furthermore, it provides insulation of a larger portion of the receiver chain from interference emanating from undesired directions. Moreover, since phase shifting and the signal combining are performed prior to down conversion in the RF phase shifting architecture, the interferer is filtered at RF stage prior to the mixer; therefore, the requirement on dynamic range of down conversion mixer is not as stringent as other types of phased array architectures [39].

The main challenge of using phase shifting at RF stage in the design of phased arrays is implementing high performance phase-shifters capable of operating at RF frequencies. Regardless of the technology used to implement phase shifters such as BST, MEMS, GaAs or CMOS, passive phase shifters, in general, tend to be excessively lossy at microwave and millimeter regime [40, 41] while active phase shifters usually suffer from low dynamic range [42, 43]. Dynamic range of phase shifters is particularly important in the operation of phased arrays as phase shifters are required to operate in the presence of strong interferers. Furthermore, phase shifter used in receive phase arrays are in the RF signal path and therefore, their noise performance can be critical for the sensitivity of receivers. Another factor that should be taken into consideration is the amplitude variation of the signal at each channel. As the signal combining and null forming at undesired directions is significantly affected by the amplitude of the signal at each channel, the phase shifters are required to not just have a low insertion loss but also maintain a constant loss within their phase tuning range. Variable gain amplifiers can be used to main the signal amplitude at each channel, however their insertion phase should be constant as their amplitudes are changing.

1.5.2.2 LO phase shifting

Fig 1.14 shows the general architecture of phased arrays based on LO phase shifting. The phase of RF signal at each channel is basically the sum of phases of IF and LO signals. Therefore, tuning the phase of LO signals would translate into changing the phase of RF signals. The advantage of this approach compared to other architectures is
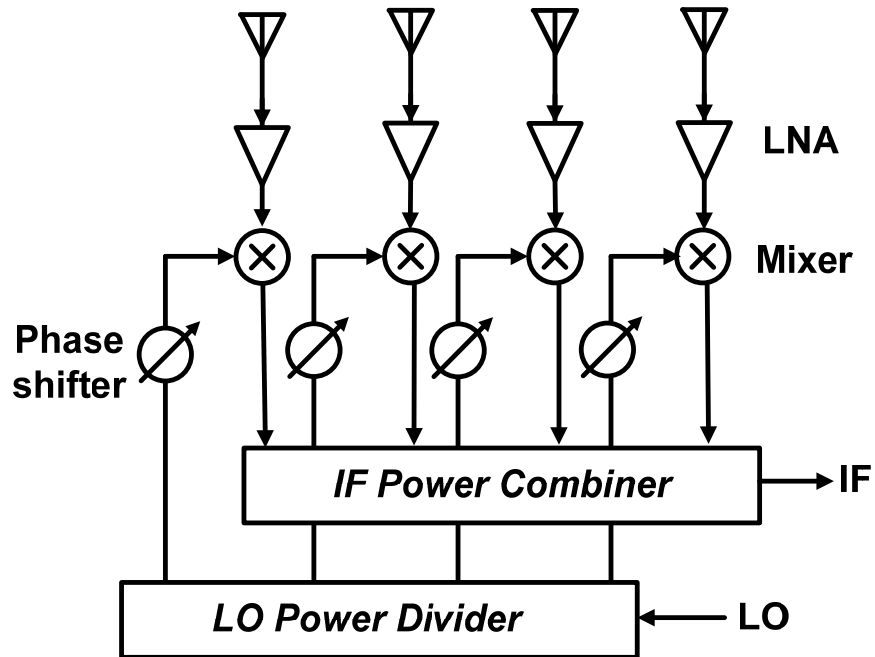
Fig. 1.14. General diagram of LO phase shifting phased array

that the phase-shifters are not placed on the signal path [44, 45]. As a result, the loss, nonlinearity and the noise performance of the phase-shifters would not have a direct impact on the overall system performance. Furthermore, performance of the required phase shifter on LO signal path, such as bandwidth, linearity and noise figure will not be as stringent as the phase shifters on the signal path [46]. However, this method compared to RF phase shifting requires a large number of mixers, therefore; in general, the overall complexity and power consumption will be higher than phased arrays based on RF stage phase shifting.
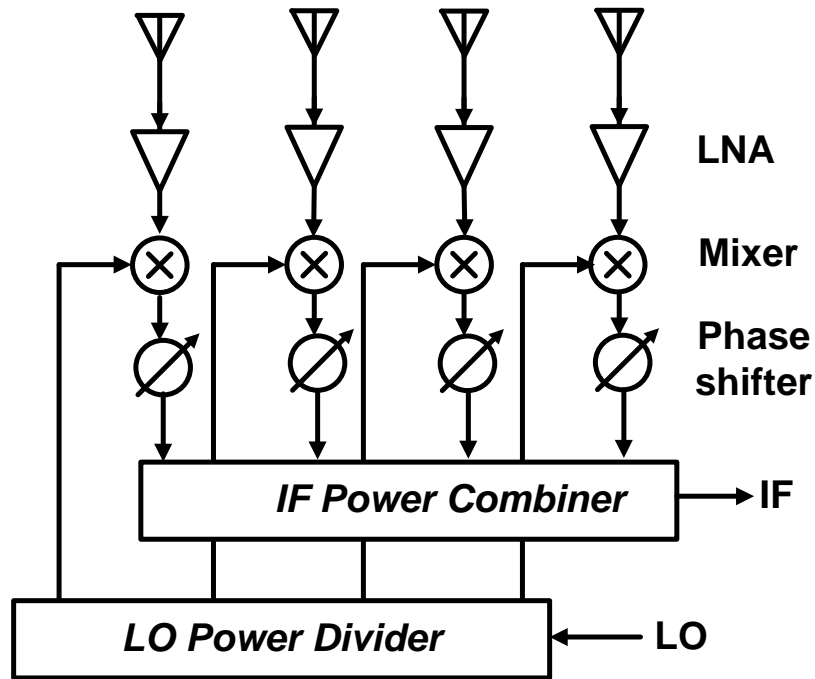
Fig. 1.15. General diagram of IF phase shifting phased array

1.5.2.3 IF phase shifting

The general architecture of phased arrays based on IF phase shifting is shown in Fig. 1.15. As mentioned before, the phase of RF signal at each channel is the sum of phases of IF and LO signals. Therefore, tuning the phase of RF signals can be achieved by tuning through tuning the phase of IF signal [47, 48]. The main advantage of this approach over RF and LO phase shifting is that the phase-shifting is performed at much lower frequencies, therefore, designing phase shifters with much better performance can be possible at IF path. As a result, the loss, nonlinearity and the noise performance of the phase-shifters can be much better when IF phase shifting is used. However, in this architecture similar to LO phase shifting phased arrays large number of mixers are

27

required that can add to the overall system complexity and its power consumption. Furthermore, since the interfere cancellation occurs only after the IF stage, all the mixers are required to have a high level of linearity capable of handling strong interference emanating from undesired directions.

1.5.2.4 Digital Phased Arrays

In digital phased array design, the signal at each array element is digitized using an Analog-to-Digital Converter (ADC) and the digital signal are then processed using a Digital Signal Processing unit (DSP) [49]. In this architecture, interference emanating from undesired directions is not canceled out after signal processing, therefore, all the elements including the RF mixer and ADC and the DSP unit must have sufficient dynamic range capable of handling the interferers. Furthermore, in general each channel requires the entire RF chain front end circuits. As a result, power consumption is relatively high in this architecture.

The main advantage of the digital array is its multifunction capability such as creating many beams [50]. An extensive variety of complex, signal-processing algorithms can be implemented using DSP units. For instance, multi-beam and multiple-input-multiple-output (MIMO) functionality can be achieved by the digital phased arrays. Such phased arrays can be capable of distinguishing among desired signals, multipath and interfering signals, as well as demonstrating their directions of arrival. Furthermore, digital phased arrays can adaptively update their beam patterns, so as to track the desired
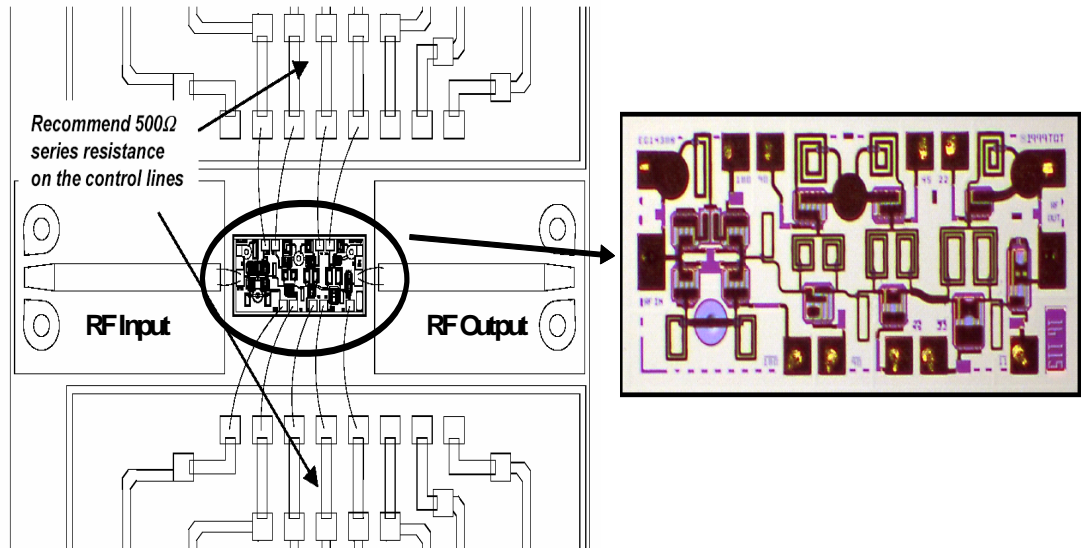
Fig. 1.16. Photograph and boding diagram for a 5-bit phase shifter

signal with the beam's main lobe and track the interferers by placing nulls in their directions.

1.6 Challenges in design of Phased Array Antennas

As discussed in the last sections, there are numerous areas that can benefit from phased arrays. However, there are disadvantages associated with the current implementations of phased arrays that can deter their broad deployment. In order to pave the way for wider employment of phased arrays in various applications, there are several challenges that should be addressed. The primary limitations of utilizing phased arrays consist of cost, size, weight, power consumption, and their high complexity. These constraints have restricted this technology to military, aerospace arena which usually require low quantity prototypes. The systems used in this arena usually can afford to

accommodate high cost and complexity of phased arrays in return of high performance to meet their stringent requirement. It is expected that by addressing these technical hurdles and substantially reducing system costs, more ubiquitous use of phased arrays particularly in commercial markets will be possible [51]. Thus, any substantial reduction in the cost and complexity of phased array systems will facilitate their much wider consumer use which requires unit costs well below what is currently possible.

The high cost and complexity of phased array typically ties in with the cost of multiple receive or transmit/receive modules, whose output and control data are multiplexed into a backend processor unit, which is separate from the T/R modules. One of the critical elements of these T/R modules is a phase shifter. Phased arrays usually require complex integration of many expensive solid-state, MEMS or ferrite based phase shifters, control lines, together with power distribution networks. Phase shifters typically contribute to a significant amount of the cost of producing a phased array antenna and it is not uncommon for the cost of the phase shifters to represent nearly half of the cost of the entire phased arrays [52]. Furthermore, a major complexity of phased array design can be attributed to the complexity of their phase shifters. Since the advent of the array theory and development of the early beam steerable phased arrays, phase shifters have been widely recognized as the most complex and sensitive part of a phased array. The complexities in the corporate feed network and biasing network for the phase shifters as well as their parasitic radiation and interactions with the radiating elements, render implementation of phased arrays very challenging. This is particularly true where a large number of phase shifters with accurate phase control are required.

Conventional linear phased arrays, capable of scanning in azimuth or elevation, require one phase shifter circuit for each antenna element. In two dimensional scanned arrays, the number of required phased shifters is even larger. Each phase shifting circuit is connected to bias lines and the associated driver circuitry for its phase control. To better illustrate the level of complexity introduced by the individual phase shifters within the array, a photograph of a five-bit digital phase shifter by Triquint along with the required bias and control connections is shown in Fig. 1.16. Independent of the type of phase shifter used, design of phased array systems is considered to be complicated and costly mostly due to the number and cost of phase shifting elements required. Thus, in order to reduce the cost of phased arrays, ongoing efforts are underway to develop new architectures that allow for designing phased arrays with reduced complexity. In the next section, different approaches proposed by researchers to allow for phased array cost and complexity reduction are discussed in more details.

1.7   Review of state of Art Phased array Design

A common approach to reduce the required number of phase shifters is based on grouping the radiating elements into a number of sub-arrays each using a single phase shifter [53-55]. The general diagram of phased arrays designed based on this approach is shown in Fig. 1.17. In general, the concept is based on replacing the linear-phase profile of the array excitation by its coarse staircase approximation in this type of phased array. As can be seen in Fig. 1.17, the array elements are divided into the groups of in-phase elements, or sub-arrays, referred to as a primary array. Each of the primary arrays assuming to be identical uses a single phase shifter. Furthermore, each of these primary
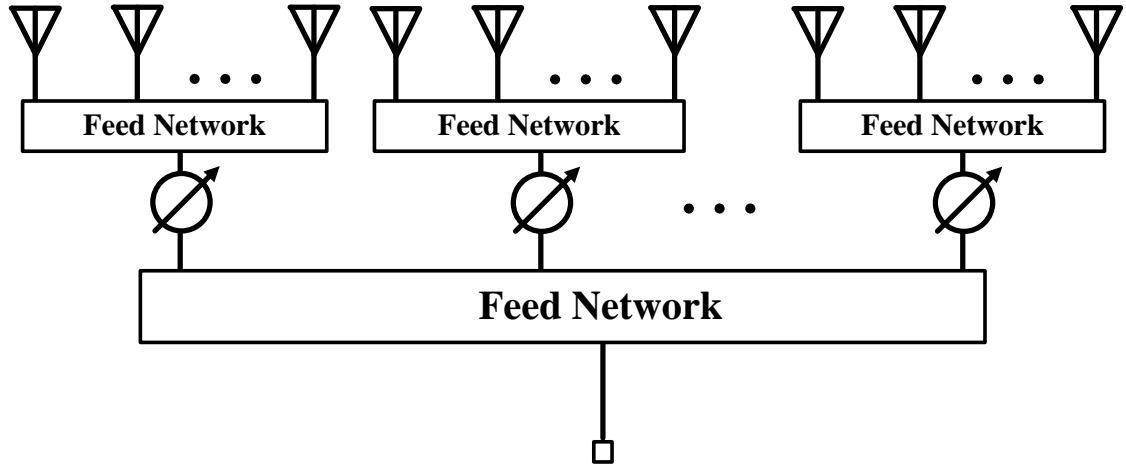
Fig. 1.17. Grouping antennas into a sub array each using one phase shifter can reduce the number of required phase shifters

arrays can be viewed as the elements of a second phased array called the secondary array. The array factor for the overall structure will be equal to the product of these two array factors. The main problem with this approach is increased side-lobes and grating lobes limiting the array scan range [56-58].

Another beam steering technique [59-61] is based on tuning an array of parasitic radiators to replace phase shifters with individual varactors. As shown in Fig. 1.18, in this approach, the sole RF port is connected to one central antenna element and a number of surrounding parasitic antenna elements are terminated with tunable reactances. Beam steering is achieved by tuning the load reactances at parasitic elements surrounding the central active element. The load reactances are usually realized by the reversely biased varactor diodes. One of the issue in this approach is it limited directivity. Since the beamforming in this approach relies on interaction of parasitic and main radiators,
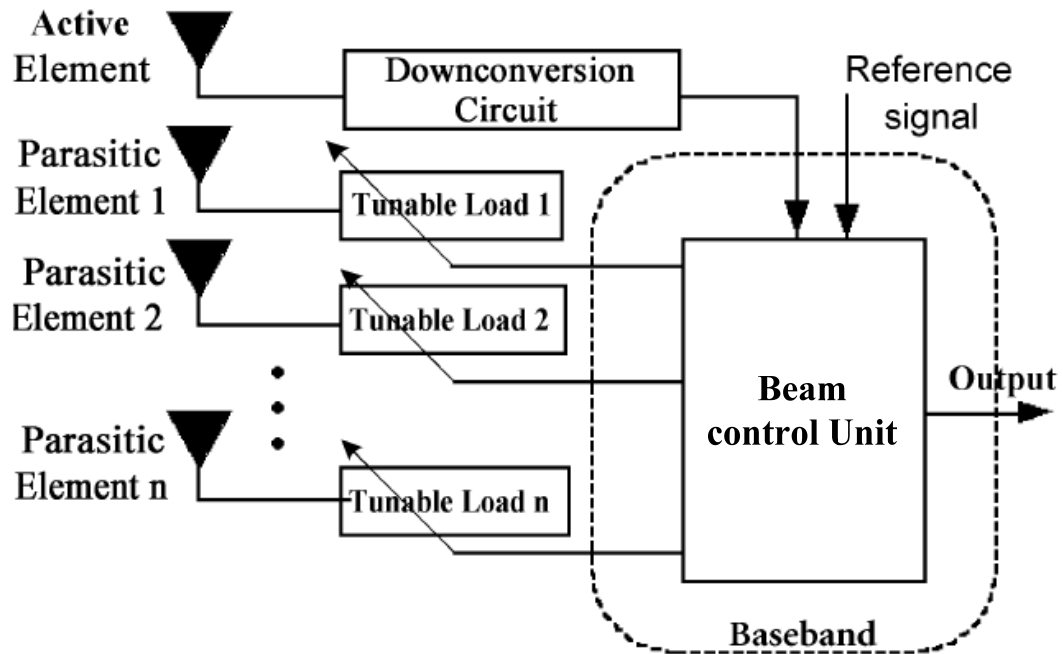
Fig. 1.18. Beam steering can be achieved by tuning the load reactances at parasitic elements surrounding a central active element [51]

achieving narrow beams can be challenging as the level of radiation from parasitic antenna elements is comparatively low to the radiation of main array element. Implementing a planar array using this technique is another issue that has been subject of research.

A phase shifter-less beam steering antenna array can also be realized by exploiting frequency-controlled scanning [62-64]. However, most practical systems require the radiating frequency to be kept fixed as the beam angle is steered. This can be achieved by using heterodyne mixing concept in the frequency-scan array. As shown in Fig. 1.19, in this approach, the phase shift between the antenna elements is usually

33
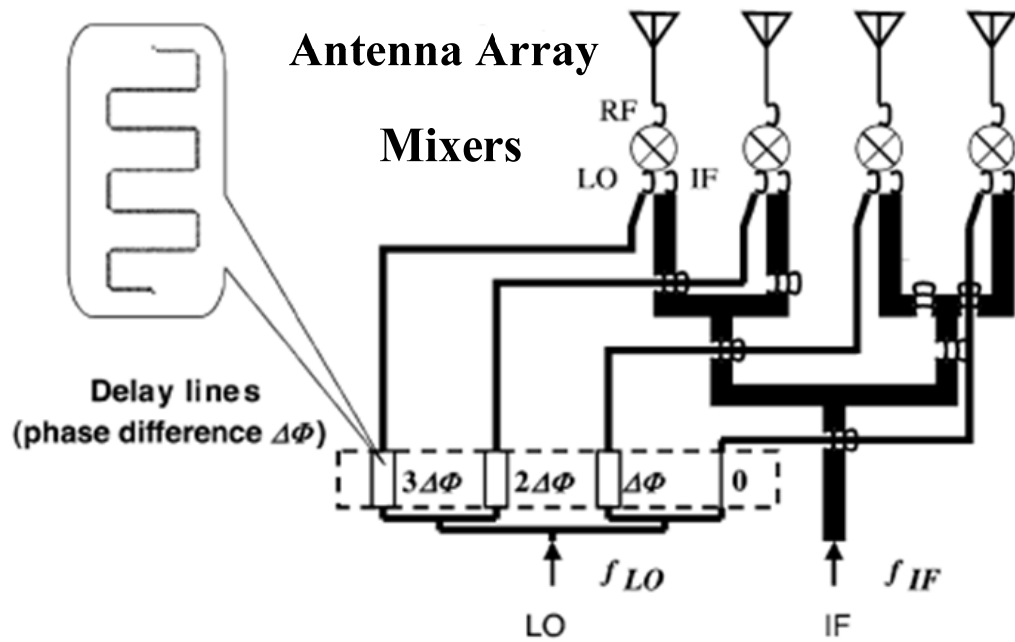
Fig. 1.19. Frequency scanning can be utilized to achieve beam steering [54]

obtained by changing the frequency of either LO signal fed to frequency sensitive network while the frequency of the IF signal is changed as well in order to maintain a constant radiation frequency.

Another phased array design approach is presented in [65-67] to control the phase progression in a phased array by detuning the peripheral elements in an array of free running coupled oscillators. The principle of operation of coupled oscillator array is based on the concept of injection-locking which was studied by Robert Adler for the first time [68]. The underlying idea is based on the fact that when an electrical oscillator is injected with an external signal whose frequency is close to the free-running frequency of

34
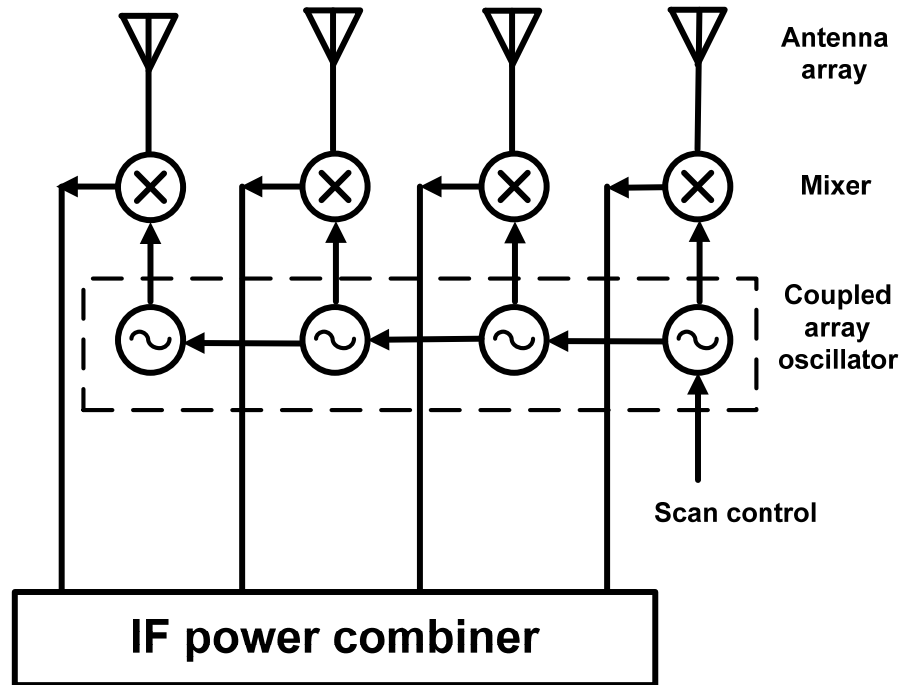
Fig. 1.20. Phased array using coupled oscillator array [56]

the oscillator, the oscillator becomes synchronized in frequency to the external signal. As shown in Fig. 1.20, the concept of injection locking can be extended to a linear array of coupled oscillators. An array of free running oscillators are arranged in a linear format and each oscillator is injected with the portion of the outputs of its nearest neighbors. As the edge oscillator elements are detuned in frequency, the oscillator outputs become synchronized to a common oscillation frequency and exhibit a linear phase progression.

1.8   Overview of Thesis

This thesis presents several new phased array design approaches that allow the complexity of phased array to be reduced. In the second chapter, a new phased array design based on extended resonance is presented. In this method, power dividing and

phase shifting tasks are performed using the same circuitry. Unlike the conventional phased arrays, this technique eliminates the need for a separate phase shifter per each antenna element hence reducing their complexity. This technique is utilized along with heterodyne mixing to allow phase shifting to be performed at a lower frequency. In this phased array design, extended resonance technique is utilized to achieve uniform power distribution at the LO/IF paths and to perform phase-shifting at the IF-stage. A new extended resonance circuit topology has been employed in the IF stage to enhance the scan range of the phased array. Furthermore, comprehensive analysis of the maximum achievable phase shift in the presented extended resonance circuit is given. Finally, a complete modular 7-element 24 GHz phased array has been demonstrated. The architecture of the proposed phased array is discussed and the measurement results are presented as well to validate the design.

In the third chapter, different types of array architectures and their required amounts of phase shift are discussed and a new bi-directional series fed phased array is introduced which demands less phase shift from phase shifters compared to any of the conventional designs of phased arrays. As the result, complexity of the phase shifters required in the array can be reduced resulting in overall phased array cost and complexity reduction. A general design procedure for a bidirectional *N*-element phased array feed network is presented. Furthermore, a compact phase shifter is designed and utilized in the phased array. The overall architecture allows one to steer the radiation beam by a single control voltage obviating the need for complex bias circuits. As a proof-of-principle, an eight-element bi-directionally fed phased array at 2.4 GHz is designed and fabricated.

The measurement results showing good agreement with the simulations are given in the chapter.

Chapter four presented a new approach to design phased arrays. Unlike the conventional designs of phased arrays requiring a separate phase shifter for each antenna element, in the proposed design, the phase progression across the antenna elements can be controlled by using only a single phase shifter. As a result, the cost and complexity of the phased arrays can be significantly reduced based on this design. The proposed phased array is composed of couplers, amplifying stages, power dividers and two phase shifters. The phase shifters are placed at the two opposite ends of a serially fed array. Furthermore, as a proof-of-principle a 2 GHz phased arrays is fabricated and tested. The measurement results showing good agreement with the simulation are presented in the chapter.

Finally, the last chapter concludes the thesis and outlines its main achievement. Furthermore, direction for future work to continue the presented works is given.

Chapter 2

A New Phased Array Design Based on Extended Resonance Technique

2.1   Introduction

In this chapter, a new method to design phased arrays based on the extended resonance technique is presented. In this method, power dividing and phase shifting tasks are performed using the same circuitry. Unlike the conventional phased arrays (Fig. 2.1) where there is a need for a separate phase shifter per each antenna element, this technique eliminates this requirement hence reducing phased arrays complexity (Fig. 2.2). In the design of the phased array, extended resonance technique is utilized with heterodyne mixing to achieve uniform power distribution at the LO/IF paths and to perform phase-shifting at the IF-stage. A new extended resonance circuit topology has been employed in the IF stage to enhance the scan range of the phased array. In addition to the design description of the IF-stage, comprehensive analysis of the maximum achievable phase shift in the new extended resonance circuit is presented. Furthermore, a modular approach to realize scalable phased array design is introduced. The design complexity associated with large phased arrays can be reduced by using the scalable phased array
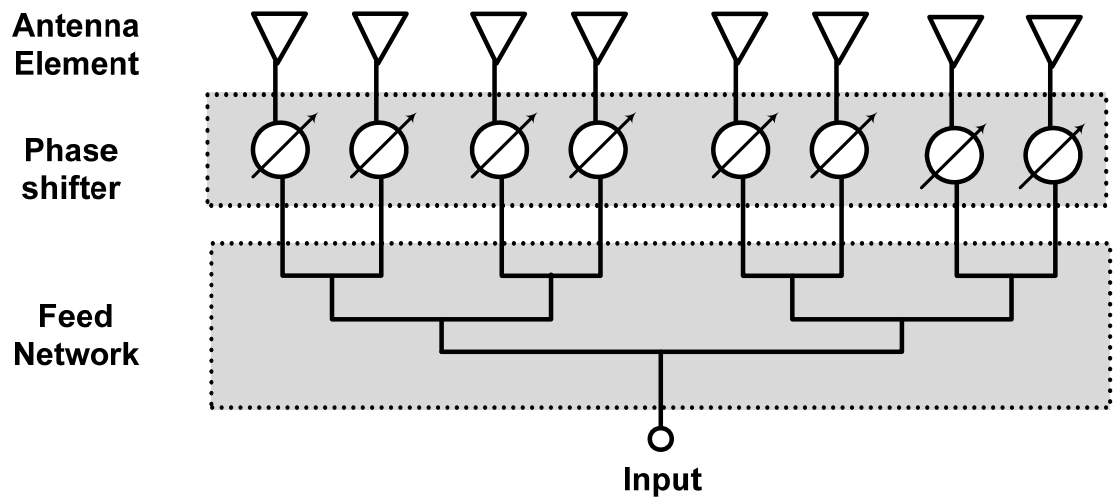
Fig. 2.1. The conventional design of phased arrays requires one phase shifter for each antenna element
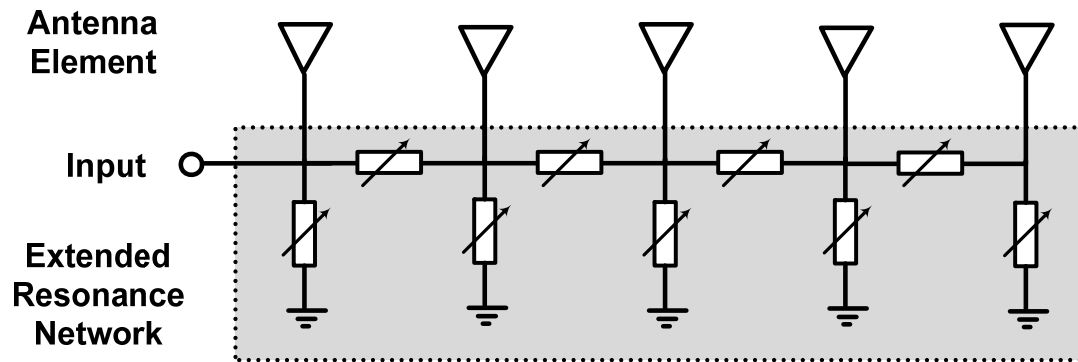
Fig. 2.2. In an extended resonance phased array, phase shifters and power dividing network are combined in a single entity

design introduced here. Finally, a complete modular 7-element 24 GHz phased array has

been demonstrated. The architecture of the proposed phased array is discussed in the next

39

sections, while the measurement results are presented in Section 2.6 to validate the design.

2.2 Extended Resonance Phased Array Concept

The extended resonance technique was originally introduced to design power combining oscillators using multiple solid-state devices [69-73]. The technique also has an excellent feature of equally power combining and dividing. To explain the theory of the extended resonance technique, we consider a circuit diagram of an extended resonance module with N ports all terminated with the same conductance *"G"* as shown in Fig. 2.3. Each series impedance X_n is chosen to transform the admittance seen at the node to its conjugate resulting in voltages with equal magnitudes at all the nodes [52].

$$\left|\frac{V_{n+1}}{V_n}\right| = 1 \tag{2.1}$$

However, a phase difference exists between these voltages, which directly depend on the value of each shunt susceptances Y_n. The shunt susceptances can be chosen according to Eqn. 2.1 to achieve a linear phase progression at nodes V_1 through V_n.

$$Y_n = (2n-1)Y_1 \tag{2.2}$$

Therefore, the phase difference between each two adjacent nodes can determined based on Eqn. 2.3.

$$\theta = 2\arctan(\frac{Y_1}{G}) \tag{2.3}$$

40
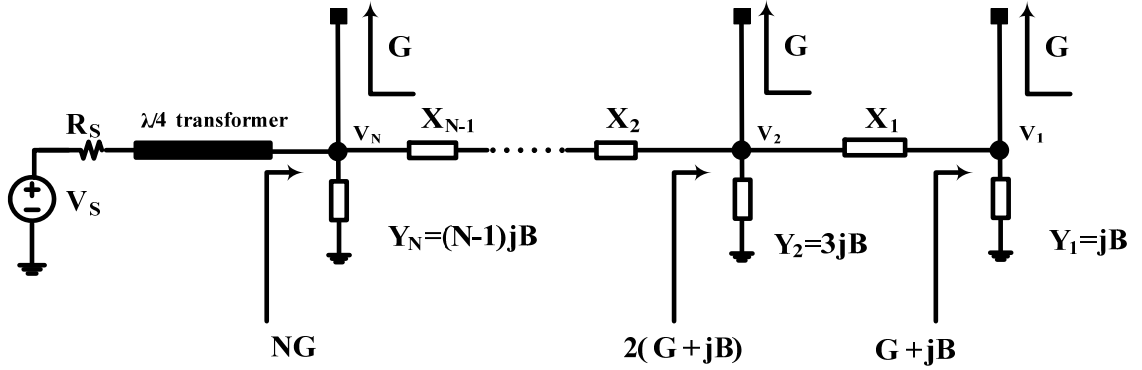
Fig. 2.3. The general structure of an extended resonance power dividing network

The required series admittance X_n to transform the admittance at the node n to its conjugate is:

$$X_n = \frac{2Y_1}{n(G^2 + Y_1^2)} \tag{2.4}$$

The shunt susceptance at the last node cancels out the imaginary admittance seen at the node. Thus, the shunt admittance at the last node can be calculated as:

$$Y_N = (N-1)Y_1 \tag{2.5}$$

The admittance seen at the last node NG is matched to the source impedance using a matching circuit.

In order to vary the relative phase of the output ports, tunable circuits can be utilized to control the value of Y_n. Furthermore, the series reactance X_n should also be tuned simultaneously to maintain the equal power division. In the next section, a design

41

of a new tunable extended resonance circuit is presented. This circuit is optimized to achieve a relatively large inter-element phase shift.

2.3 A new extended resonance circuit to enhance maximum achievable inter-element phase shift

As mentioned before, in order to vary the relative phase of the output ports, tunable circuits can be utilized to control the value of Y_n and the series reactance X_n simultaneously to maintain the equal power division. In general, if the shunt susceptance Y_1 can be tuned from jB_{min} to jB_{max}, the maximum achievable phase shift can be determined by:

$$\Delta\theta = 2[arctan(\frac{B_{max}}{G}) - arctan(\frac{B_{min}}{G})] \tag{2.6}$$

Based on Eqn. 2.6, the maximum achievable phase shift depends not only on the susceptance variation $(jB_{max}-jB_{min})$ but also on the susceptance value as well. It can be shown that for a fixed susceptance variation- $(jB_{max}-jB_{min})$- there is an optimum susceptance that can result in the maximum achievable phase shift. This can be exploited to increase the phase shift in the extended resonance circuit.

In the previous extended resonance circuits [74-76], Y_n and X_n were replaced with a series of varactor diodes as shown in Fig. 2.4. Therefore, the phase shift between power divider ports when the varactors are tuned is:

$$\Delta\theta = 2[arctan(\frac{\omega C}{G}) - arctan(\frac{\omega C}{tG})] \tag{2.7}$$
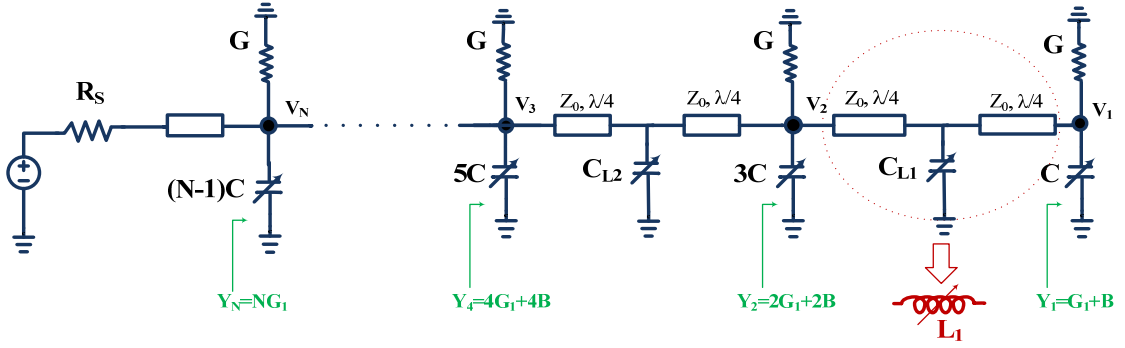
Fig. 2.4. The extended resonance circuit using just varactors as shunt susceptance

where t is the tunability of the varactor (the ratio of the maximum capacitance to the minimum capacitance). Note that varactors at various ports have different values, but they have the same tunability, t.

It can be shown that depending on the tunability of the varactor, there exists an optimum normalized capacitive susceptance, which results in the maximum phase shift between power divider ports, or maximum scan angle for the phased array [52].

To achieve the maximum phase shift it can be shown that value of capacitor should be [52] :

$$\frac{wC_{opt}}{G} = \sqrt{t} \tag{2.8}$$
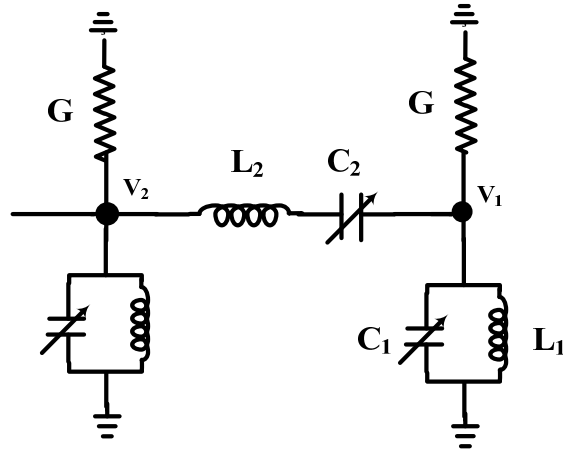
Fig. 2.5. The proposed extended resonance circuit, with a block shown above, can considerably increase the maximum achievable phase shift

The maximum phase shift then will be given by:

$$\Delta\theta_{max} = \pi - 2.tan^{-1}\{\frac{2\sqrt{t}}{t-1}\} \qquad (2.9)$$

In order to extend the phase shift range beyond the limit given by Eqn. 2.9, the modified design shown in Fig. 2.5 is presented. In this design, an inductor L_1 is incorporated in shunt with the varactor C_1 to increase the achievable phase shift. In this design, although the overall susceptance variation (jB_{max}-jB_{min}) remains the same, the optimum inductance value can be determined to maximize the achievable phase shift. As the shunt varactor C_1 is tuned, the series reactance X_n should transform the admittance seen at the node V_1 to its conjugate in the entire tuning range. Such a reactance capable of providing both inductive and capacitive impedance can be provided by placing a varactor
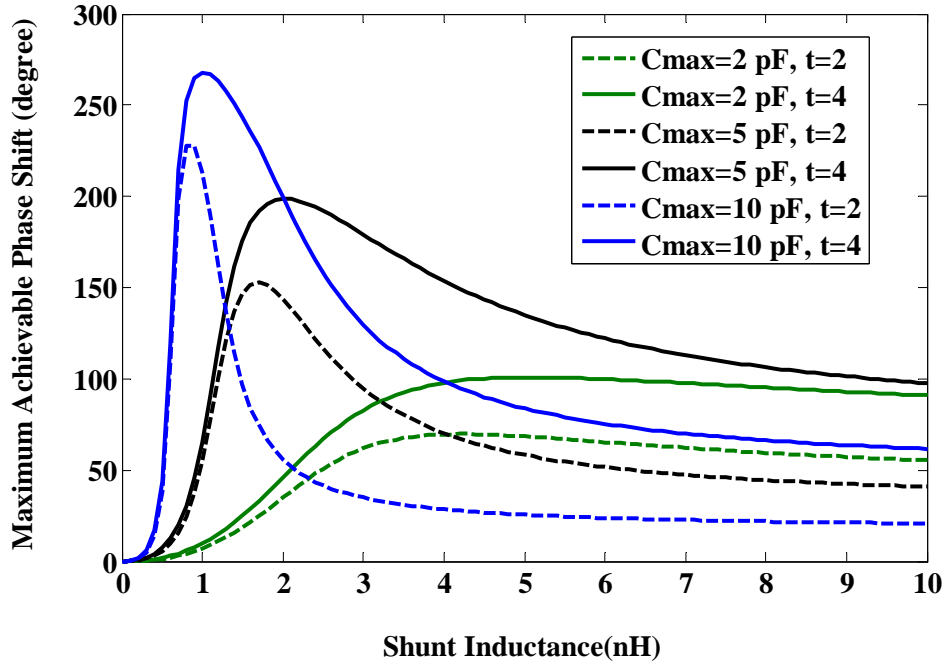
Fig. 2.6. Maximum achievable inter-element phase shift versus the shunt inductance for various varactors at 2 GHz

C_2 in series with an inductance L_2 as shown in Fig. 2.5. The maximum inter-element phase shift for such a structure is given by:

$$\Delta\theta = 2[arctan(\frac{\omega C_{max} - \frac{1}{L_1\omega}}{G}) - arctan(\frac{\frac{1}{L_1\omega} - \frac{\omega C_{max}}{t}}{G})] \qquad (2.10)$$

The graph of the maximum achievable phase shift versus shunt inductance L_1 for different varactors is shown in Fig. 2.6. For a given varactor capacitance, there is an optimum shunt inductance value that maximizes the phase shift across the two nodes in the circuit. This inductance value can be calculated based on the varactor maximum capacitance C_{max} and its tunability "t" as:
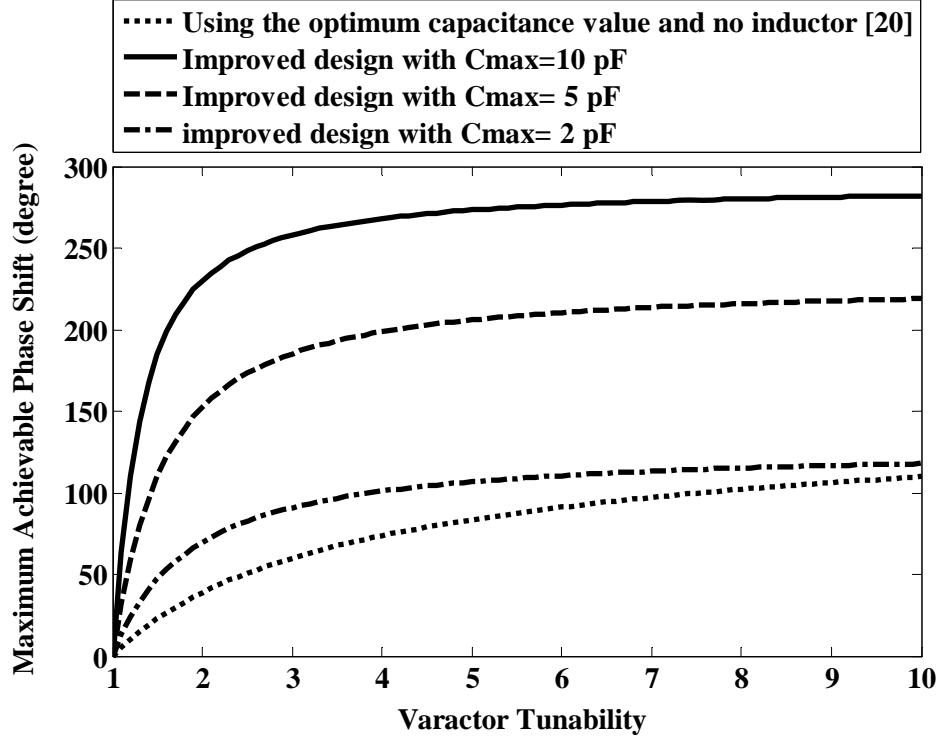
Fig. 2.7. Maximum achievable inter-element phase shift versus the varactor tunability for various varactor capacitances at 2GHz

$$L_{opt} = \frac{2t}{\omega^2 C_{max}(t-1)}$$ (2.11)

The maximum inter-element achievable phase shift is then given by:

$$\Delta\theta_{max} = 4\,tan^{-1}\left[\frac{\omega C_{max}(t-1)}{2Gt}\right]$$ (2.12)

The plots in Fig. 2.7 compare the maximum achievable inter-element phase shift

in the design of the extended resonance without any inductor [75] with the improved
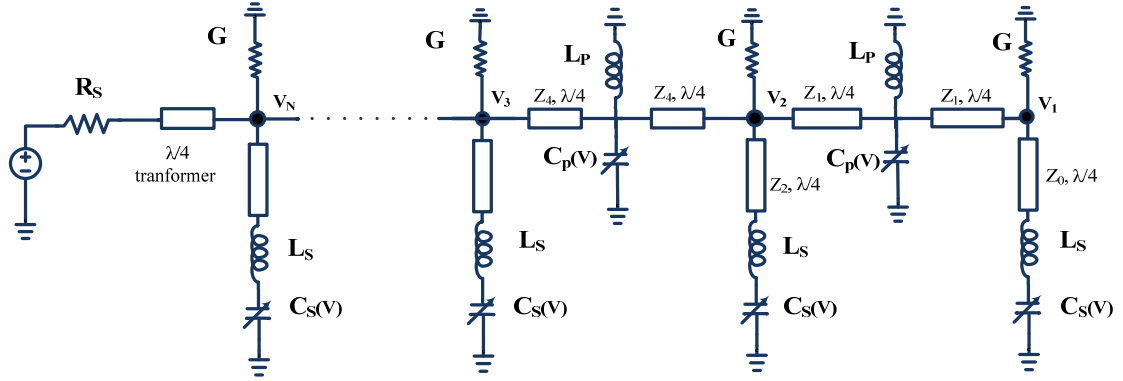
Fig. 2.8.   The impedance transformers can be employed to facilitate the implementation of the extended resonance circuit

design for different varactor capacitance values. Low loss varactors based on MEMS, BST and GaAs technologies with the typical tunabilities less than 2, 3 and 8, respectively, can provide phase-shifts in the ranges of 10-20, 50-60 and 90-100 degrees in the design based on [52], whereas the new design described here can achieve a considerably larger phase shift employing the same varactors as seen in Fig. 2.7. This improvement in the maximum achievable phase shift is even more significant if a varactor with a larger capacitance value is used. Based on Eqn. 2.12, a varactor with a larger tunability and capacitance value can result in a larger phase shift when an optimum inductance is employed (Fig. 2.7).

In the extended resonance circuit shown in Fig. 2.5, varactors with different capacitance values are required. In order to facilitate the implementation of the extended resonance circuit, a different circuit topology (Fig. 2.8) is presented that can be designed using similar varactors. In this circuit, the series combination of C_2 and L_2 (Fig. 2.5) is replaced with a varactor $C_p(V)$ in shunt with an inductor L_p inserted between two quarter-

47

wave transformers. The shunt combination of C_l and L_l (Fig. 2.5) is also replaced with a quarter-wave transformer connected to a varactor $C_S(V)$ in series with an inductor L_S, as shown in Fig. 2.8. In order to achieve the maximum phase shift calculated in Eqn. 2.12, the quarter-wave transformer is designed to transform the series combination of C_s and L_s to the shunt combination of C_l and L_l with the optimum inductance value given by Eqn. 2.11. Furthermore, in order to allow the same varactor to be used through the entire circuit, the impedances of the quarter-wave transformers are determined to provide the susceptance ratios required in the extended resonance circuit. Moreover, the number of bias voltages can be reduced dramatically in this structure. Two bias voltages can tune the varactor capacitances through the entire circuit, one for tuning each of the varactors $C_S(V)$ and one for tuning each $C_p(V)$ (Fig 2.8).

The direction of the radiation beam of series-fed phased arrays changes with frequency variation resulting in array beam squint. In order to investigate the frequency response of the extended resonance phased array, several phased arrays are designed and their beam squint characteristic versus frequency has been studied. The plots in Fig. 2.9 and Fig 2.10 show the inter-element phase shift and scan angle variation versus frequency, respectively, for a phased array designed to have a scan angle of 15 degrees. Three different circuits employing different varactors having tunabilities of 2, 5 and 10 are designed to achieve this scan angle. The results shown in the Fig. 2.9 and Fig. 2.10 suggest that beam squint is alleviated by increasing the varactor tunability. Based on Fig. 2.9 and Fig 2.10, as the tunability increases from 2:1 to 5:1, the beam squint slightly improves however as the tunability increases beyond 5:1, there is minimal improvement in frequency response of the phased array. The Fig. 2.11 and Fig. 2.12 show the inter-
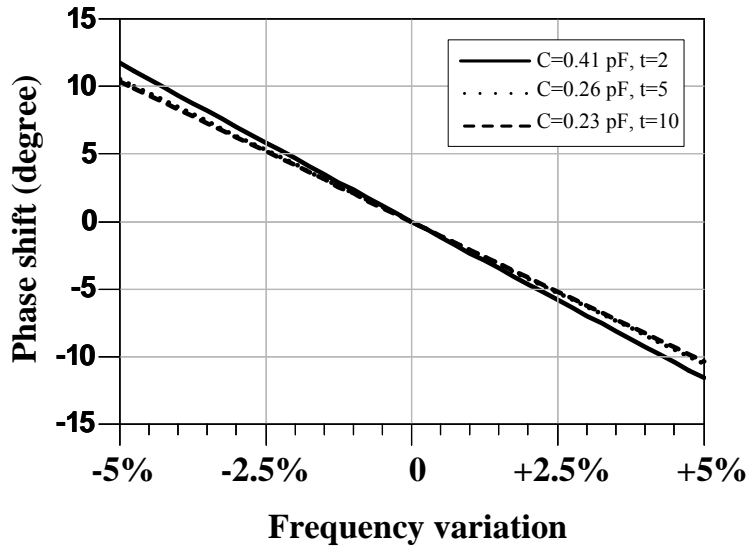
Fig. 2.9.　　　Inter-element phase variation versus frequency for the 15 degree-scan range phased array using different varactors
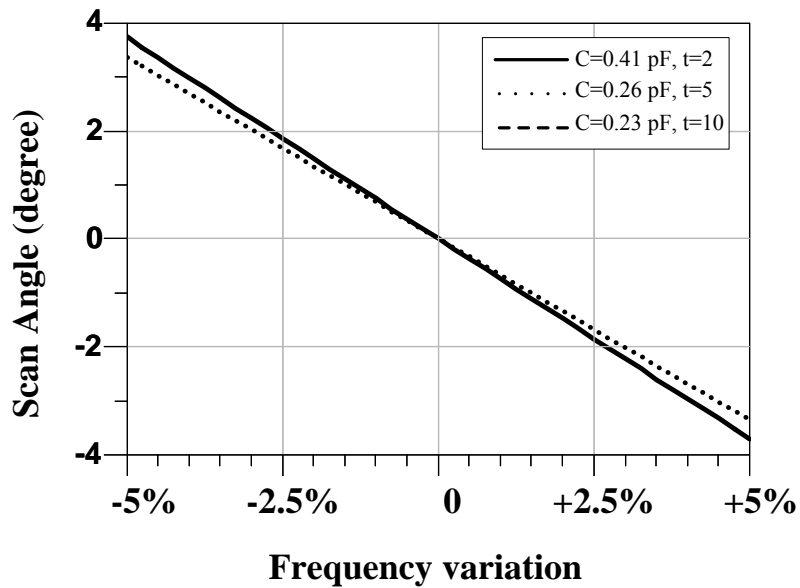
Fig. 2.10.　　　Scan angle variation versus frequency for the 15 degree-scan range phased array using different varactors
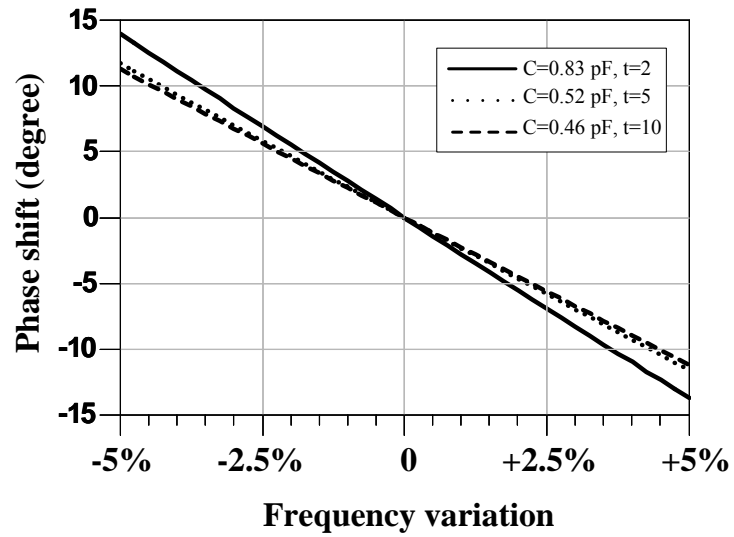
Fig. 2.11.   Inter-element phase variation versus frequency for the 30 degree-scan range phased array using different varactors
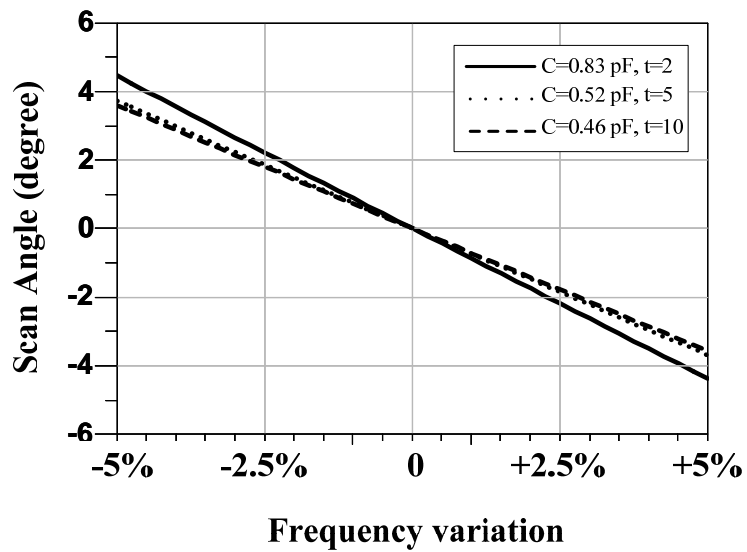
Fig. 2.12.   Scan angle variation versus frequency for the 30 degree-scan range phased array using different varactors

50
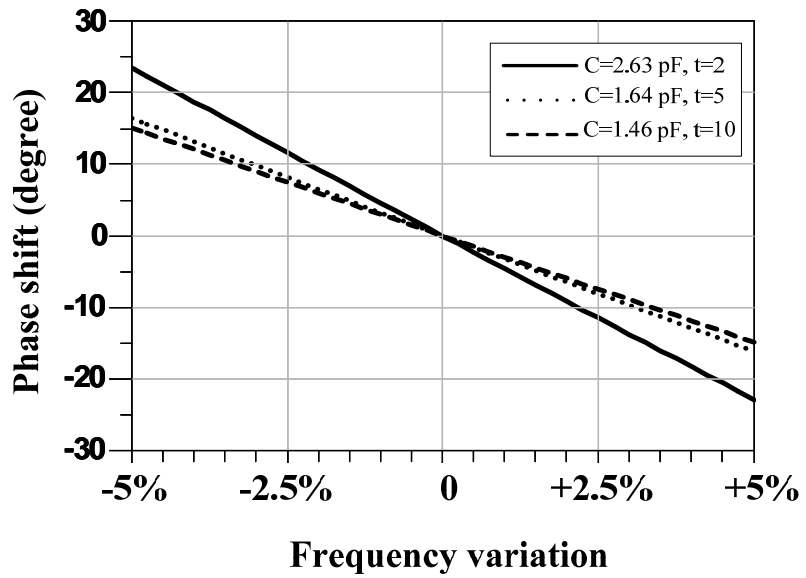
Fig. 2.13.   Inter-element phase variation versus frequency for the 90 degree-scan range phased array using different varactors
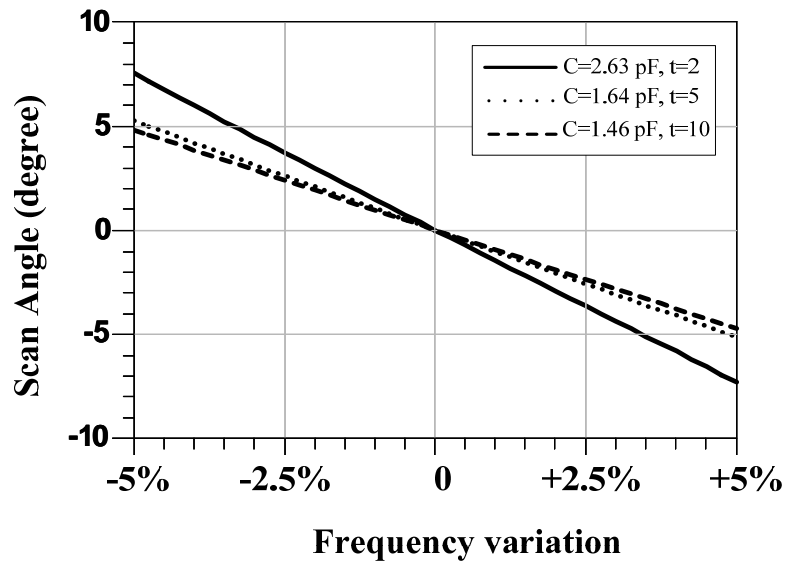
Fig. 2.14.   Scan angle variation versus frequency for the 90 degree-scan range phased array using different varactors

element phase shift and scan angle variation versus frequency for an array designed to achieve a scan angle of 30 degrees. Compared to the graphs given the array having a scan angle of 15 degrees, the beam squint degrades as the scan angle increases. Here, again the beam squint is alleviated by increasing the varactor tunability. The plots of inter-element phase shift and scan angle variation versus frequency for an array having a scan angle of 90 degrees are shown in Fig. 2.13 and Fig. 2.14.

The phased array frequency bandwidth requirement depends on the application which the phased array is intended. Long range automotive radars for automotive cruise control and crash warning systems require a bandwidth of approximately 1% at the center frequency of 24 GHz. Furthermore, these radars are required to have a beam as narrow as 3 degrees which should be steered within scan range of 15 degrees around broadside. Based on Fig. 2.12, for such a scan angle, the beam of the extended resonance phased array tilts within a range as narrow as +/-0.4 degrees. Such a low frequency beam squint capability demonstrates extended resonance phased array as a promising solution for automotive long range radars [77].

2.4 Modular Extended Resonance Phased Array

One of the challenges in the area of phased array systems is how to extend very large phased arrays. The maximum gain of an antenna array can be calculated as [46]:

$$G_{array} = G_{antenna} + 20\,log_{10}\,N \tag{2.13}$$

where N is the number of array elements.
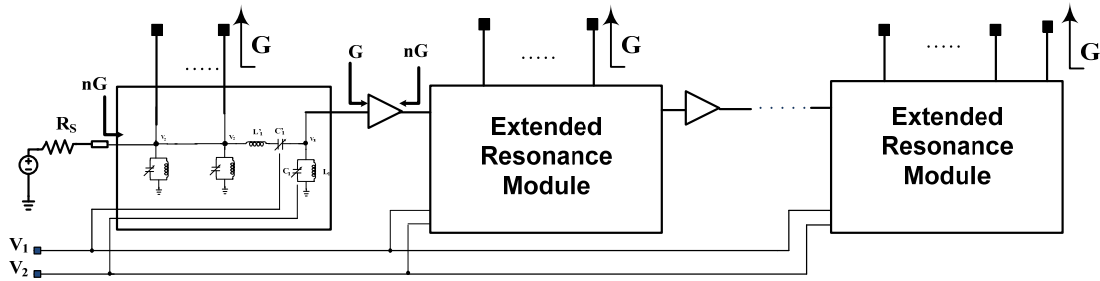
Fig. 2.15. The modular design of transmit extended resonance phased array

Based on Eqn. 2.13, increasing number of array elements increases the gain of antenna array. Moreover, the spatial selectivity of phased array can be enhanced by increasing number of array elements. Consequently, the noise performance of phased array system if used in receive mode can be enhanced. Furthermore, increasing the gain of phased array alleviates the output power requirement of power amplifier if phased array used in transmit mode [46]. In general, increasing the number of array elements increase the design complexity of phased array. Power combing among a large number of radiating elements can be exceedingly complex. Furthermore, the lossy passive signal distribution networks can cause an excessive amplitude drop along the feed network of phased arrays.

In the extended resonance circuit, the shunt susceptance values increase as odd multiples of the first shunt susceptance value across the circuit, therefore as the number of array elements increases, the value of the required shunt susceptances can be prohibitively large. Furthermore, the loss of passive elements accumulates across the circuit and degrades the uniform array excitation as the number of array elements is increased. In order or address the aforementioned design issues, a modular approach to

53

the design of extended resonance phased array is presented. In this design, several identical extended resonance circuits are placed in tandem through amplifier stages (Fig. 2.15), that is the last antenna at each module is replaced with an amplifier. After boosting the signal level, it is injected into the next module. Therefore, the same design can be used to extend the number of array elements realizing scalable phased array design. The design complexity associated with large phased array design can be reduced by using the scalable phased array presented here.

The amplifier stages are designed to inject signals with equal power levels into each module in order to maintain a uniform power distribution across the entire antenna array. Therefore, the gain of the amplifier can be determined by Eqn. 14 assuming a lossless circuit.

$$G_{amplifier} = 20 \, log_{10} \, N \qquad\qquad (2.14)$$

Here, N is the number of array elements.

In reality, the amplifying stages should compensate for the circuit loss through the circuit as well. The amplifier should be matched to G, the admittance of the antennas, in order to maintain the uniform power distribution across each module. The output of the amplifier is matched to NG to avoid any mismatch and reflection at the input of each extended resonance module.

2.5 Heterodyne Modular Extended Resonance Phased Array

In order to apply extended resonance technique to microwave and millimeter wave applications, low loss tunable elements required to operate at the mentioned frequencies. Designing low loss tunable elements at such high frequencies can be challenging. In this section, the design of an extended resonance phased array using a heterodyne concept is presented. Exploiting heterodyne concept for phased array design allows the tunable elements to operate at frequencies much lower than the actual operating frequency of phased array.

2.5.1 Overview of Heterodyne Modular Extended Resonance Phased Array

As depicted in Fig. 2.16, the heterodyne phased array is composed of identical IF power dividing/phase shifting and LO power dividing extended resonance modules. The LO power dividing network, designed based on the extended resonance technique, distributes the LO signal equally to the LO ports of the mixers. The IF-network is a tunable extended resonance network that, in addition to uniformly distributing the IF-signal to the mixers' IF-ports, controls the phase of the IF signals. Thereby, the phased array beam can be controlled by tuning the IF network. The identical IF and LO extended resonance modules are connected in tandem through amplifying stages. The amplifying stages are designed to inject the same power level into each module in order to maintain a uniform power distribution across the entire networks. Furthermore, through heterodyne mixing of the IF and LO signals, the insertion phase of the amplifying stage in the IF network is canceled out by the insertion phase of the amplifying stage at the LO network.

The extended resonance modules provide a linear phase progression across their output ports [75]. Here, the initial phase progression across the IF ports is canceled out by the phase progression across the LO ports to set the beam corresponding to the mid-point of the scan range at broadside. In order to steer the beam, the phase shift between the RF signals can be tuned by utilizing varactors in the IF or LO networks. Phase shifting at the IF stage is preferred due to the better performance of varactors at lower frequencies. The tunable IF modules are realized based on a modified extended resonance circuit topology discussed previously.

The signal at an IF port can be presented by Eqn. 2.15.

$$S_{IF(n)} = A_{IF} \cos(\omega_{IF} + n\theta_0 + n\Delta\theta) \qquad (2.15)$$

Furthermore, the signal at the corresponding LO port is given by Eqn. 2.16.

$$S_{LO(n)} = A_{LO} \cos(\omega_{LO} + n\phi_0) \qquad (2.16)$$

Therefore, the signal fed to the corresponding antenna element can be determined according to Eqn. 2.17 assuming the mixer gain to be A_{mixer}.

$$S_{RF(n)} = A_{mixer} A_{IF} \cos(\omega_{IF} + 2\omega_{LO} + 2n\phi_0 + n\theta_0 + n\Delta\theta) \qquad (2.17)$$

Therefore, the frequency of RF transmit signal is given by Eqn. 2.18.

$$f_{RF} = f_{IF} + 2f_{LO} \qquad (2.18)$$
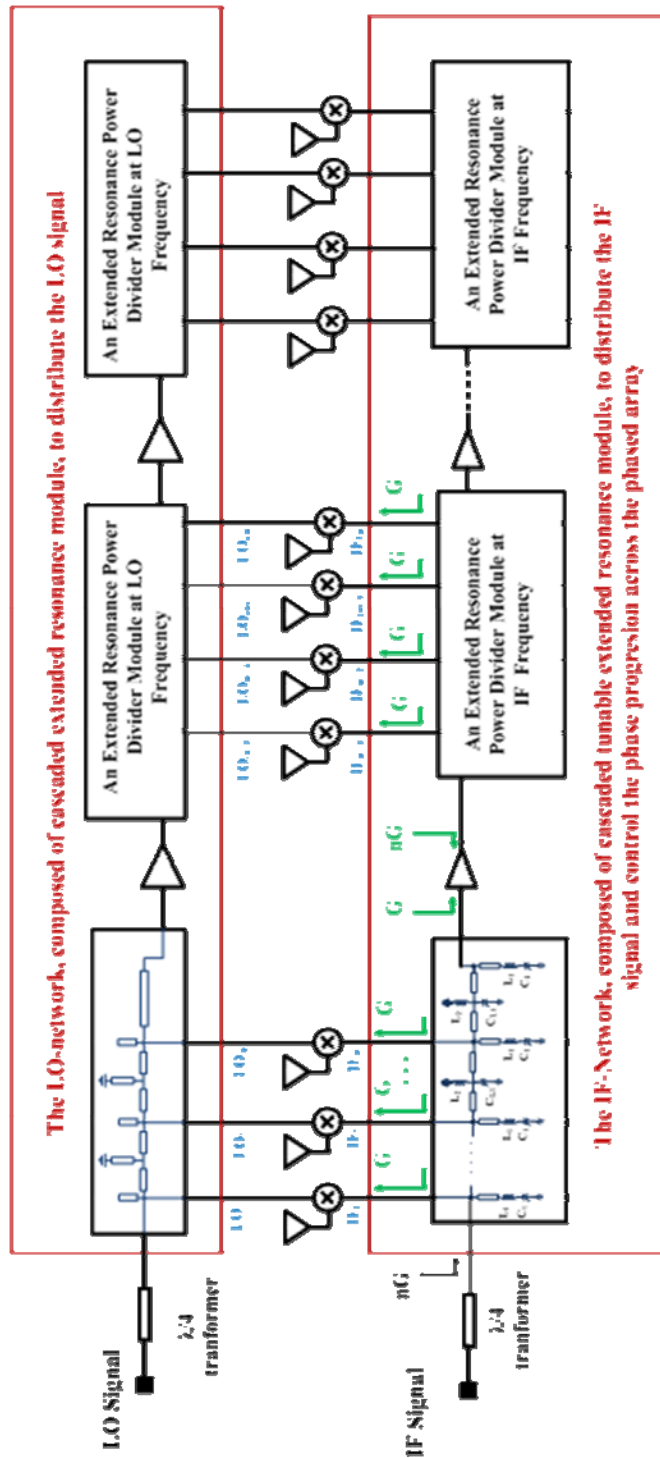
Fig. 2.16. The proposed phased array is a heterodyne-mixing structure that exploits the extended resonance technique to achieve a uniform power distribution and to control the phase progression across the phased array

57

Furthermore, the initial phase progression across the IF ports is canceled out by the phase progression across the LO ports allowing scanning around the broadside. Therefore, the relationship given by Eqn. 2.19 should be met to set the initial beam corresponding to the mid tuning range at broadside.

$$\phi_0 = \frac{-\theta_0}{2}$$

(2.19)

2.5.2 IF Circuit design

The IF-network, designed at 2 GHz, is composed of two tunable, four-port extended resonance power dividing modules cascaded through an amplifying stage. The IF power dividing module is shown in Fig. 2.17. In order to achieve an equal power division through the entire IF-network, the designed amplifying stage has a gain of 7 dB, matched to 50 ohm at the input and 10 ohm at the output. In addition to IF signal distribution, the power dividing modules provide the required phase shift to steer the beam. The phase shift can be controlled by tuning the varactors $C_s(V)$ and $C_p(V)$ as shown in Fig. 2.6. The capacitance of the varactors $C_s(V)$ and $C_p(V)$ can be tuned from 0.2 pF to 1.2 pF and 0.4 pF to 2.4 pF, respectively, as the bias voltages change from 0.5 volts to 12 volts. The $C_p(V)$ bias voltage VB_1 is applied through a single bias circuit at the input of each block, while separate, but identical, bias circuits are designed to tune the capacitance of varactors $C_s(V)$ using bias voltage VB_2. The RF-choke inductors used in the bias circuit design have an inductance of 154 nH, while the capacitance of the DC-blocks are 850 pF. The inductors used in the design are L_S=3.3 nH and L_P= 9.5 nH. The characteristic impedances of the quarter-wave transformers range from 30 ohms to 90 ohms through the
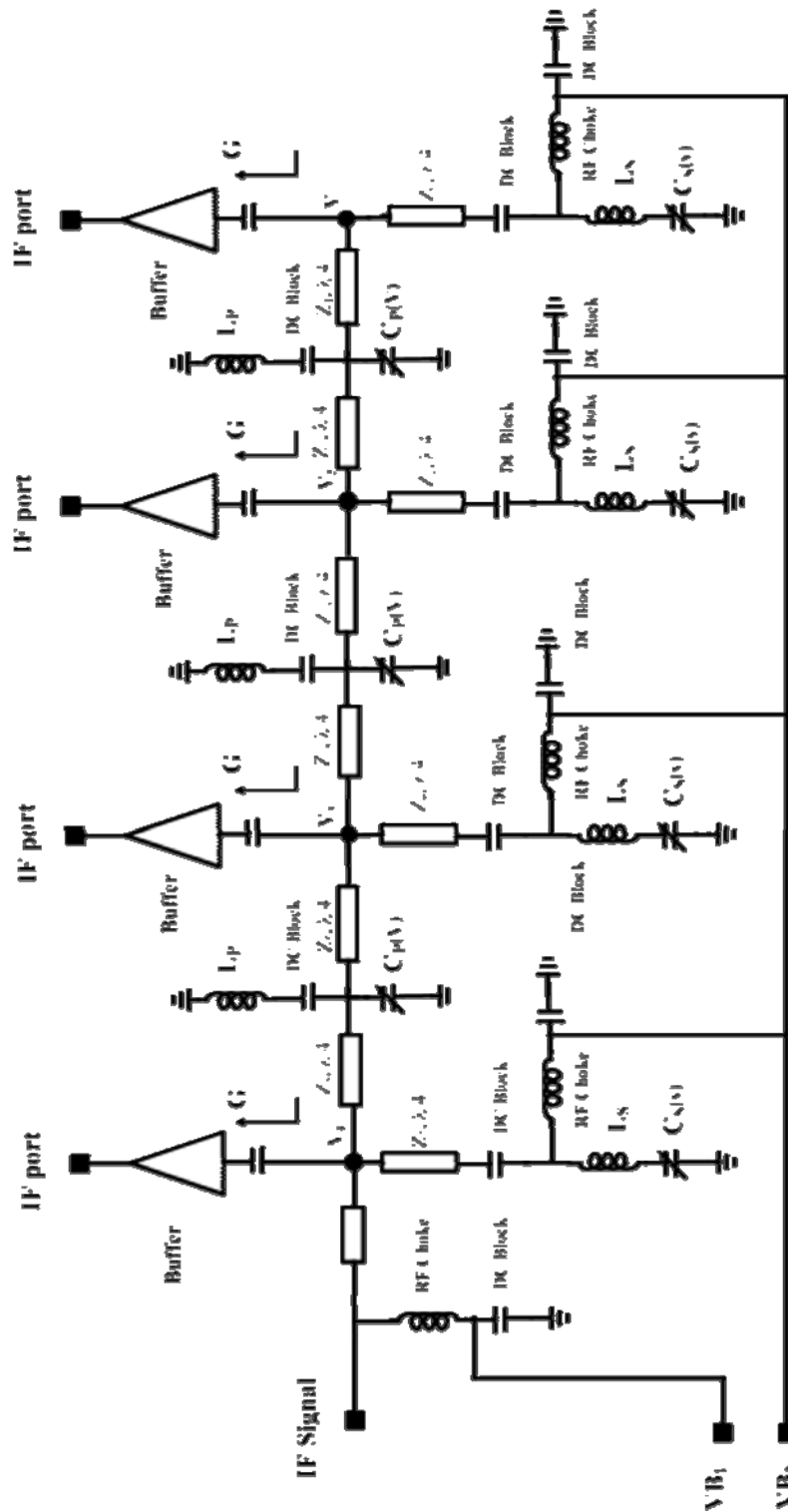
Fig. 2.17. The IF extended resonance module at 2 GHz
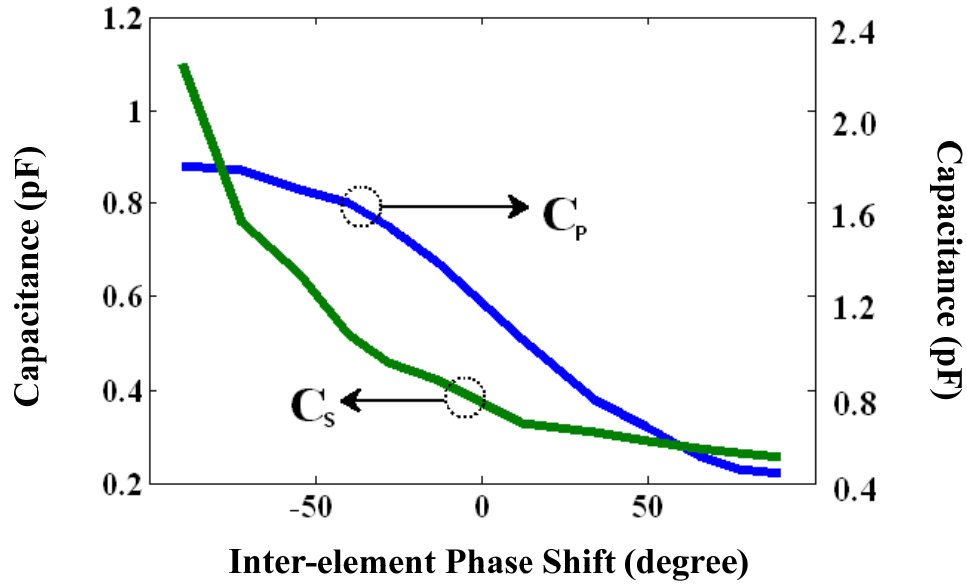
Fig. 2.18. The inter-element phase shift can be controlled by tuning the varactors capacitances

entire design. In order to provide isolation between the power divider and mixers circuits, the buffer amplifiers are employed at the IF stage. The graph of the resultant inter-element phase shift versus the capacitance of varactor $C_s(V)$ and $C_p(V)$ is shown in Fig. 2.18.

2.5.3 LO Circuit design

The LO network is composed of two cascaded extended resonance power dividing modules designed at 11 GHz. The LO power dividing module is shown in Fig. 2.19. The sub-harmonic mixers double the frequency of the LO signals and up-convert the 2 GHz IF signals to 24 GHz transmit signals. In the design of the LO power dividing modules, microstrip lines are utilized to achieve a compact, low loss structure at the design frequency. Furthermore, a matching circuit is used to improve the impedance
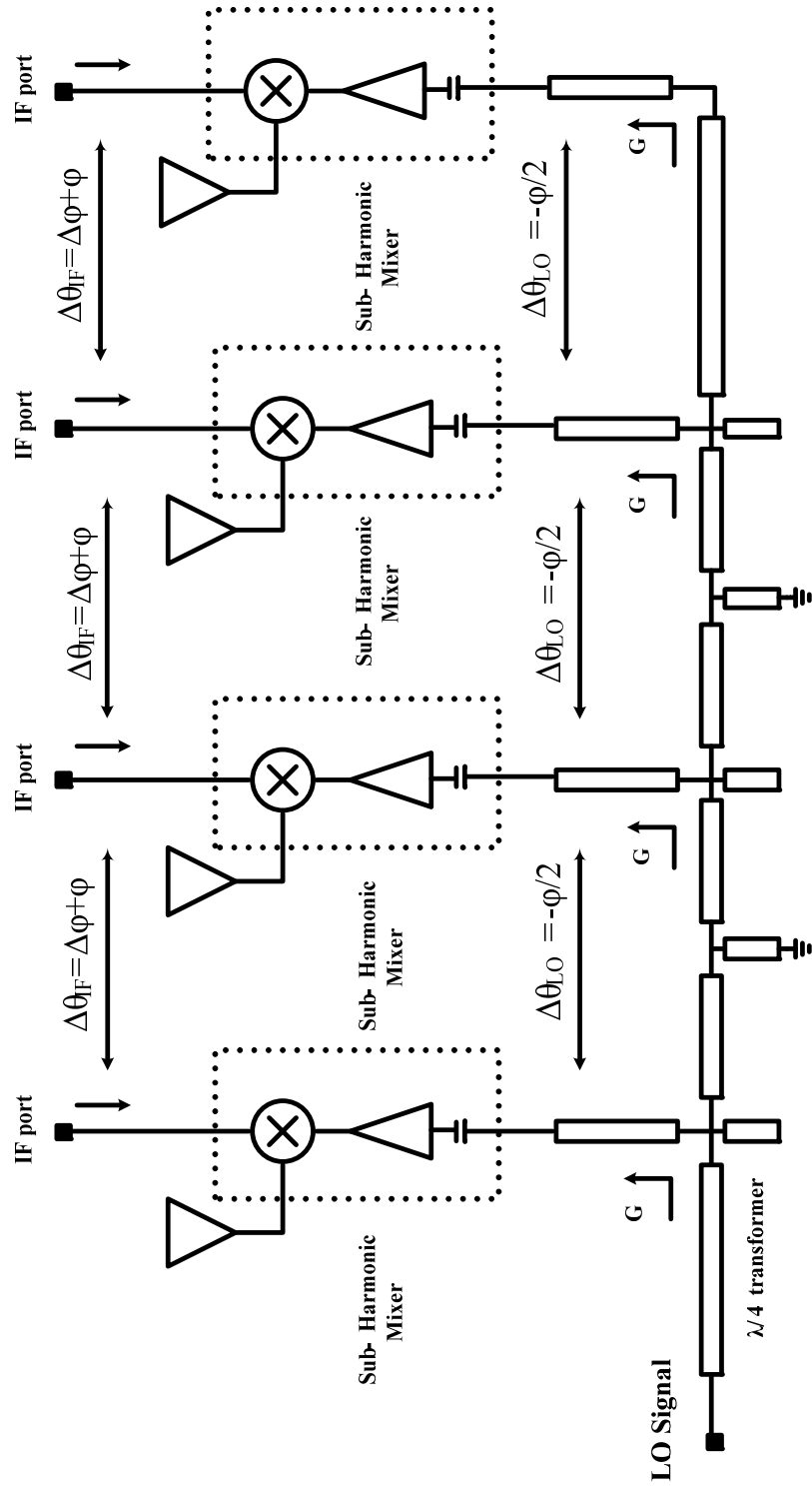
Fig. 2.19. The LO extended resonance module at 11 GHz
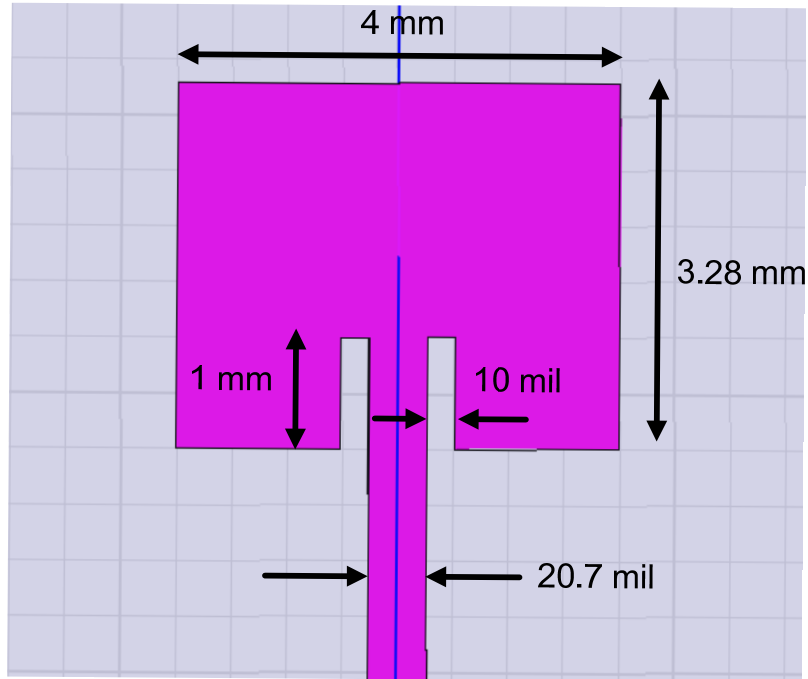
Fig. 2.20. The patch antenna designed for center frequency of 24 GHz

match at the mixers LO-ports. Moreover, the phase progression across the LO-network cancels out the phase progression across the IF network to set the beam at broadside.

2.5.4 Antenna design

Microstrip patch antennas are used as radiating element in the presented phased array. The patch antenna at the center frequency of 24 GHz was designed based on the procedure given in [78]. Based on this procedure, the width of the antenna is given by:

$$W = \frac{c}{2f_0} \sqrt{\frac{2}{\varepsilon_{r_{eff}} + 1}}$$

(2.20)
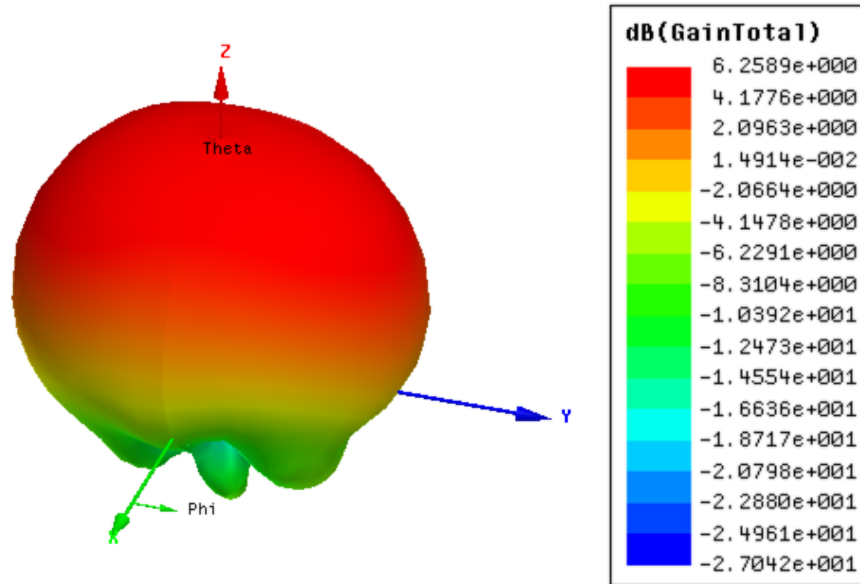
Fig. 2.21. The radiation pattern of the patch antenna at 24 GHz

and ε_r is the dielectric constant of the substrate. The effective dielectric constant of the microstrip antenna is calculated according to Eqn. 2.21.

$$\varepsilon_{r-eff} = \frac{\varepsilon_r + 1}{2} + \frac{\varepsilon_r - 1}{2}\left[1 + 12\frac{h}{W}\right]^{-1/2} \qquad (2.21)$$

where h is the substrate thickness. Once W and ε_{r-eff} is calculated, the extension length of the microstrip patch due to the fringing effects can be calculated using.
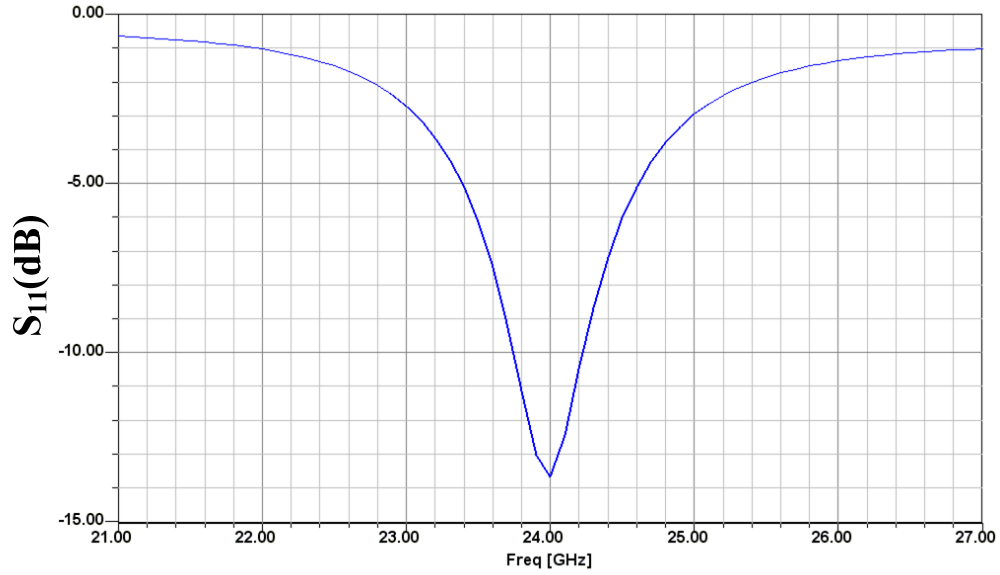
Fig. 2.22. Return loss of the antenna at 24 GHz

$$\Delta L = h \times 0.412 \frac{(\varepsilon_{r\_eff} + 0.3)(\frac{W}{h} + 0.246)}{(\varepsilon_{r\_eff} - 0.258)(\frac{W}{h} + 0.8)} \tag{2.22}$$

Therefore, the length of the microstrip patch is given by:

$$L = \frac{c}{2f_0\sqrt{\varepsilon_{r-eff}}} - 2\Delta L \tag{2.23}$$

Preliminary design of a 24 GHz microstrip patch antenna was done using the given equations and the substrate parameters. Then, the antenna was simulated using
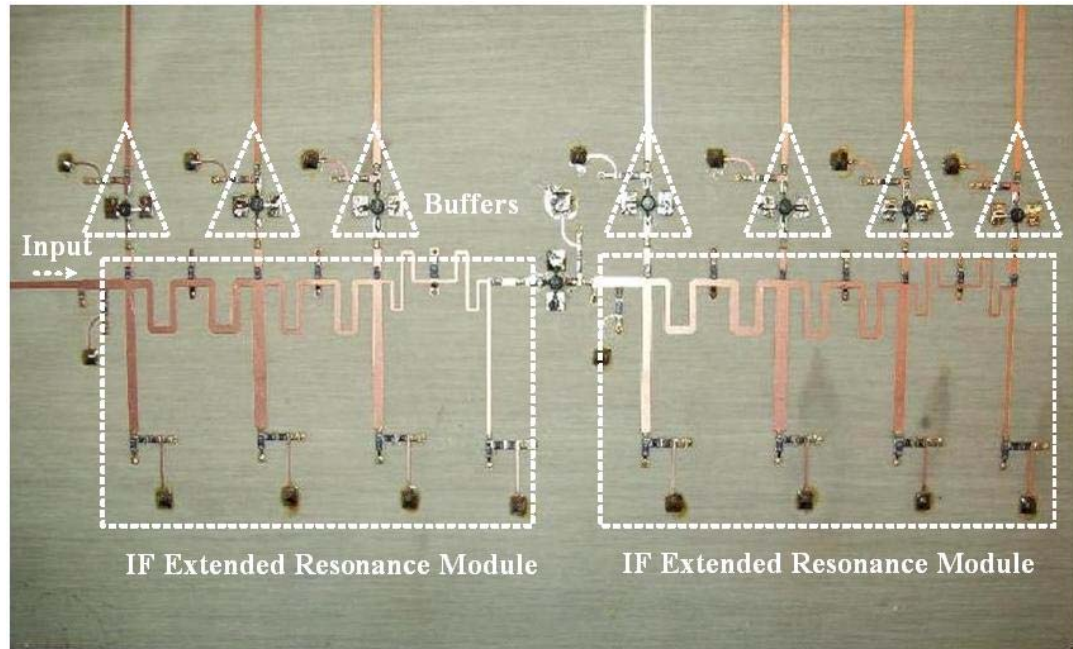
Fig. 2.23. The photograph of the IF circuit

Ansoft HFSS and based on simulation results, the dimensions were optimized to achieve the correct resonant frequency. The final patch antenna with its dimension is shown in Fig. 2.20. The simulated radiation pattern of the final microstrip patch antenna is shown in Fig. 2.21. The antenna is designed to be matched to 50 ohm. The simulated return loss of antenna is shown in Fig. 2.22. The 10 dB return loss-bandwidth of the antenna is approximately 500 MHz at the center frequency of 24 GHz.

2.6   Fabrication and Measurement results

A seven-element phased array is fabricated as shown in Fig. 2.23. As can be seen, the IF-circuit is fabricated on a RO4003C from Rogers Corporation with a thickness of 20 mils and a dielectric constant of 3.55. The flip-chip GaAs varactor MA46H120 from MACOM is used for phase shifting. The varactors have an approximate quality factor of

Measured   ----- Simulated
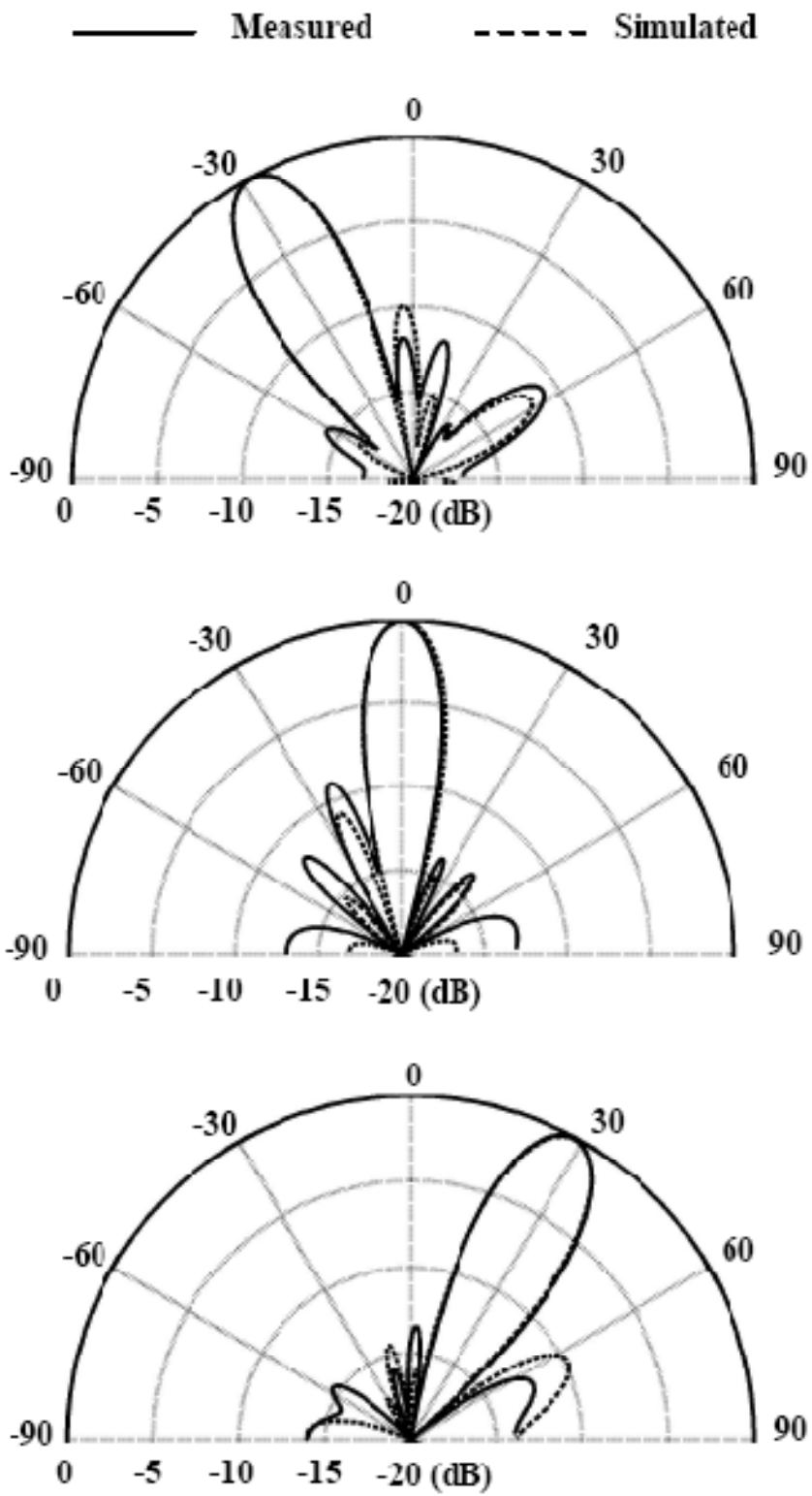
Fig. 2.24. The measured array factors of the IF-network compared to the simulation
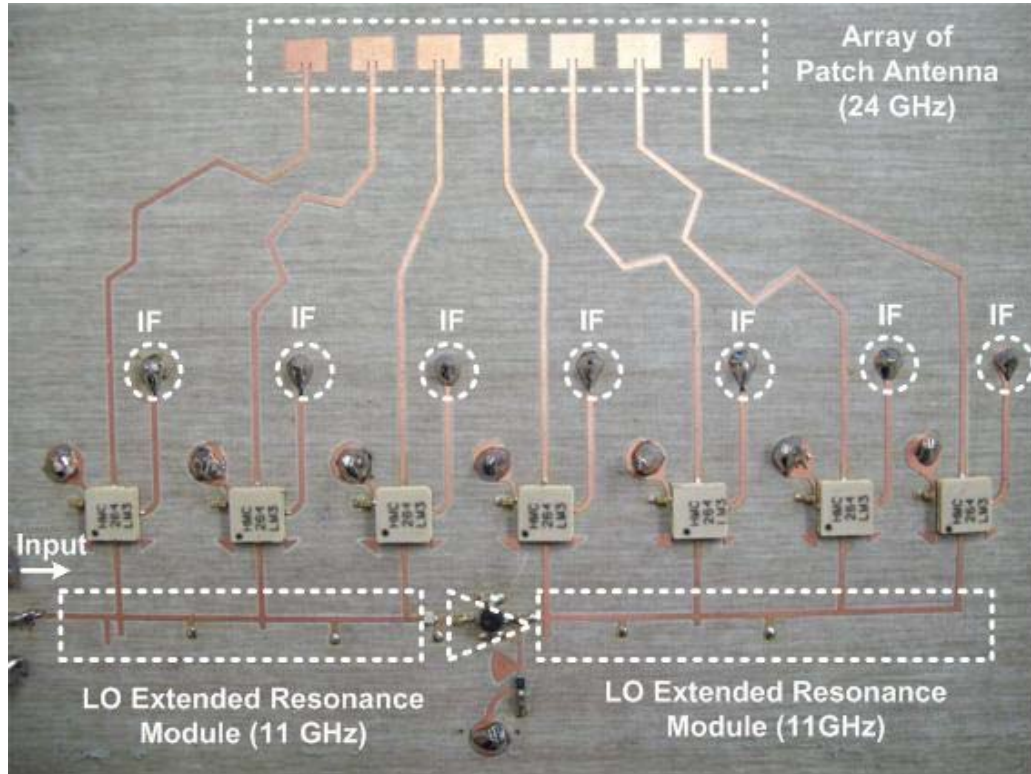
Fig. 2.25. The photograph of the LO circuit and the patch-antenna elements together with their feed lines

50 at a bias voltage of 4 volts and 5:1 tunability at 2 GHz. The amplifier ERA1+ from Mini-circuits is employed to cascade the IF power dividing modules. The same amplifier is used as the buffer at the IF ports. The IF-circuit can be used as a stand-alone circuit for beam steering at 2 GHz. The S-parameters of the IF ports are measured at various bias points and the calculated array factors are shown in Fig. 2.24. A scan angle of approximately 60 degrees can be achieved at the IF-circuit while the side lobes are maintained below -10 dB. The 3-dB beam width of the array factor varies from 15 degrees to 18 degrees within the entire scan range.

The LO-circuit together with the antenna elements are fabricated on a separate circuit board as shown in Fig. 2.25. The substrate used is Rogers RO4350 with a

Anechoic Chamber

Ka band Horn Antenna
(MFR-01456)

LNA

Rotation Control

Spectrum Analyzer
(HP 8563E)

Processing Unit
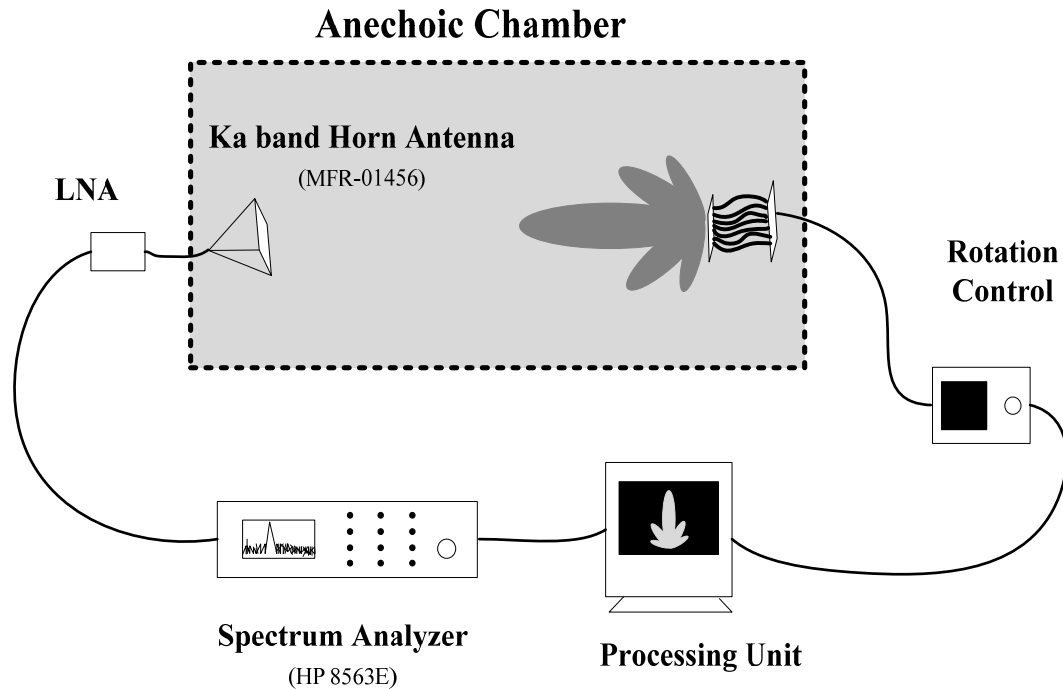
Fig. 2.26. The phased array radiation pattern measurement setup

thickness of 10 mils and a dielectric constant of 3.66. The LO signal at 11 GHz provided by a signal generator is applied to the input of the LO circuit. The extended resonance modules in the LO circuit are cascaded through RFMD LN300 amplifiers. The Sub-harmonic mixers HMC264LM3 with integrated LO frequency doublers from Hittite Microwave are used in the phased array. The LO amplifiers are included in these mixers obviating the need for a high LO power.

The IF signals from the IF circuit board are injected into the IF ports of the mixers on the LO circuit board. The outputs of the mixers are connected to patch antennas at 24
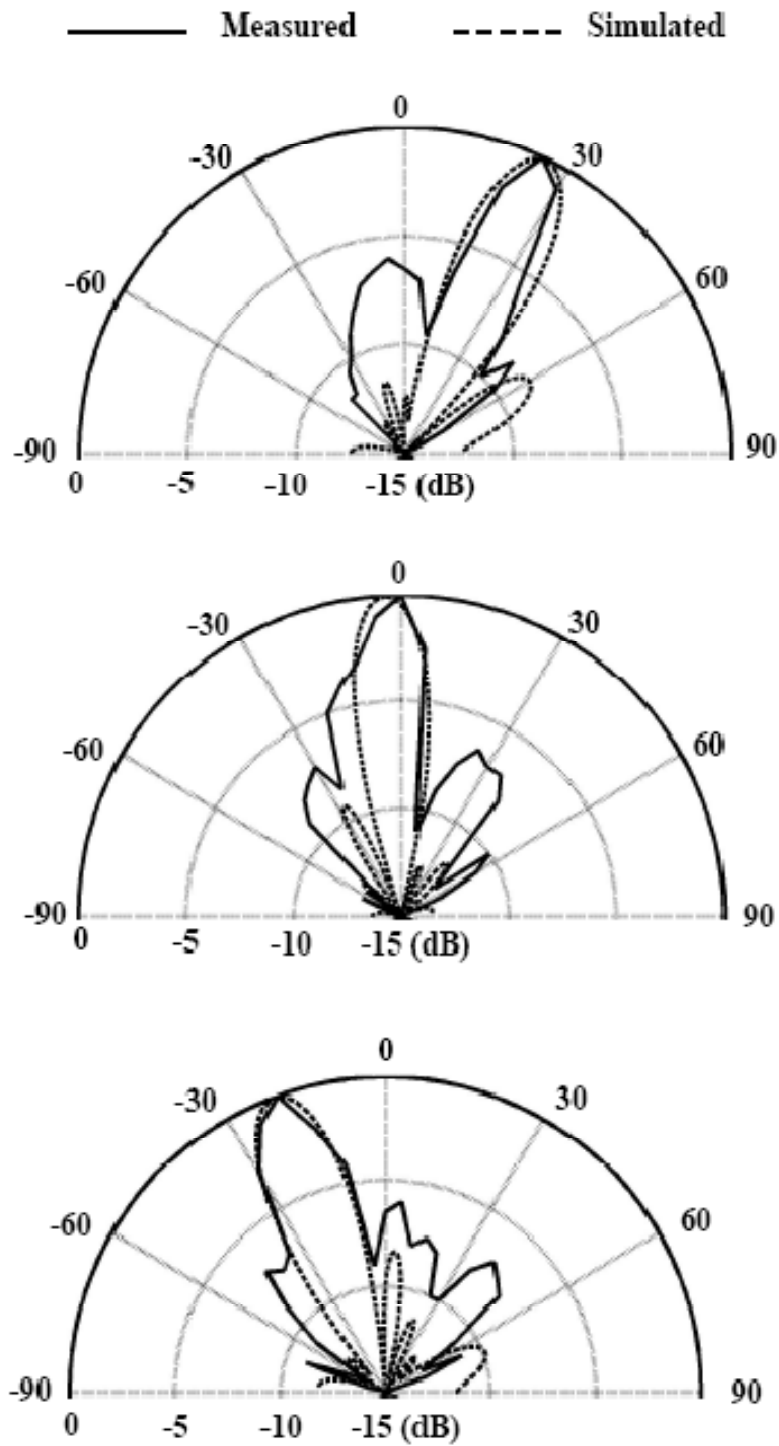
Fig. 2.27. The measured array patterns at 24 GHz compared to the array factors calculated using the simulated S-parameters
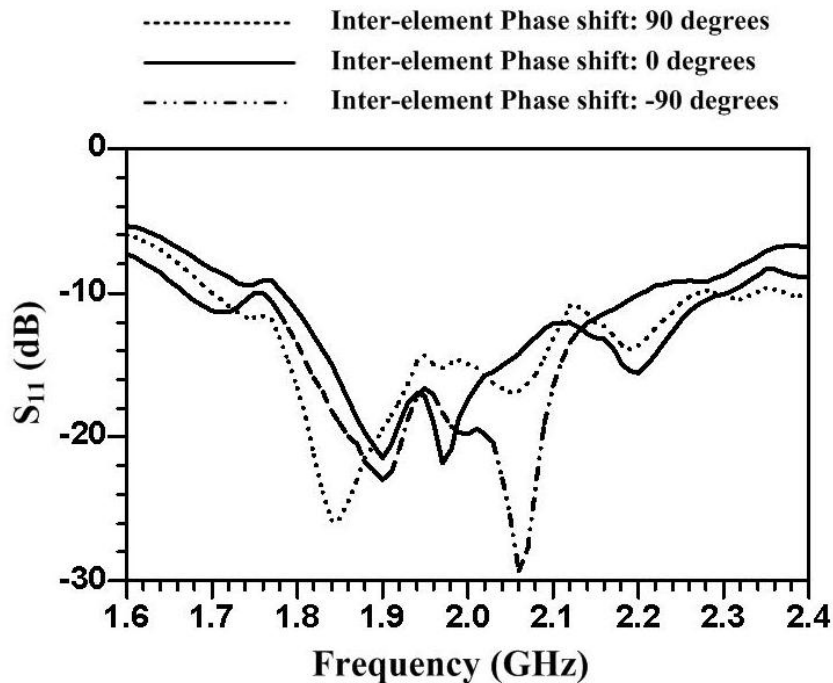
Fig. 2.28. Measured input reflection coefficient of the IF circuit versus frequency at different scan angles

GHz. The patch-antennas are placed $\lambda/2$ apart and each has a gain of 5 dBi. The dimensions of these antennas are 4 mm by 3.28 mm.

The measurement set-up in an anechoic chamber is shown in Fig. 2.26. A Ka band horn antenna MFR-01456 is used as the receive antenna to measure the array pattern. The receive-signal is amplified by an LNA before being measured by a spectrum analyzer and then the computer processes the data to determine the radiation pattern. The computer also controls the rotation angle of the phased array. The radiation patterns corresponding to the broadside and maximum scan angles are measured. The measured results are compared with the array factors calculated using the simulated S-parameters as shown in Fig. 2.27. A scan angle of approximately 50 degrees is achieved. One source of

70

— · — · — · — Array Factor at 2050 MHz

—————— Array Factor at 2000 MHz

— — — — — · Array Factor at 1950 MHz

| 0 | -10 | -20 | -30 | -20 | -10 | 0 |

Array Factor in dB

Fig. 2.29. The array factor based on measured S-parameters at 2 GHz versus frequency

discrepancy between the measured array patterns and the calculated array factors is the radiation from the meandered microstrip lines.

Any modulation in a heterodyne system usually happens at the IF stage. Therefore, it is necessary to understand the effect of frequency variation within the IF-path on the performance of the proposed phased array system. The input return loss and the array factor are measured at the IF-circuit at different frequencies. As can be seen in Fig. 2.28, the return loss of the IF-circuit is maintained greater than 10 dB at a bandwidth of above 20% in the entire scan range. Based on the measured results, the beam tilts approximately within +/- 7 degrees within a bandwidth of 100 MHz. The change in peak gain of the array is approximately 1 dB while the side lobes are maintained below 10 dB

71

in the 100 MHz bandwidth (Fig. 2.29). Symmetrical design of the series fed phased array can alleviate the beam squint.

TABLE 2.1
Comparison between the presented extended resonances phased array and the published series-fed phased arrays

	[79]	[80, 81]	[82]	[52]	[83]	**Presented Phased Array**
Number of antenna elements	4 patches	5 patches	30 leaky wave	4 patches	4 patches	**7 patches**
Center frequency	2.45 GHz	5.8 GHz	3.33 GHz	2 GHz	2.4 GHz	**2 GHz**
Scan Range	30 degrees	22 degrees	60 degrees	20 degrees	49 degrees	**60 degrees**
Number of tuning voltages	6	1	1	4	3	**2**
Return loss bandwidth	1.02%	4.6%	NA	NA	3%	**20%**
Beam squint	NA	5.6° per 1% frequency variation	2.7° per 1% frequency variation	NA	0.4° per 1% frequency variation	2.8° per 1% frequency variation
Gain variation within scan range	NA	0.4 dB	13 dB	1.8 dB	1.5 dB	**1.8 dB**

Table 2.1 summarizes the performance of the proposed electronically steerable antenna array against other series-fed steerable arrays presented in the literature. The proposed antenna array achieves a much wider electronic scan-angle range compared to the other designs shown in the table 2.1. The design proposed in [85] can achieve a comparable scan range at the price of 13 dB array gain variation, whereas, the extended resonance phased array demonstrates a gain variation of only 1.8 dB within the entire scan range. Furthermore, the extended resonance phased array requires a fewer number of

tuning voltages to control the beam of phased array compared to the works presented in [82], [52], [86]. The return loss bandwidth of the extended resonance phased array is much broader than any of the other designs while it demonstrates relatively low beam squint capability as well. The beam squint can be alleviated in the extended resonance phased array by reducing its scan range.

2.7 Conclusion

A new design of phased array based on extended resonance technique is presented. The extended resonance technique is capable of reducing the complexity of phased arrays by achieving phase shifting and power dividing within a single network. A new circuit topology to enhance the scan range of extended resonance is reported and the maximum achievable inter-element phase shift across the tunable extended resonance network is studied. Moreover a modular approach to realize a scalable phased array design is proposed which can significantly reduce design complexity associated with large phased arrays. Furthermore, a 24 GHz modular transmit phased array based on the extended resonance technique is reported. This technique is used along with heterodyne-mixing concept which allows the design to benefit from the better performance of tunable elements like varactors at lower frequencies. Finally a seven-element 24 GHz modular transmit phased array is fabricated and tested. The measured results show a good agreement with the simulation.

Chapter 3

A New Bi-Directional Series-Fed Phased Array

3.1   Introduction

As mentioned before, the large number of required phase shifters and their high circuit complexity is one of the main reasons behind the high cost and complexity of phased arrays. Furthermore, the cost and complexity of the individual phase shifters in a phased array depends on the required phase shift. As an example, one type of phase shifters so called "varactor-loaded-transmission line" is shown in Fig. 3.1. In this type of phase shifter, the maximum achievable phase shift is determined by the number of varactor and inductor stages. Therefore, overall phase shifter complexity is directly proportional to the maximum phase shift required from phase shifter. By designing phased arrays that demand less phase shift from phase shifters, the cost and complexity of phased array can be reduced.
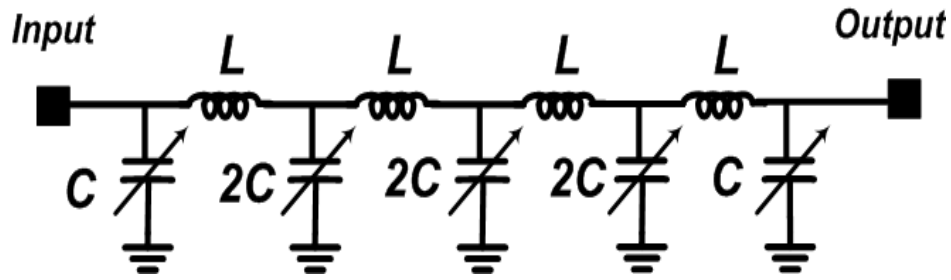
Fig 3.1. The complexity of varactor loaded transmission line is determined by the amount of phase shift required from the phase shifter

The required amount of phase shift from a phase shifter can depend on the design of the array feed network. In this chapter, different types of array architectures are discussed and their required amounts of phase shift are compared. A new bi-directional phased array is introduced which demands less phase shift from phase shifters compared to any of the conventional phased array designs. The detailed design of the feed network is given in this chapter. Furthermore, a new compact phase shifter design is presented in this chapter as well. Utilizing this phase shifter within the proposed bi-directional phased array allows the array beam to be steered by a single control voltage. The entire phased array is fabricated and its measurement result is reported.

3.2 Overview of phase Shift Requirement in Different Types of Phased Arrays

In general phased arrays are designed based on either a parallel or a serial feed network [84]. In parallel feed networks, which are often called corporate feeds, the input
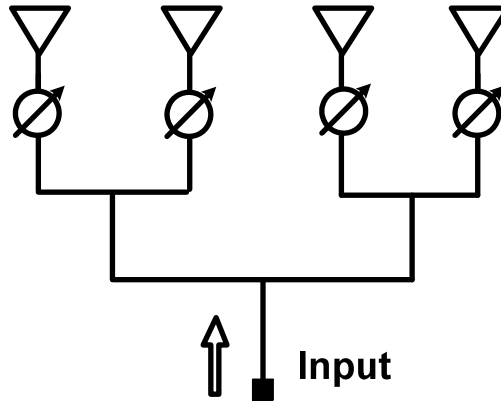
Fig 3.2. Phased arrays using parallel feed network require maximum phase shift of *(N-1)θ* from phase shifters to achieve inter-element phase shift of *θ*
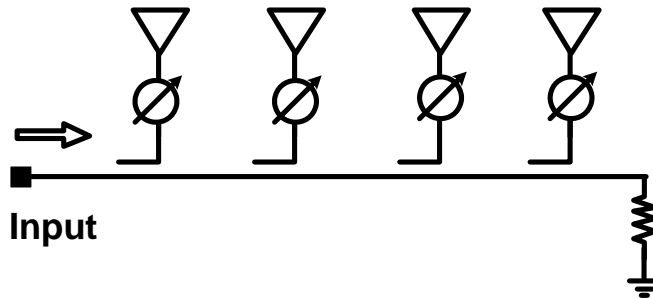
Fig 3.3. Series-fed phased array with phase shifters inserted in parallel require maximum phase shift of *(N-1)θ* from phase shifters to achieve inter-element phase shift of *θ*
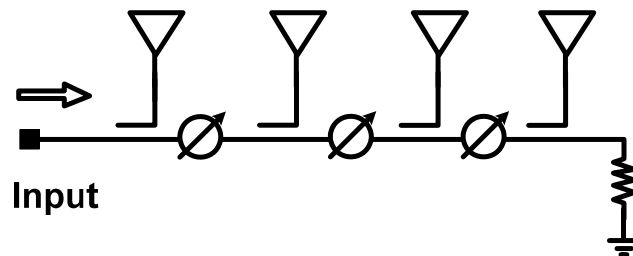
Fig 3.4. Series-fed phased array with phase shifters inserted in series require maximum phase shift of *θ* from phase shifters to achieve inter-element phase shift of *θ*
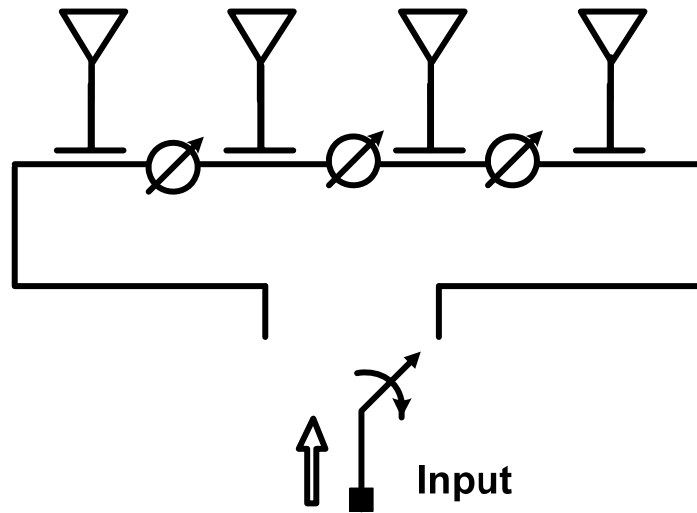
Fig 3.5. Bi-directional series-fed phased arrays require maximum phase shift of *θ/2* from phase shifters to achieve inter-element phase shift of *θ*

signal is divided in a corporate tree network to all the antenna elements as shown in Fig. 3.2. In phased arrays using corporate feed network, the phase shift at each individual element is controlled separately through a phase shifter. In general, for an N-element phased array with a corporate feed network, to achieve inter-element of θ, maximum phase shift of *(N-1)θ* is required from phase shifters. Series feed networks are simpler, more compact and with lower feed line losses compared to parallel networks [85]. In a series-fed array the input signal, fed from one end of the feed network, is coupled serially to the antenna elements. Also the other end of the network is usually terminated with a matched load. In serially fed arrays, the phase shifters can be inserted either in parallel (Fig. 3.3) or in series along the feed line as depicted in Fig. 3.4, which demands a reduced phase shift for a given scan angle. In an *N*-element serially fed array, placing the phase

shifters in series rather than in parallel reduces the required amount of phase shift by a factor of (N-1) [34]. To further reduce the required amount of phase shift, such arrays can be bi-directionally fed, as shown in Fig. 3.5. Bi-directionally series-fed arrays have been implemented using both hybrid [79, 86] and integrated circuits [87]. The bidirectional series-fed phased array presented in [79] uses phase shifters having variable characteristic impedances that are adjusted according to the feeding direction. In [86], two different beams are formed by switching the source between the two opposite ends of a dual feed travelling patch antenna array. The authors in [87] combined a bi-directional series feed network with a parallel-fed architecture in order to reduce the required phase tuning range. Finally, the bi-directional fed series fed array presented in this chapter reduces the phase shift required for a given scan angle to half of the conventional series fed arrays illustrated in Fig 3.4. The detailed design of this phased array is given in the next section.

3.3 A New Bi-Directional Series-Fed Array to Reduce the Required Amount of Phase Shift

3.3.1 Bi-Directional Phased Array Overview

In this chapter, we propose a new bi-directional series-fed phased array approach that can reduce the required phase shift to half of the phase shift needed in the conventional serially fed arrays shown in Fig. 3.4. Furthermore, unlike the approach described in [79], the phased array presented here does not require any adjustment in the feed network as the feeding direction of the array is changed. The approach reported here allows the same phase shifter design to be used throughout the entire phased array substantially reducing array design complexity. Since a compact, low complexity phase
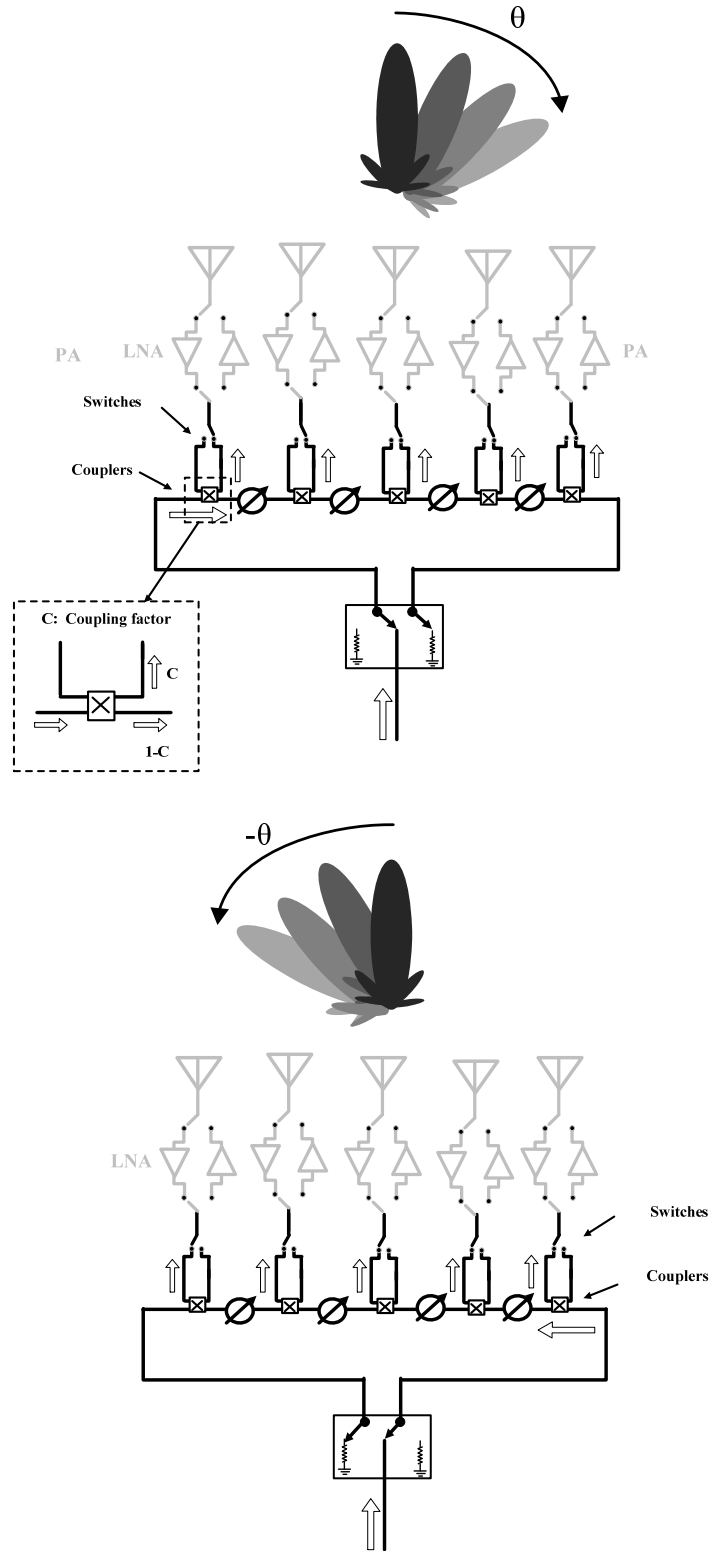
Fig 3.6. The new bidirectional phased array utilizes directional couplers, switches and phase shifters with a single control voltage to achieve beam steering.

shifter can be used throughout the array, array beam can be controlled by a single bias voltage, obviating the need for complex bias circuits. In the next section, the theory of bidirectional phased array is presented. In the following sections, the implementation and measurement results of an eight-element phased array designed based on the presented architecture are discussed.

3.3.2   Operation Theory of the Bi-directional Series-Fed Phased Array

A new bi-directional array composed of identical couplers and switches connected in tandem along with phase shifters is shown in Fig. 3.6. All of the phase shifters are identical and simultaneously tuned by a single control voltage through the feed network. By using a matched single pole, double throw (SPDT) switch, the array can be fed from either ends. If the phase shifters provide an inter-element phase shift ranging from 0 to θ, the array radiation beam can be steered from 0 to $\varphi_1 = arcsin(\theta/\pi)$ assuming that the array elements are $\lambda/2$ apart. When the feed direction is switched, the phase shifters provide an inter-element phase shift ranging from $-\theta$ to 0 allowing for the beam to be steered from 0 to $\varphi_2 = -arcsin(\theta/\pi)$. As a result, array beam can be steered by $2arcsin(\theta/\pi)$.

3.3.3   Bi-Directional Feed Network Design

As the array feed direction is switched, it is important to maintain the array directivity, beamwidth and side-lobe levels the same. In order to achieve this, all of the couplers used in the array are identical. Furthermore, using the identical couplers obviates the need to design each individual array element separately, thereby reducing design complexity. In order to determine the optimum coupling factor, its effect on the array
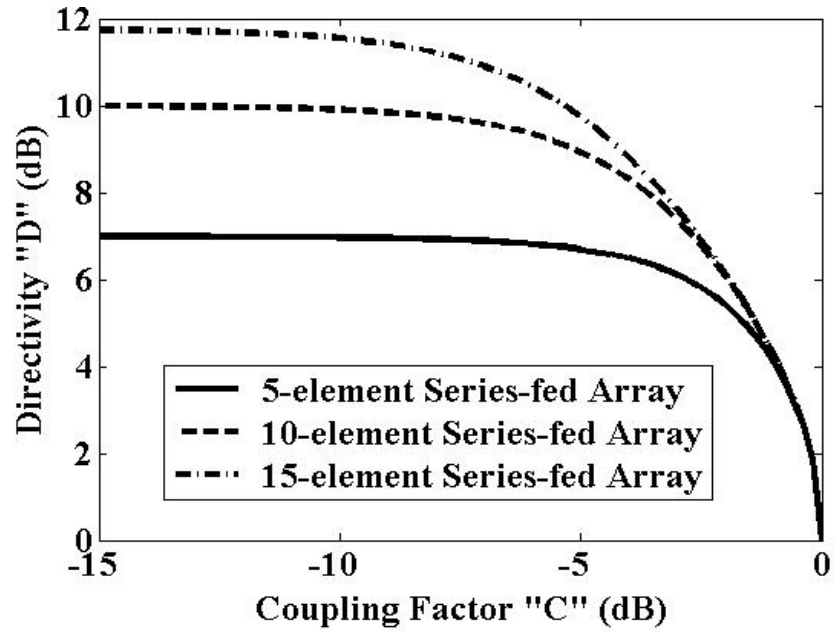
Fig 3.7. Array directivity versus the coupling factor for different array sizes
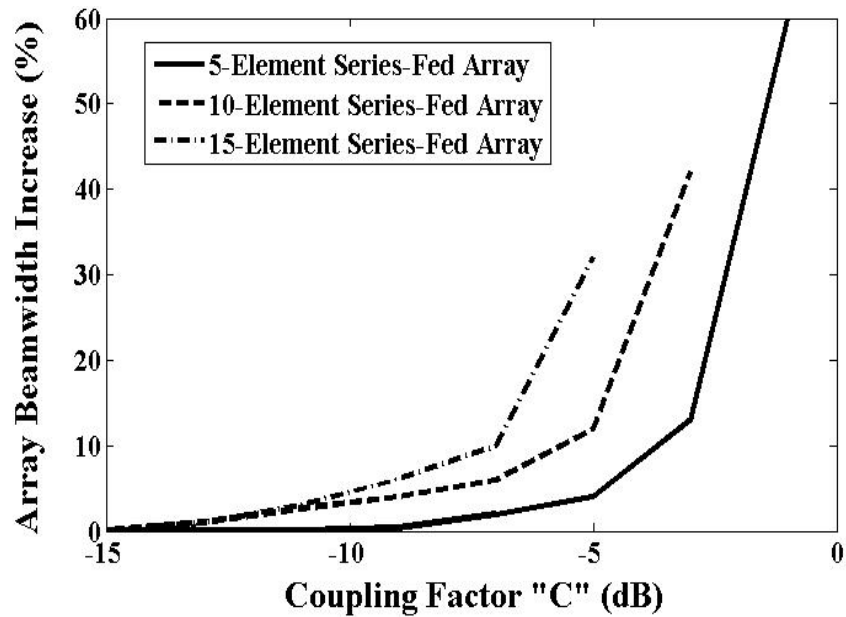
Fig 3.8. Increase in array beamwidth compared to a uniformly excited array versus the coupling factor for different array sizes

amplitude excitation is investigated. Assuming the phase shifters and the couplers are ideal and lossless and all the couplers have the same coupling factor *"C"*, the normalized signal level at each antenna element is given in Eqn. 3.1.

$$\bar{S}_n = (1 - C)^{n-1} C \qquad (3.1)$$

where *"n"* is the antenna element number.

According to Eqn. 3.1, the signal amplitude at each array element drops along the feed-line resulting in a linear amplitude tapering that affects the array directivity and beam-width. To investigate the effect of amplitude tapering on the array factor, the array directivity *"D"* has been calculated (2). As shown by (2), array directivity depends on the number of array elements *"N"* as well as the coupling factor *"C"*. The antenna elements here are assumed to be omnidirectional with $\lambda/2$ spacing.

$$D = \frac{C^{\frac{1}{2}}}{1-(1-C)^{\frac{1}{2}}} \left[\sqrt{\frac{1-(1-C)^{\frac{N}{2}}}{1+(1-C)^{\frac{N}{2}}}} \right] \qquad (3.2)$$

Based on Eqn. 3.2, directivity of a bidirectional array having 5, 10 and 15 elements versus the coupling factor *"C"* is plotted in Fig. 3.7. As can be seen, by reducing the coupling factor, one can improve the array directivity. This also mitigates the array beam broadening caused by amplitude tapering across the array (Fig. 3.8). At the same time, the power dissipated in the matched termination within SPDT switch increases as *"C"* is reduced. The relationship between the power dissipation normalized
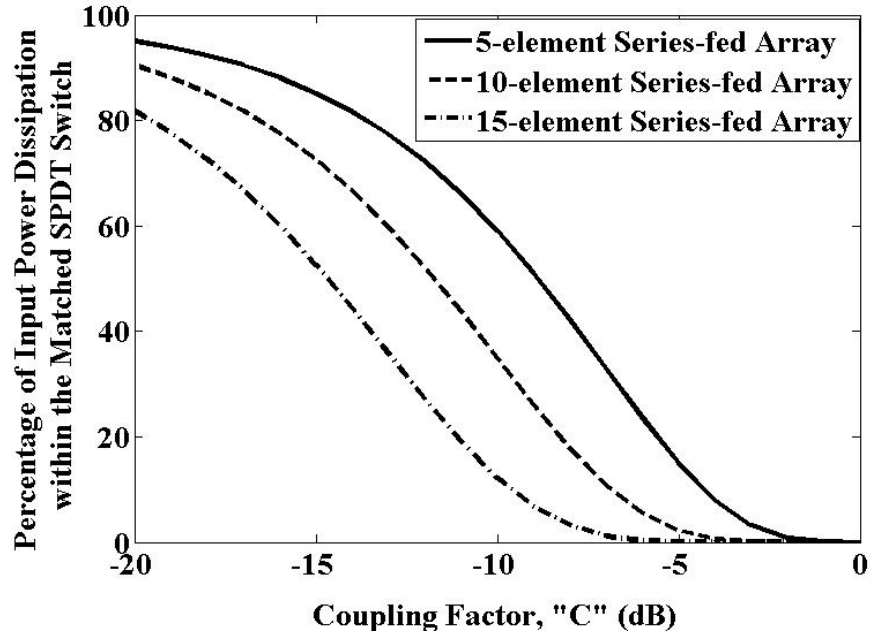
Fig 3.9. The percentage of input power dissipated within the matched SPDT switch versus the coupling factor for different array sizes

to the input *"P_{dis}"*, the coupling factor *"C"* and the number of array elements *"N"* is shown in Eqn. 3.3.

$$\bar{P}_{dis} = (1-C)^N \tag{3.3}$$

A plot of the dissipated power percentage as a function of the coupling factor *"C"* for various array sizes is given in Fig. 3.9. As can be seen, reducing coupling factor increases the power dissipated at the matched termination within the SPDT switch at the input to the array.

When determining the size of bidirectional array to meet a certain directivity goal, the dissipated power *"P_{dis}"* should be also taken into account. In general, one can use

83
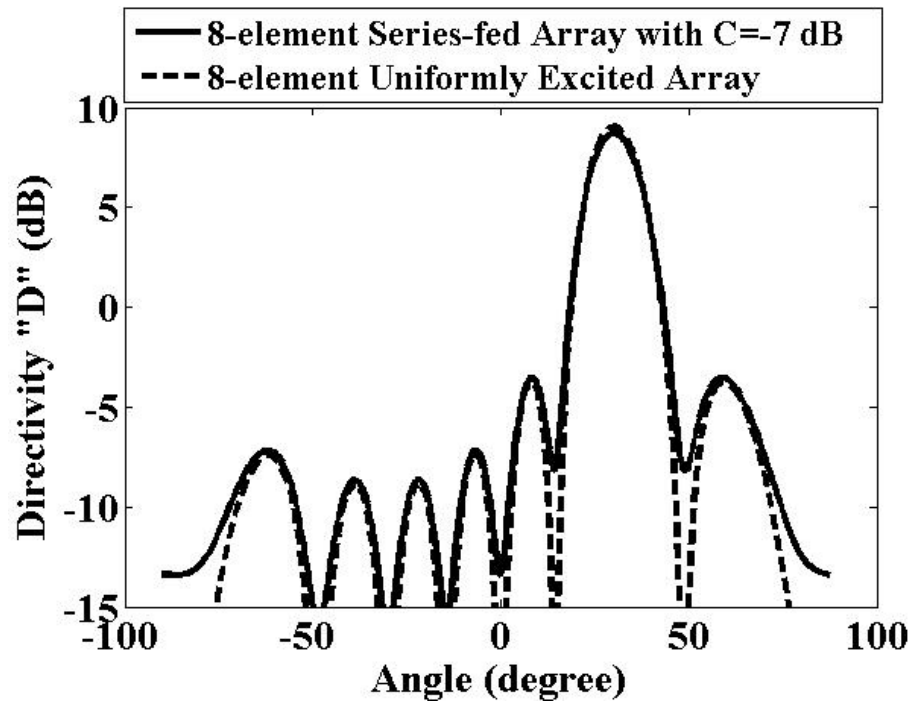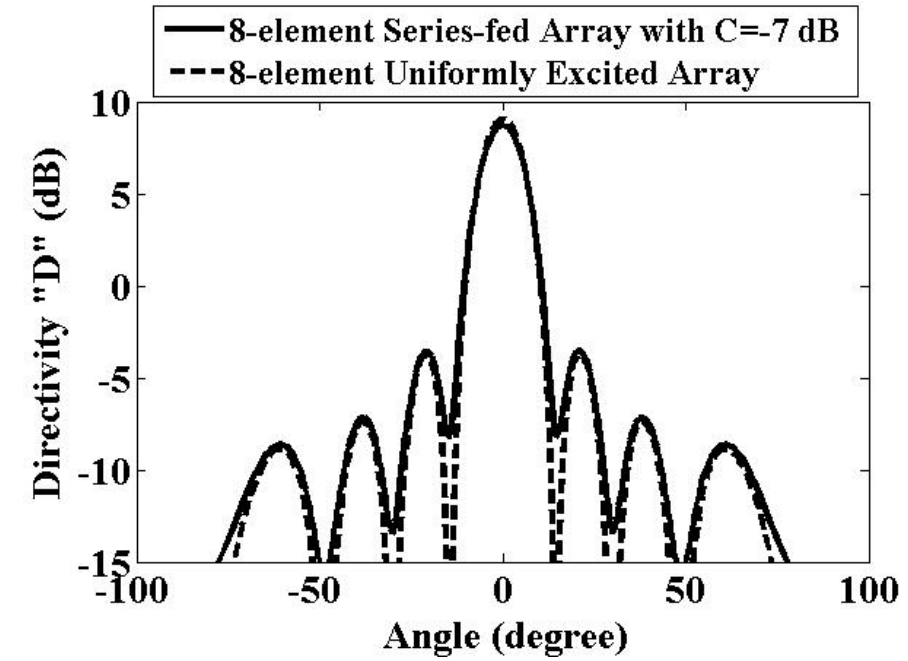
Fig 3.10. Directivity of an eight-element series-fed array compared to an eight-element uniformly excited array at (a) scan angle of zero and (b) scan angle of thirty degrees.
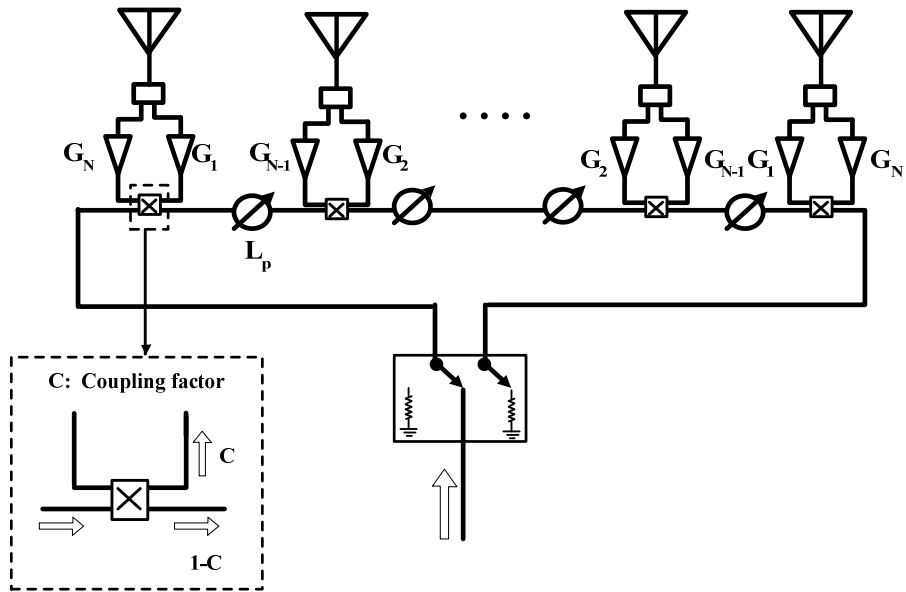
Fig 3.11. Amplifier can be used in the receive phased array to achieve a particular amplitude tapering
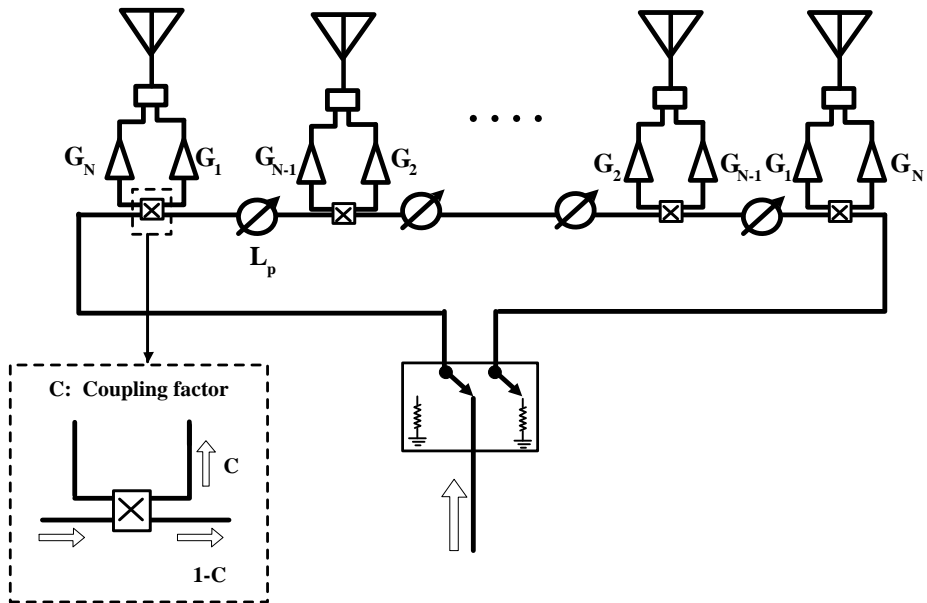
Fig 3.12. Amplifier can be used in the transmit phased array to achieve a particular amplitude tapering

Fig. 6 to determine the numbers of array elements and a range of coupling factors to achieve a required directivity. Subsequently, based on Fig. 3.9, the minimum number of array elements can be chosen to maintain the dissipated power below a target goal. It can be shown that by appropriately choosing the coupling factor; one can achieve a directivity similar to that of a uniformly excited array using the same number of array elements while less than 15% of the input power is dissipated within the matched SPDT switch.

For the eight-element phased array presented in this paper, the coupling factor is set to -7 dB. In this case 15% of the input power is dissipated in the SPDT termination. The array factors for this design compared to a uniformly excited eight-element array for scan angles of zero and thirty degrees are shown in Fig. 3.10. As can be seen, the difference between the patterns is negligible. Therefore, by selecting an appropriate coupling factor, one can achieve a radiation pattern which is very close to the theoretical pattern for a uniformly excited array with the same number of array elements.

It should be noted that the emphasis of this chapter is only on the power distribution and phase shifting. The phased array can contain low noise amplifiers and power amplifiers as depicted in Fig. 5. Therefore, the performance of LNAs and PAs ultimately should be considered to determine the dynamic range and efficiency of the overall array.

Different amplitude tapering may be required across the array to meet a particular sidelobe level requirement. Amplifiers can be used in the array for receive mode (Fig. 3.11) and transmit mode (Fig. 3.12) to achieve any amplitude tapering desired. Using

amplifiers also allows for compensating the effect of phase shifter insertion loss on the array factor. In general, if array amplitude tapering of $a_1 \ldots a_n$ is desired across the array, gain for array element n, G_n, can be calculated according to Eqn. 3.4 assuming the gain of the first element to be G_1 (shown in Fig. 3.11 and Fig. 3.12).

$$\frac{G_n}{G_1} = [\frac{L_p}{1-C}]^{n-1}(\frac{a_n}{a_1}) \tag{4}$$

where L_p is the insertion loss through the phase shifter.

3.4   A New Phase Shifter Design

One of the key and essential components of most of phased arrays is phase shifter. As mentioned before, a major complexity of phased array is attributed to the phase shifters required. Furthermore, performance of phase shifters used in the phased array significantly affects the performance of the entire phased array. Critical parameters in phase shifter design are phase tuning range, RF insertion loss, variation of insertion loss versus phase shift, power handling and bandwidth [88]. In the next section, a brief overview of common approaches to design phase shifter will be given. In the following section, design of a new compact phase shifter for the use in bi-directional phased array will be discussed.
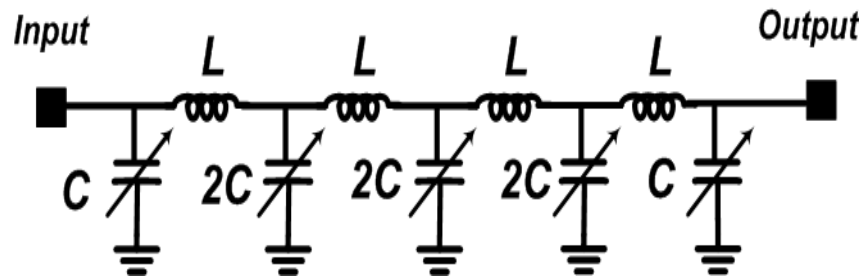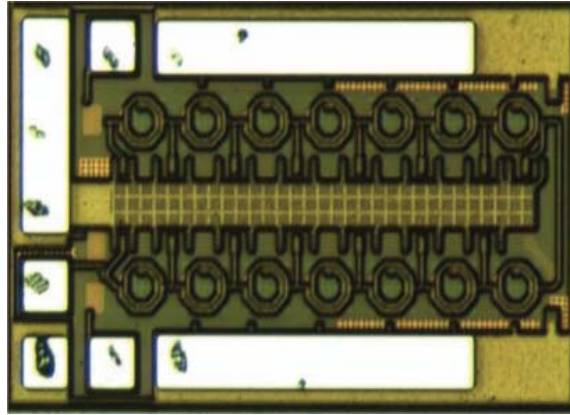
Fig 3.13. A photograph and general diagram of loaded transmission line phase shifter

3.4.1 Overview of Common Phase Shifter Design Approaches

A variety of phase shifters have been investigated for use in phased arrays. The most comment approaches to design phase shifters are based on a varactor loaded line, reflective type, vector modulated or switch based phase shifters. In varactor loaded transmission line design, the electrical length of the line is varied by tuning the varactors (Fig. 3.13). Various varactor technologies have been used in this type of phase shifters including MEMS varactors [89-91], BST varactors [92-94] or solid state varactors [95-97]. Reflective type of phase shifter is shown in Fig. 3.14. In this type of phase shifter, a
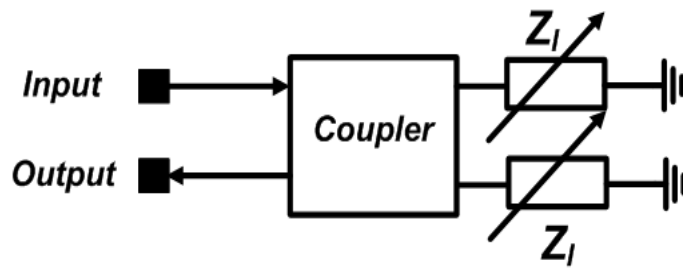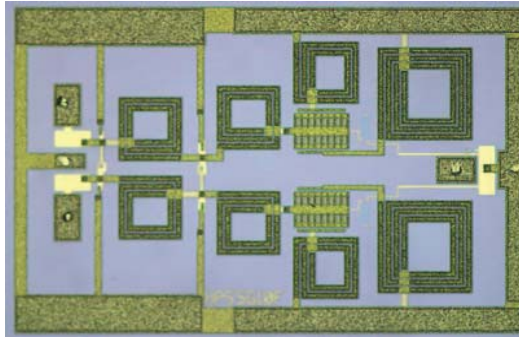
Fig 3.14. A photograph and general diagram of reflective type phase shifter
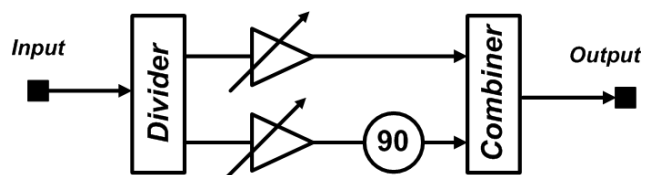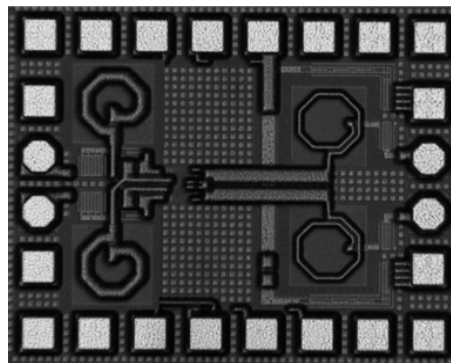
Fig 3.15. A photograph and general diagram of vector modulated phase shifter
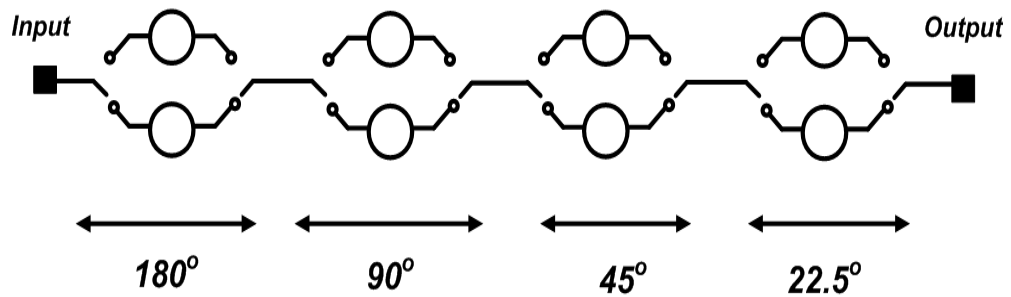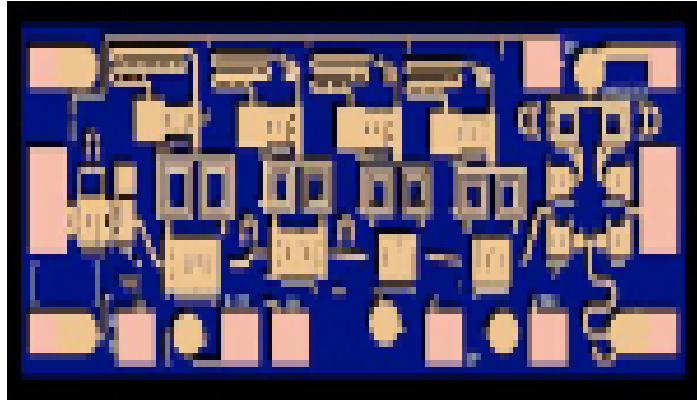
Fig 3.16. A photograph and general diagram of switch line phase shifter

circulator or a couple is terminated with tunable reactances (Fig. 3.14). Tunable

reactances reflect the incident signal with a phase shift which depends on the value of the

reactance. The amount of phase shift can be tuned by using varactors to change the value

of reactance. Vector modulated phase shifter is another type of phase shifter that is

mainly used for integrated circuits (Fig. 3.15). In this phase shifter, signal is divided into

two paths with different gains and 90 degree phase difference. The signal at the output is

the vector sum of the two signals. It can be shown that the phase of the output signal

depends on the amplitude ratio of the two signals. Therefore, by tuning the amplitude

$Y_0 - jB$ Y_0

V_{out} jX V_{in}

jB jB

Y_0 $Y_0 + jB$
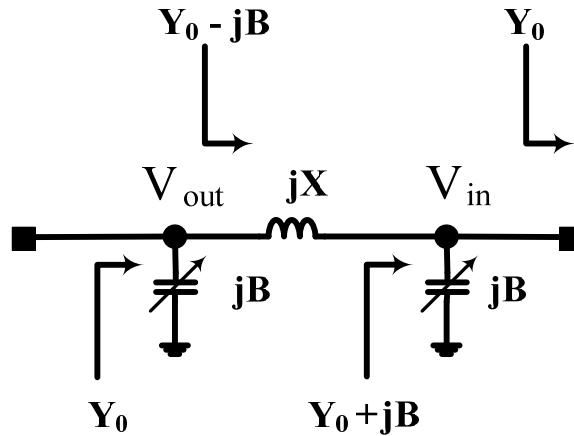
Fig 3.17. The circuit diagram of the phase shifter.

ratio of the two signals, the phase of overall signal can be tuned. Switch based phase

shifters use switches to select different phase delays (Fig. 3.16). The phase delays can be

implemented based either on distributed or lumped elements.

3.4.2 Phase Shifter Design

The phase shifter used in the array is designed based on the extended resonance

technique as shown in Fig. 3.17 [98]. The phase shifter is assumed to be matched to

$Z_0=1/Y_0$. A varactor with a susceptance jB is connected in shunt at the input node. The

admittance seen at this node, Y_0+jB, is then transformed to its conjugate value, Y_0-jB, by

using a series reactance jX. The inductive value can be calculated based on Eqn. 3.5.

Finally, a similar varactor jB is added in shunt to cancel out the imaginary part of the

impedance.

91
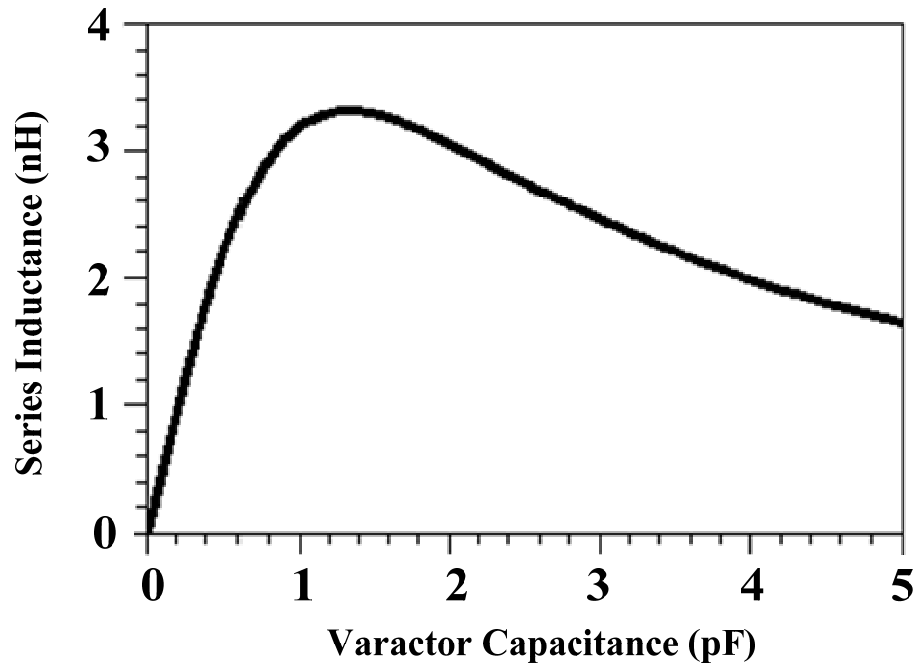
Fig 3.18. The required series inductance versus the varactor capacitance to maintain the same voltage amplitude at the input and the output node

$$X = \frac{2B}{Y_0^2 + B^2} \tag{5}$$

Analysis of the circuit shows that for a fixed value of *"B"* the voltage at the input node, V_{in}, and the voltage at the output node, V_{out}, have the same magnitudes but are different in phase. The phase difference between V_{out} and V_{in} is given by Eqn 3.6.

$$\Delta\theta = 2\arctan(\frac{B}{Y_0}) \tag{6}$$

92
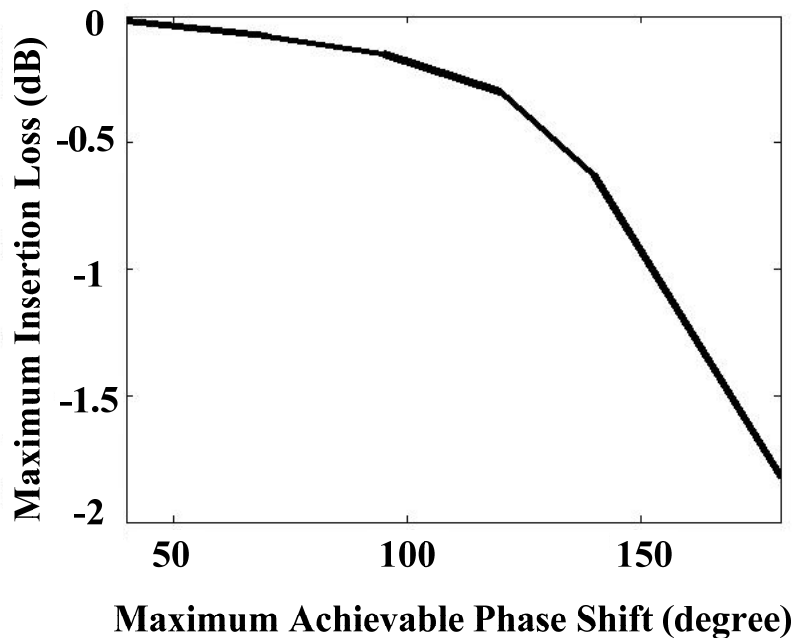
Fig 3.19. Maximum insertion loss versus maximum achievable phase shift when a fixed reactance value is used.

In order to vary the phase shift, the susceptance jB is tuned by controlling the varactor bias voltage. In general, as the varactors are tuned, the series reactance jX should also be tuned to maintain the voltage magnitude at the nodes V_{out} and V_{in} the same. However, for simplicity's sake, the jX can be fixed at a value that allows the variation of the amplitude ratio of the output voltage, V_{out}, to the input voltage, V_{in} to be minimized. For a 2.4 GHz phase shifter with the characteristics impedance of 50 ohm, the required series inductance versus the capacitance of varactor is plotted in Fig. 3.18. As can be seen, at the point where the slope of the graph is zero, the required variation of inductance versus varactor capacitance is minimal. Therefore, by choosing this optimum value of series inductance, the variation of voltage amplitude ratio for
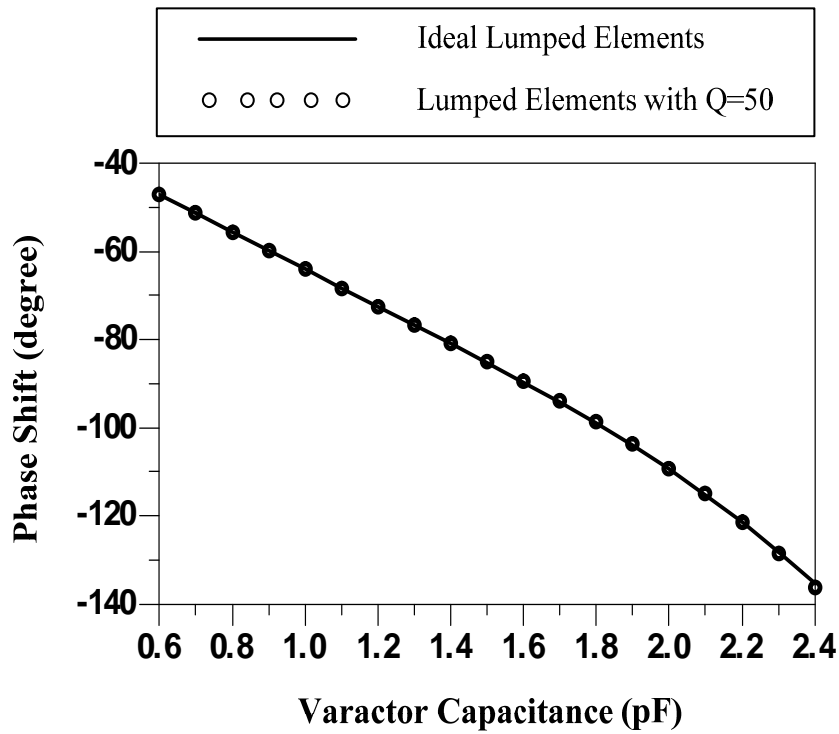
Fig 3.20. Simulated phase shift through the phase shifter.

nodes V_{out} and V_{in} is minimal. In general, the optimum value of series reactance jX_{opt} can be calculated as Eqn. 3.7.

$$X_{opt} = \omega L_{opt} = \frac{1}{Y_0} \qquad (7)$$

Phase shifters with different varactors are designed using the corresponding optimum reactance given by Eqn. 3.7. The maximum phase shifter insertion loss within the tuning range of varactor capacitance versus the maximum achievable phase shift is shown in Fig. 3.19. As expected, as the maximum phase shift is

94
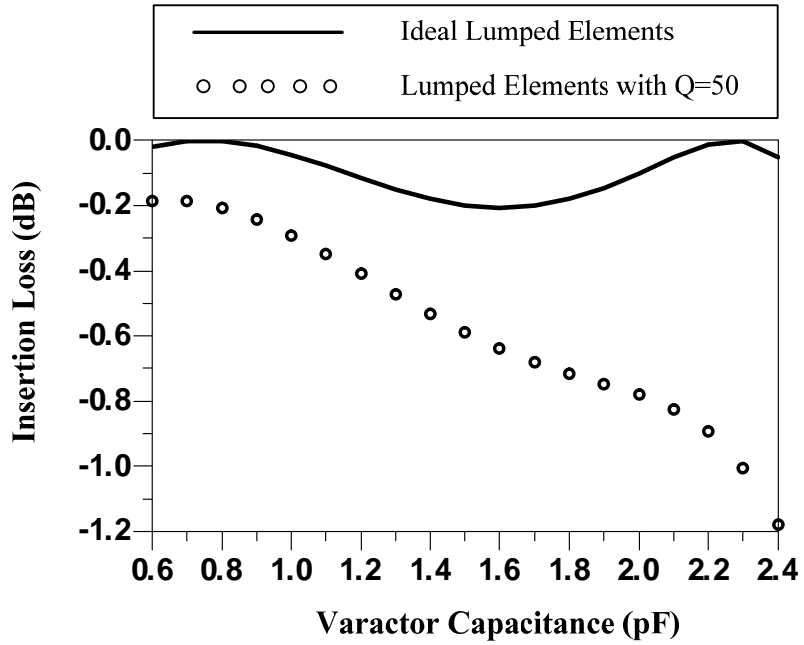
Fig 3.21. Simulated insertion loss through the phase shifter
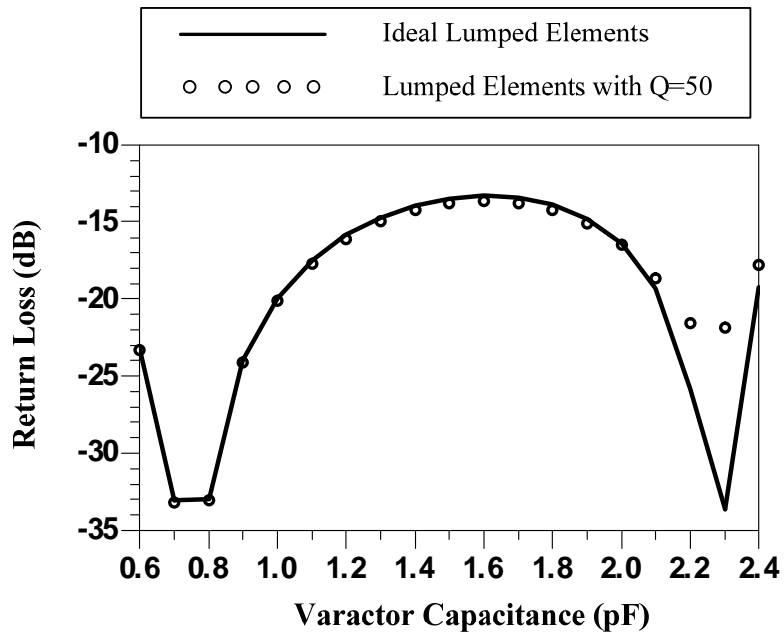
Fig 3.22. Simulated return loss of the phase shifter.
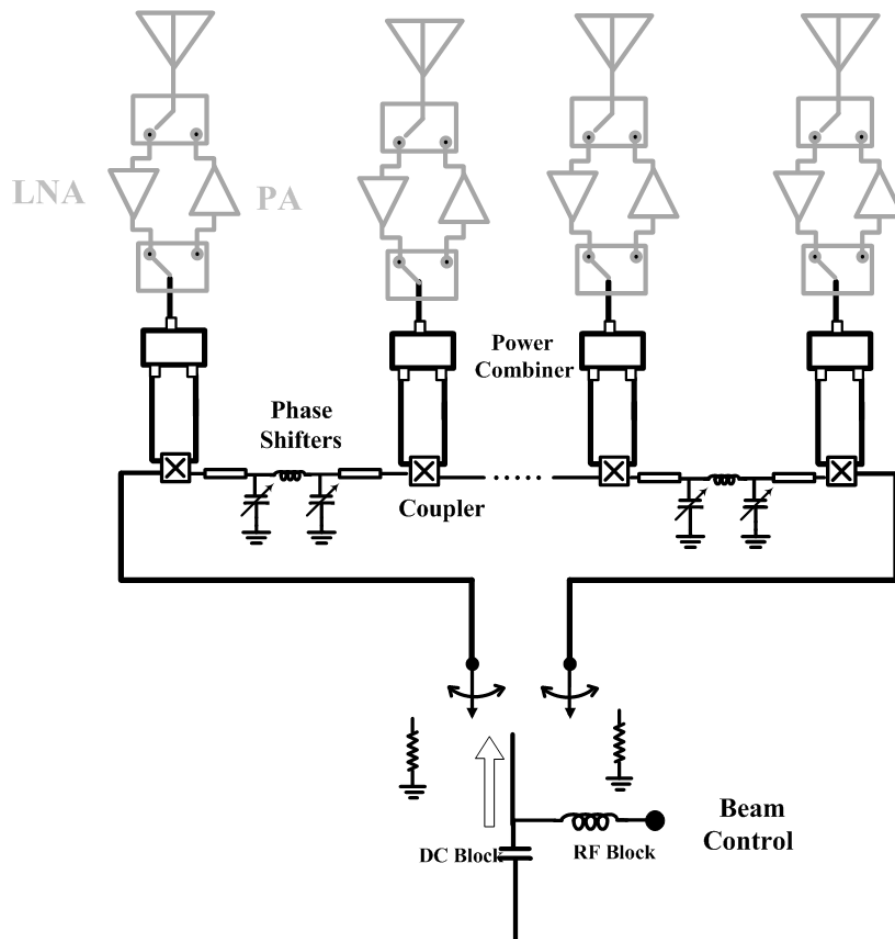
Fig 3.23. A single voltage applied to the bias network at the input controls the phase shift across the entire phased array

increased, the maximum insertion loss due to fixing the value of series reactance increases as well.

Based on the design procedure described, a phase shifter is implemented using varactor diodes and a lumped inductor at 2.4 GHz. The varactor capacitance used in the design is tuned from 0.6 to 2.4 pF with the inductor value of 2.1 nH. The phase shift through the phase shifter has been simulated both with ideal element as well as lumped

96
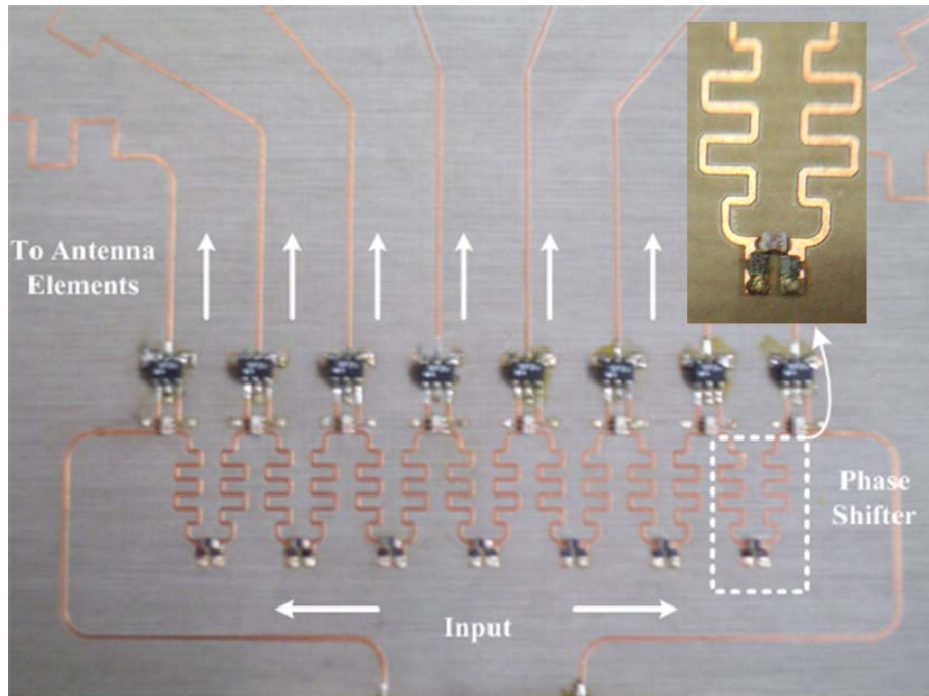
Fig 3.24. A Photograph of the eight-element bidirectional phased array operating at 2.4 GHz

elements with $Q = 50$ (Fig. 3.20). The phase shift through the phase shifter can then be

tuned approximately from -45 to -150 degrees. The loss through the phase shift has also

been simulated (Fig. 3.21). The loss through the phase shifter due to the mismatch

doesn't exceed 0.2 dB over the entire range. When varactor diodes and inductors with a

finite quality factor ($Q = 50$) are used, the maximum insertion loss increases to 1.2 dB. In

this case, the return loss is maintained below -15 dB in the entire tuning range. (Fig.

3.21).

In order to utilize this phase shifter in the design of the bidirectional phased array,

a fixed delay is introduced at each phase shifter by inserting two transmission lines as
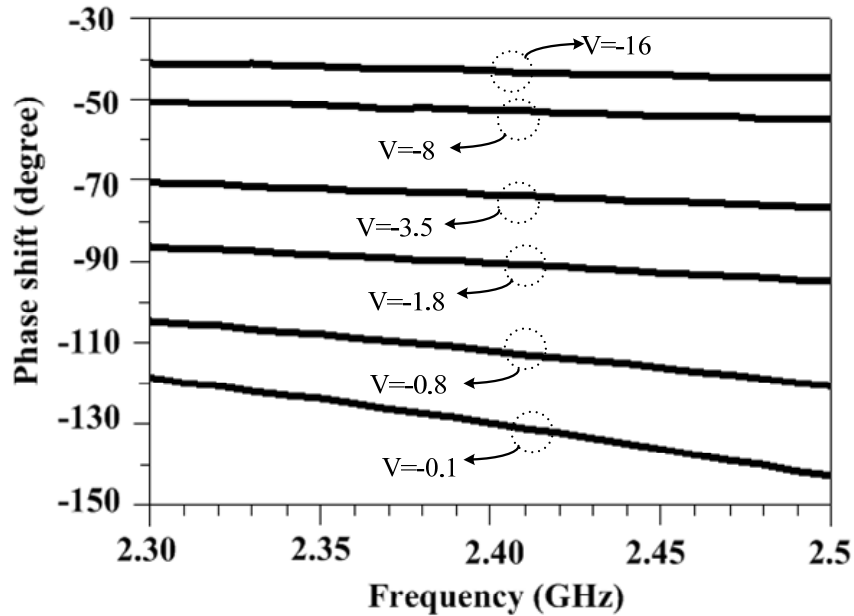
Fig 3.25. Measured phase shift through the phase shifter versus frequency for different control voltages.

shown in Fig. 3.23. The phase shift across the entire array is controlled through the bias circuit at the input to the bidirectional array (Fig. 3.23).

3.5 Fabrication and Measurement Results

An eight-element phased array at 2.4 GHz is designed and fabricated on Rogers RO4003C with a dielectric constant of 3.55 and a thickness of 8 mils (Fig. 3.24). The surface-mount couplers CP0805A2442BW from AVX with a coupling factor of 10 dB are used in the design. The surface-mount power combiners from Mini-circuits (SP-2U2+) combine the power from the output ports of the couplers.
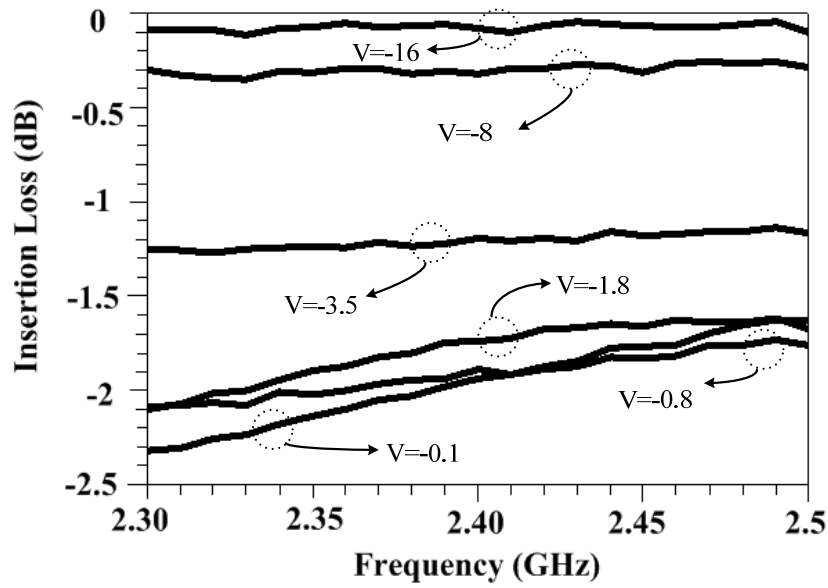
Fig 3.26. Measured insertion loss through the phase shifter versus frequency for different control voltages
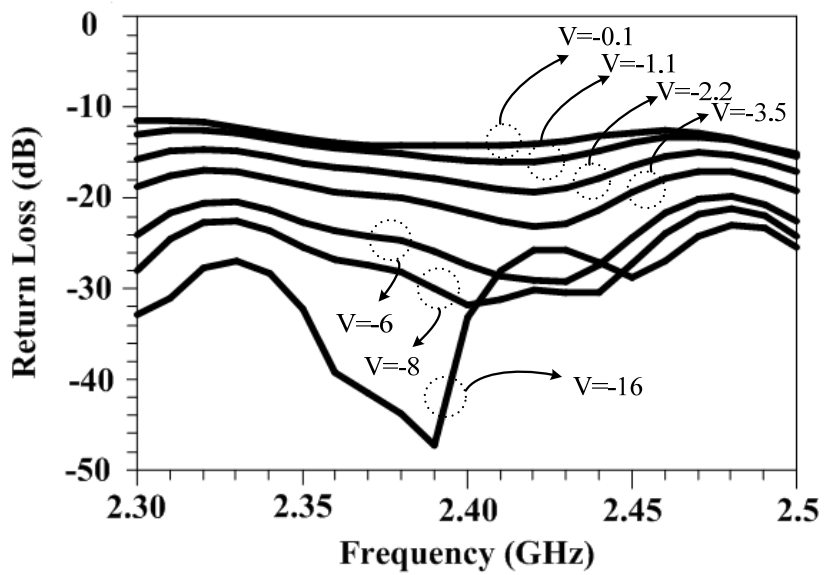
Fig 3.27. Measured return loss of the phase shifter versus frequency for different control voltages

Measured
──────

Simulation
‑ ‑ ‑ ‑ ‑ ‑

Scan angle of +/- 30 degrees

Measured
──────

Simulation
‑ ‑ ‑ ‑ ‑ ‑

Scan angle of +/- 15 degrees
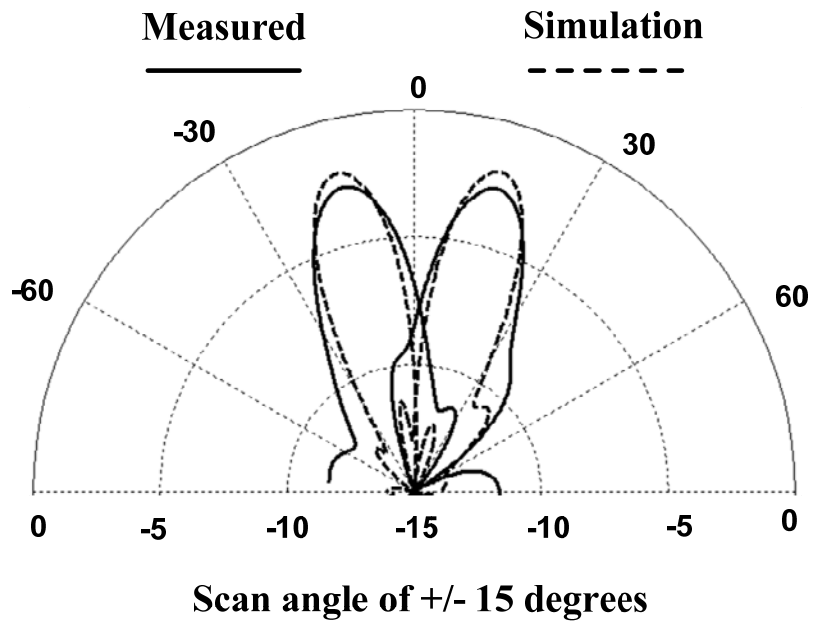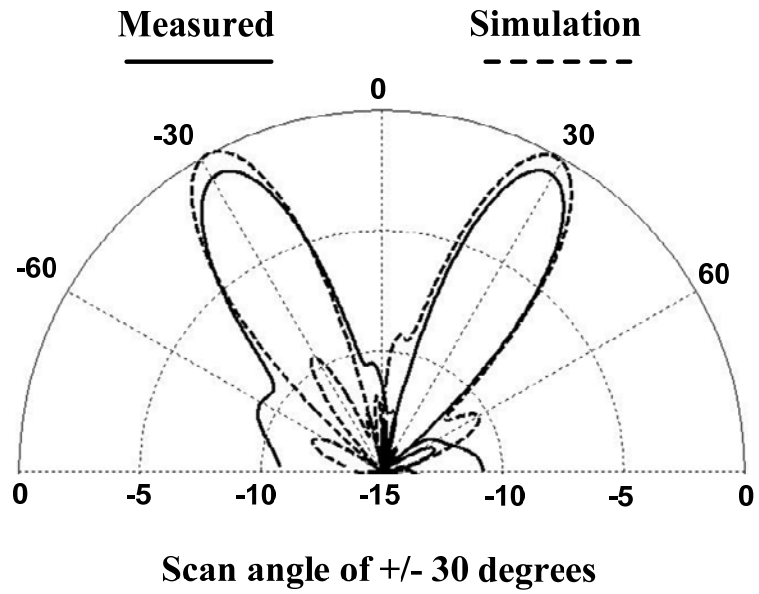
Fig 3.28. Comparison between the measured and simulated array factors for the eight-element phased array
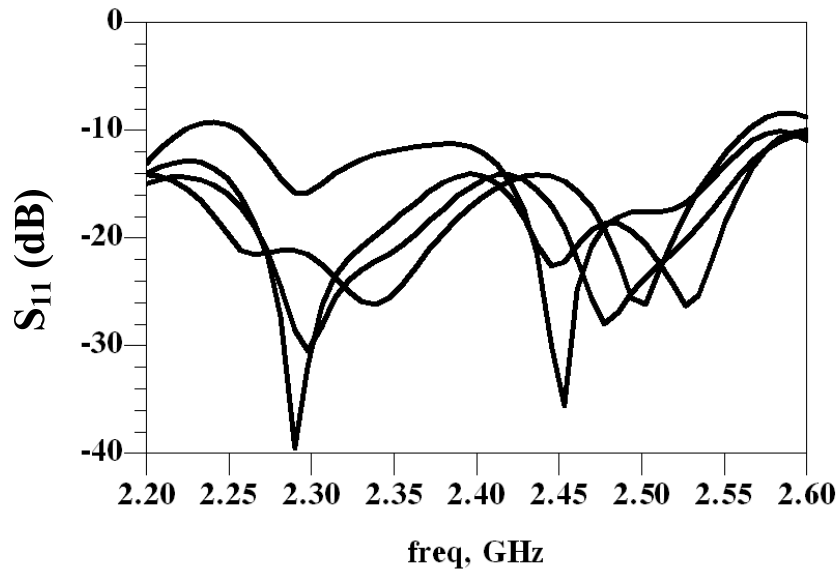
Fig 3.29. Input return-loss for different bias voltages

The phase shifter used in the design is fabricated and measured separately. The varactor diode used in the phase shifter is MA46H120 from MA/COM with a tunability of 4:1 and quality factor of 50 at the bias voltage of 12 volts and the design frequency. Two varactor diodes are placed in shunt to provide a capacitance tuning range of 0.6 pF to 2.4 pF as the bias voltage is varied from -0.1 volts to -16 volts. The lumped inductor used in the design is 0403HQ-2N1XJL from Coilcraft with an inductance value of 2.1 nH and a quality factor of 80 at the design frequency. A single bias voltage from 0.1 to 16 volts is used to tune the capacitance of the varactors. The measured phase shift versus frequency is shown in Fig. 3.25. As can be seen, the measured phase shift through the phase shifter can be tuned from -40 to -130 degrees, while its insertion loss varies from 0.2 dB to 1.8 dB over the tuning range (Fig. 3.26). The phase shifter return loss also remains below 15 dB within the entire tuning range (Fig. 3.27).

101

The array beam is controlled by a single bias voltage applied at the input to the phased array. The S-parameters for the entire are measured as a function of varactors bias voltage with the input signal switched between the two directions. The corresponding array factors are then calculated assuming a linear array with $\lambda/2$ antenna spacing. A scan angle of 60 degrees has been achieved as the tuning voltage is varied from -0.1 to -16 volts. The calculated array factors for scan angle of +/- 15 degrees and +/-30 degrees are compared with the simulated results in Fig. 3.28. The 3-dB beamwidth is 17 degrees at scan angle of 15 degrees and 14 degrees at the scan angle of 30 degrees while the side-lobes are maintained at approximately below -10 dB. Based on the measurement result, the input reflection coefficient S_{11} at the design frequency is better than -10 dB over the entire scan range. As shown in Fig. 3.29, the reflection coefficient is maintained below -10 dB within a bandwidth of approximately 400 MHz corresponding to a fractional bandwidth of 17%.

Table 3.1 summarizes the performance of the proposed phased array against other series-fed steerable arrays presented in the literature. The proposed antenna array achieves a much wider electronic scan-angle range compared to the designs shown in Table 3.1. The design proposed in [85] can achieve a comparable scan range at the price of 13 dB array gain variation, whereas, the bi-directional series-fed phased array demonstrates a gain variation of 2.7 dB in the entire scan range. Furthermore, the bi-directional series-fed phased array requires only one tuning voltage to control the phased array beam. The return loss bandwidth of the bi-directional phased array described here is much broader than any of the other designs.

TABLE 3.1
Comparison between the bi-directional series-fed phased array presented in this chapter and the
published series-fed phased arrays

	[79]	[80, 81]	[82]	[52]	[83]	**The Presented Phased Array**
Number of antenna elements	4 elements	5 elements	30 leaky wave	4 elements	4 elements	**8 elements**
Center frequency	2.45 GHz	5.8 GHz	3.33 GHz	2 GHz	2.4 GHz	**2.4 GHz**
Scan Range	30 degrees	22 degrees	60 degrees	20 degrees	49 degrees	**60 degrees**
Number of tuning voltages	6	1	1	4	3	**1**
Return loss bandwidth	1.02%	4.6%	NA	NA	3%	**17%**
Gain variation within scan range	NA	0.4 dB	13 dB	1.8 dB	1.5 dB	**2.7 dB**

3.6 Conclusion

A new series fed bi-directional phased array is reported. The phased array uses a bi-directional series feed network to reduce the required phase tuning range. As the result, complexity of the phase shifters required in the array can be reduced resulting in overall phased array cost and complexity reduction. A review of different topologies of phased array and the required phase shift is given in this chapter. The operation theory of the bi-directional phased array is discussed and the required phase shift for a given scan range is determined. A general design procedure for a bidirectional phased array feed network is presented and effect of design parameters on the array factor is discussed. Moreover,

review of common approaches to design phase shifters are given in this chapter and a new, compact phase shifter is designed and utilized in the phased array. The phase shifter has been fabricated and measured. The overall phased array architecture allows one to steer the radiation beam by a single control voltage obviating the need for complex bias circuits. An eight-element phased array based on the presented design is fabricated and tested. The agreement of the measured results with the simulation verifies the design.

Chapter 4

A Novel Design of Low Complexity Phased Arrays

4.1 Introduction

In this chapter, we propose a new approach to the design phased arrays with low complexity. Unlike the conventional design of phased arrays requiring a separate phase shifter for each antenna element (Fig. 4.1), in the proposed design, the phase progression across the antenna elements can be controlled by using only a single phase shifter (Fig. 4.2). As a result, the cost and complexity of the phased arrays can be significantly reduced based on this design. The proposed phased array is composed of couplers, amplifying stages, power dividers and two phase shifters. The phase shifters are placed at the two opposite ends of a serially fed array. In the next sections the proposed design of the phased array is discussed. Finally in the last section, the implementation and measurement results for an eight-element phased array operating at 2 GHz are presented.
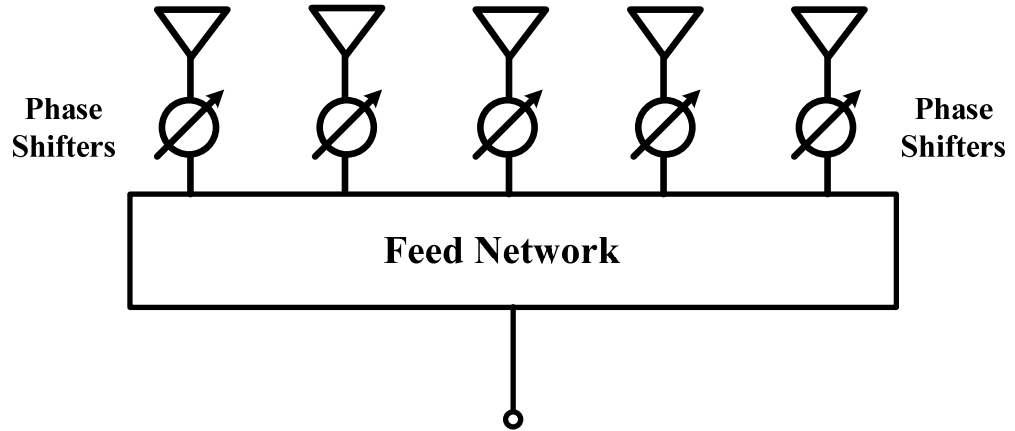
Fig. 4.1. Conventional design of phased arrays requires a separate phase shifter for each antenna
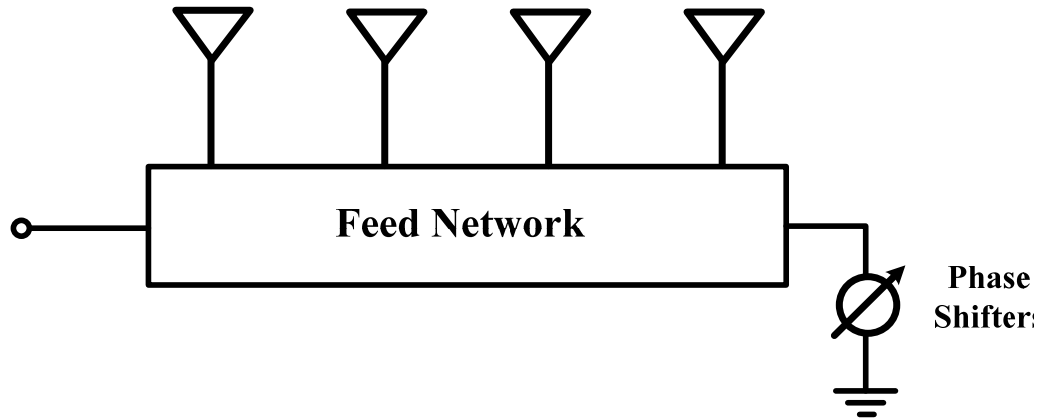
Fig. 4.2. The proposed phased array design requires a single phase shifter placed at the opposite end of a serially excited antenna array to the input

4.2　The Concept for a phased array with only a single phase shifter

In most of the existing phased array designs, the phase of the signal at each antenna element is separately controlled by a phase shifter. However, in the presented approach, the phase of signals in the entire phased array can be controlled by a single phase shifter. The block diagram shown in Fig. 4.3 illustrates the concept of the proposed approach. The signal at each radiating-element is the vector sum of two signal components, a_i and b_i provided by distributing the input signal through two feed networks with unequal power division. The signals across each feed network are in phase while the phase difference between the two signal paths is controlled by a single phase shifter. The signal phase shift at each radiating element depends on the phase and amplitude ratio of the two signal components a_i and b_i at each radiating element. The phase shift θ_i at antenna element E_i is given by:

$$\theta_i = \arctan\left(\frac{Sin\phi}{\dfrac{a_i}{b_i} + Cos\phi}\right) \tag{4.1}$$

where Φ is the signal phase shift through the phase shifter as shown in Fig. 4.3
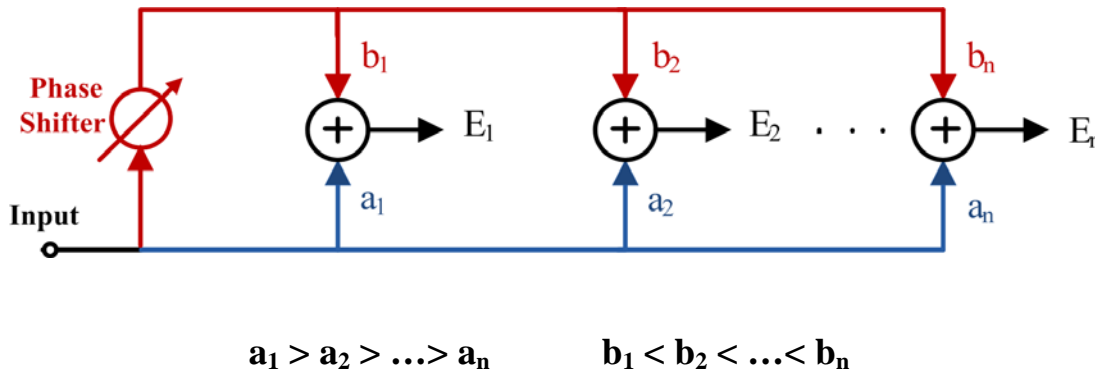
Fig. 4.3. The block diagram of phased arrays based on the proposed approach requiring a single phase shifter throughout the entire phased array
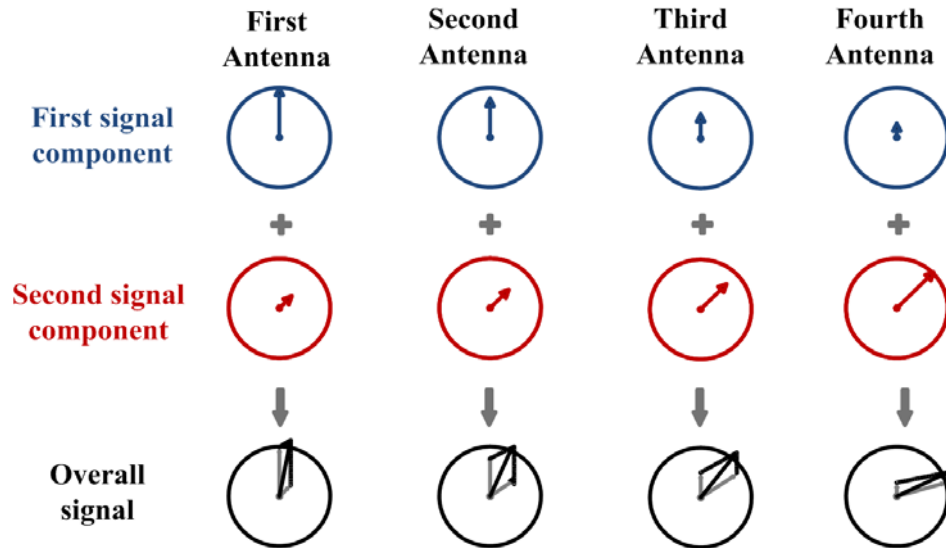
Fig. 4.4. Phase progression in the entire array can be controlled by tuning the phase of one component of the signals at the antenna elements

Based on Eqn. 4.1, the phase shift at each antenna element Φ_i is a function of a_i/b_i. Therefore, by providing different amplitude ratios for a_i and b_i, a different phase
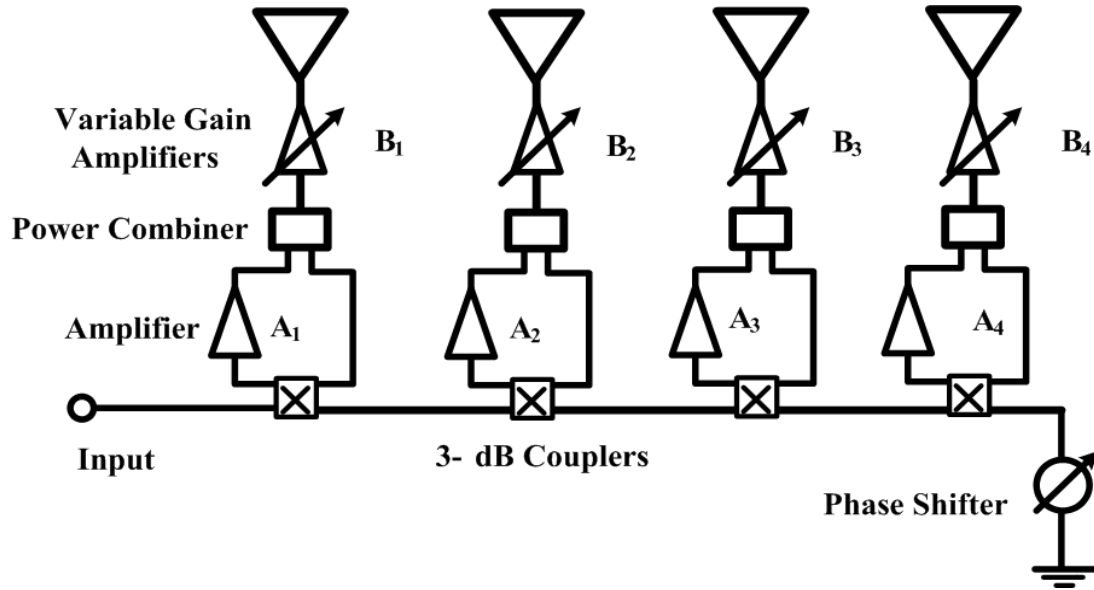
Fig. 4.5. The block diagram of phased arrays based on the proposed approach requiring a single phase shifter throughout the entire phased array

shift can be achieved across the array with a single phase shifter. The amplitude ratio for the two signals at each array element can be determined to provide an appropriate phase progression across the array. In this design, the first signal component fed into each antenna element progressively decreases, while the second signal component progressively increases across the array. The vector diagram shown in Fig. 4.4 illustrates how the phase progression is achieved across the phased array.

The maximum achievable scan angle θ_{max} in phased arrays designed based on this approach can be approximated using Eqn. 4.2. The equation is derived assuming the phase shifter can provide a maximum phase shift of 360 degrees. Therefore, the maximum inter-element phase shift can be determined by splitting the maximum achievable phase shift from phase shifter by the number of array elements.

$$\theta_{max} = \frac{180}{\pi} a\,sin(\frac{2}{N})$$

(4.2)

N is the number of antenna elements.

As can be seen, the maximum achievable scan range is dependent on the number of antenna elements used in the array. As the number of antenna elements increases, the maximum scan range decreases. For applications where a wide scan range is not needed, the presented method can be exploited to substantially reduce the number of phase shifters. For example, long range automotive radars for automatic cruise control or pre-crash warning systems require radiation beams as narrow as 3 degrees which should be steered within 15 degrees around the broadside. In order to achieve such a beamwidth, at least 24 antenna elements are needed to be used in the design of phased array. Based on Eqn. 4.2, to achieve 15 degrees of scan angle, one phase shifter is required for each 9 antenna elements. Assuming the modular approach introduced in the chapter 2 can be used, it means 3 phase shifters are required for the entire phased array designed based on the presented approach. A low number of phase shifters required compared to the conventional phased array designs which usually require a single phase shifter per each antenna element renders this approach as a promising solution for the design of long range automotive radars.

The single phase shifter phased array design methodology presented here is general and can be exploited to construct both active as well as passive phased arrays. Furthermore, both receive mode and transmit mode phased arrays can be realized based on the presented approach.
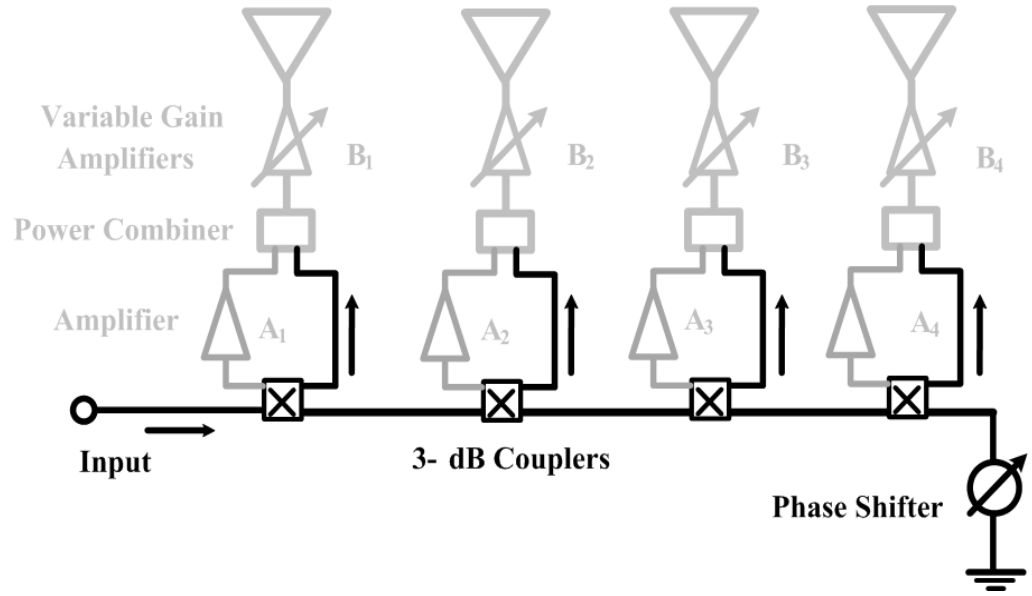
Fig. 4.6. The first signal components are achieved as the signal is traveling away from input
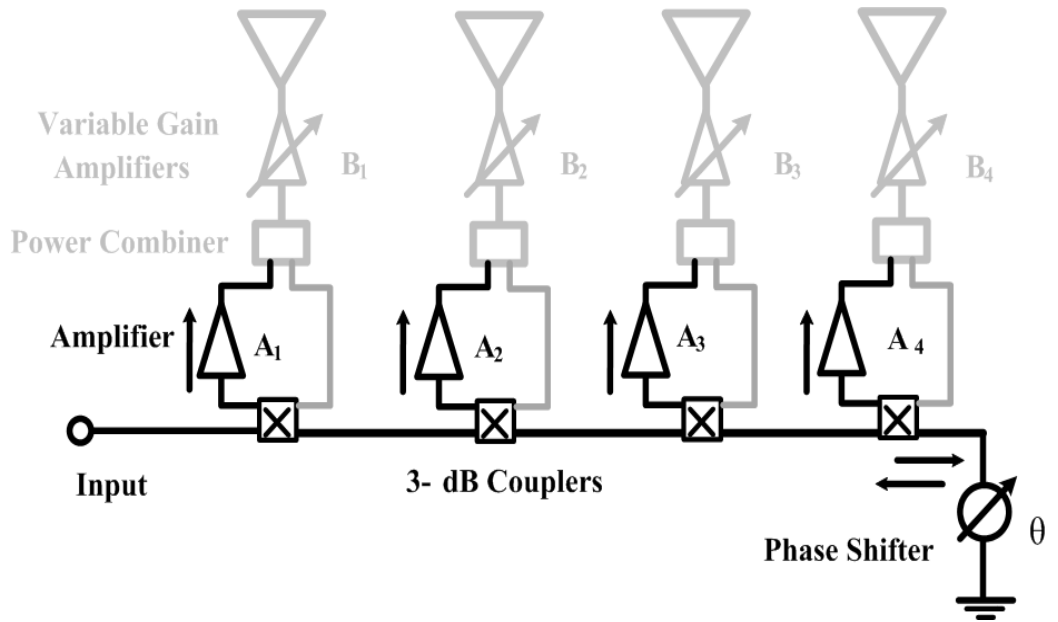
Fig. 4.7. The second signal components are achieved as the phase shifted signal is reflected back into the feed network

111
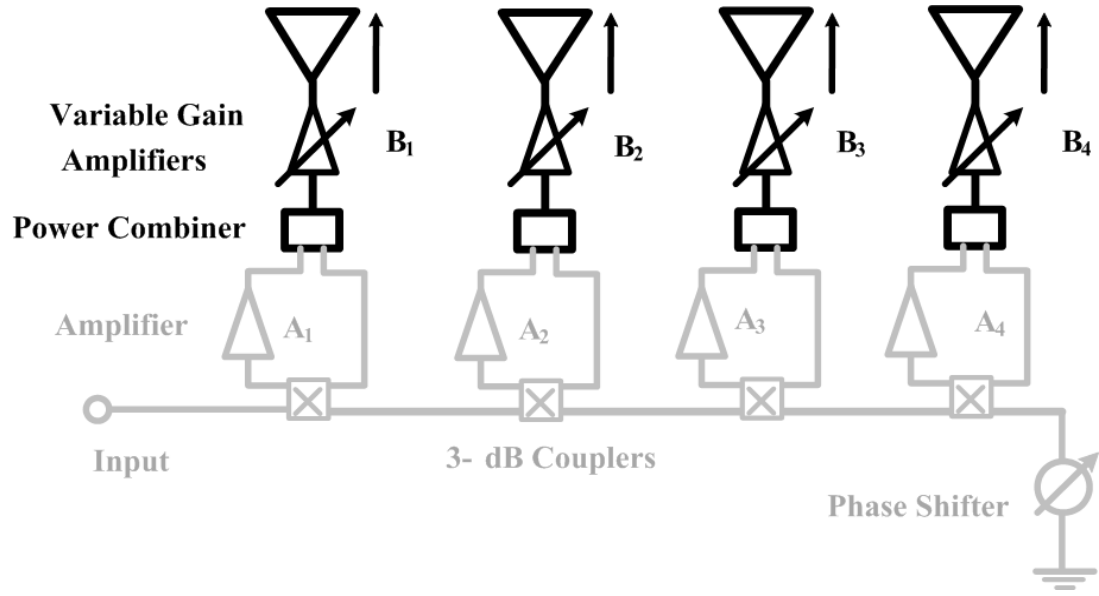
Fig. 4.8. The overall signal the each antenna element is achieved by combining two signal components
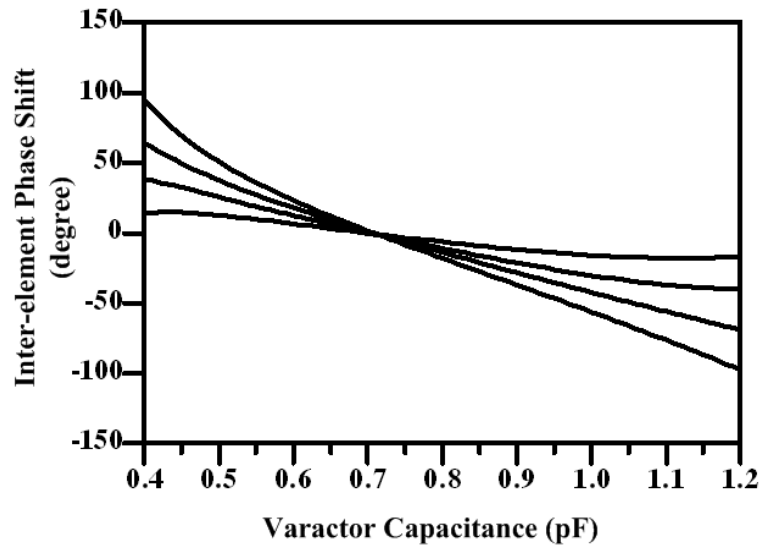
Fig. 4.9. Approximately linear phase progressing can be achieved across the array

One circuit implementation of the presented approach is discussed in the next section.

4.3   Phased array architecture

The circuit diagram of the proposed phased array is shown in Fig. 4.5. The phased array is composed of a serial feed network and a phase shifter.   The opposite end of serially fed array is connected to a phase shifter. The phase shifter, which consists of varactor diodes and inductors, reflects the incident signal back after providing a phase shift. In the next sections, the serial feed network and phase shifter designs are presented.

4.3.1   Feed network design

As can be seen in Fig. 4.5, the series feed network is composed of directional couplers and amplifiers. The signal at each antenna port is the vector sum of the two signal components travelling in opposite directions.   First signal components are generated when the input signal is travelling away from the input. The second signal components are generated when the input signal is phase shifted and reflected back into the feed network. The first signal component is coupled through the directional coupler's coupled port, while the second signal component is coupled through the isolated port of the coupler. The first signal component at each antenna element has a fixed phase which is maintained for all the antenna elements. However the second signal component has a variable phase controlled by the phase-shifter. By tuning the phase of the second signal component, a variable progressive phase-shift across the sub-array can be achieved. The amount of the phase shift at each antenna element depends on the relative amplitude of the two signal components. In an array with linear phase progression, the closer an
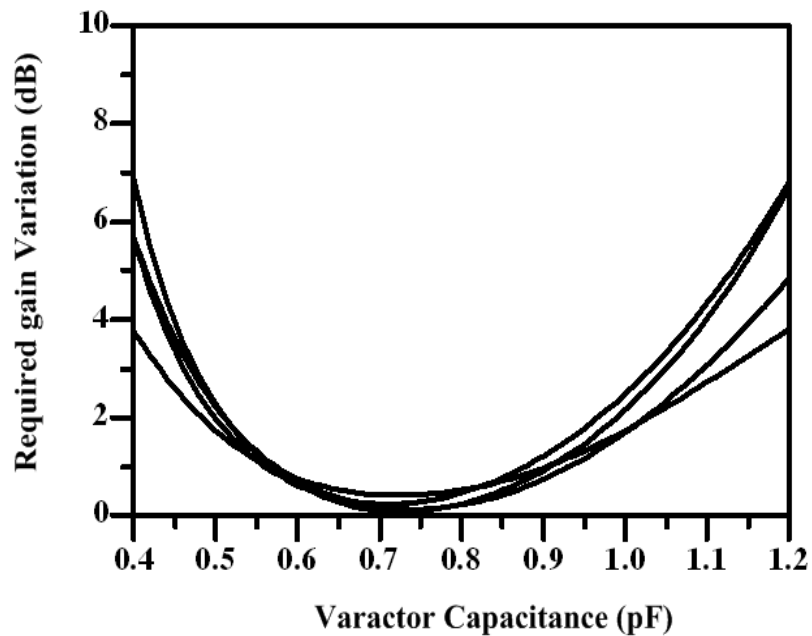
Fig. 4.10. The amplitude variation at the antenna elements as the phase progression is tuned

antenna element is to the phased array input, the larger the amount of phase shift it would require. Therefore, as the amplitude of the first component of the signal decreases, the amplitude of the second component increases. To provide proper signal amplitudes across the array, 3 dB hybrid couplers are used in the design. Furthermore, in order to compensate for the amplitude difference between the input signal and the reflected signal by the phase shifter, amplifiers $A_1...A_4$ with appropriate gains are incorporated in the design. The phase shift at each antenna is shown in Fig. 4.9. As can be seen by choosing appropriate coupling factor, approximately linear phase progression can be achieved across the array.
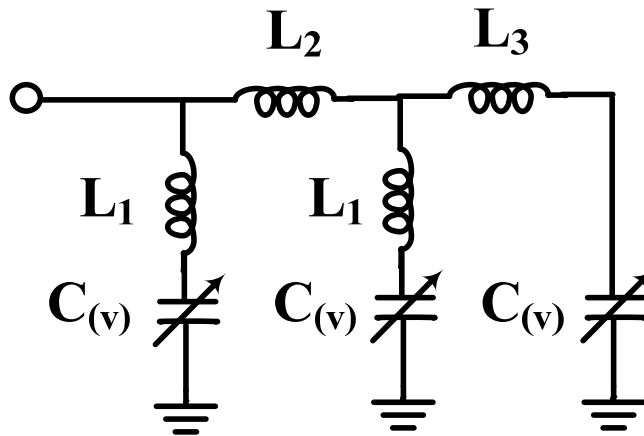
Fig. 4.11. Circuit diagram of the phase shifter

The signal at each antenna port is the vector sum of the two signal components, therefore by tuning the phase of one component the overall amplitude of vector sum varies. The amplitude variation at the antenna elements are shown in Fig. 4.10. A maximum amplitude variation of 7 dB is required to keep the uniform array excitation. To maintain the amplitude of the signal at each array element, variable-gain amplifiers $B_1...B_4$ are employed before the antenna elements.

4.3.2 Phase shifter design

The circuit structure of the reflective phase shifter is shown in Fig. 4.11. The phase shifter circuit is designed using several varactor diodes and lumped inductors. The phase shifter behaves like an open circuited transmission line with an adjustable electrical
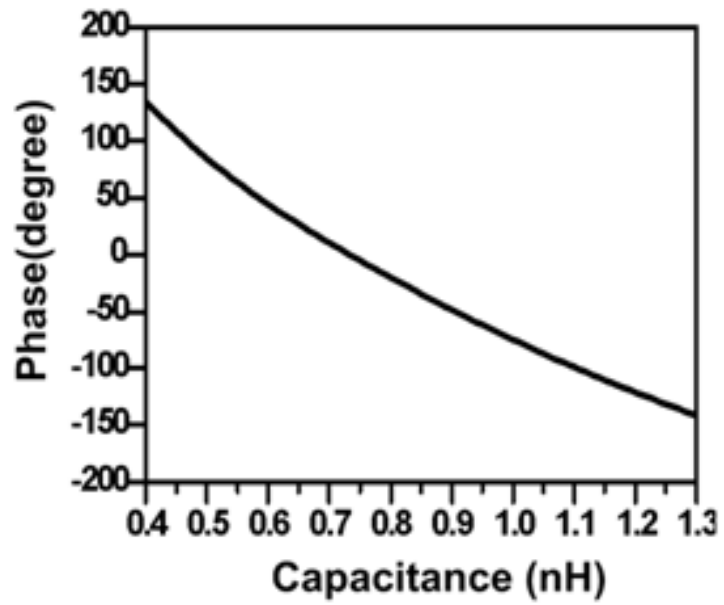
Fig. 4.12. Phase shift of the signal reflected by the phase shifter
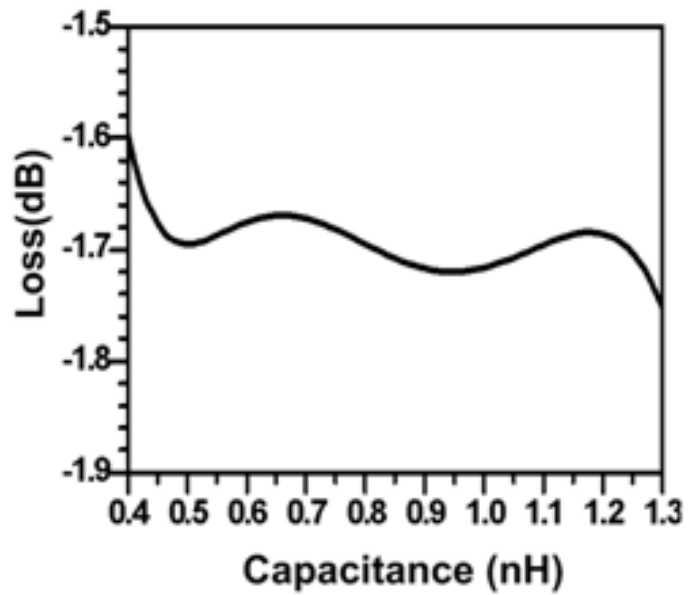
Fig. 4.13. Loss of the signal reflected by the phase shifter
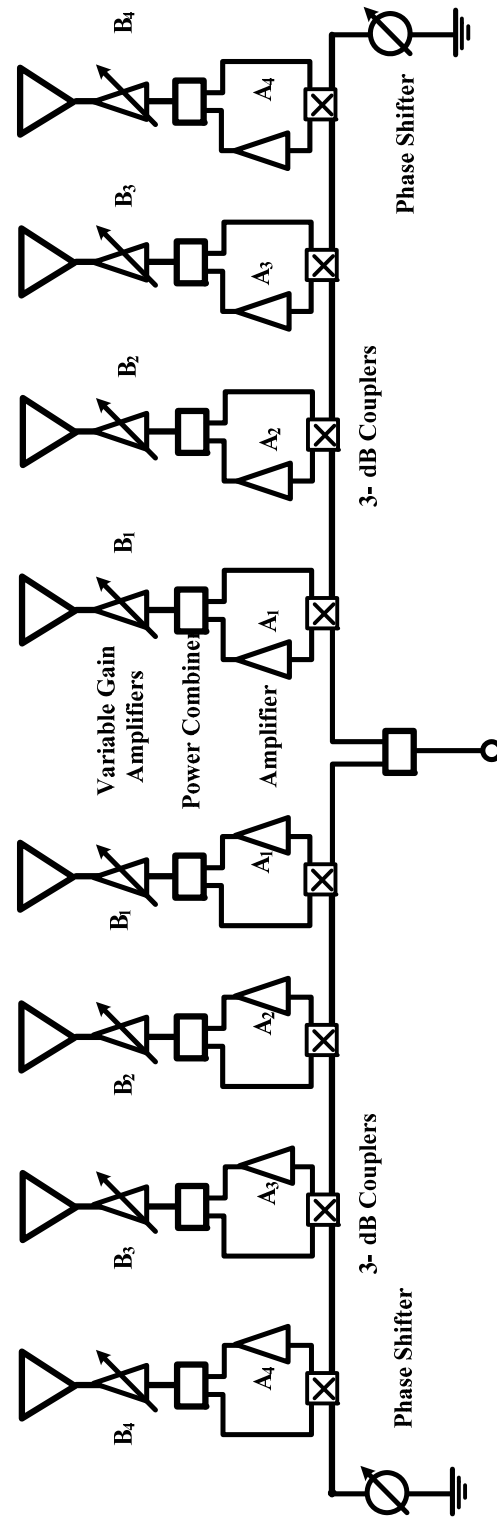
Fig. 4.14. Two sub-array are connected to form a symmetrical structure fed from the center

117

length. The effective electrical length of the line can be controlled by tuning the varactor capacitance. The amount of phase shift can be controlled by varying a single bias voltage applied to the phase shifter. In this design, the varactor capacitance is tuned from 0.3 pF to 1.2 pF. The inductance values for L_1, L_2 and L_3 are 1.7 nH, 4.7 nH, 7.1 nH. The resultant phase shift can be tuned from -150 to 150 degrees (Fig. 4.12) while the reflection loss varies from 1.5 dB to 1.8 dB within the entire tuning range (Fig. 4.13).

4.3.3   Symmetrical array design

A symmetrical phased array is designed based on the phased array design approach previously described. The block diagram of the proposed phased array is shown in Fig. 4.14. Series fed arrays usually suffer from frequency scanning. One way to alleviate this problem is to design a symmetrical array. Therefore, by placing two sub-arrays together and feeding a symmetrical structure from the center is expected to enhance the spontaneous bandwidth of the phased array. The phased array is composed of two identical serially fed sub-arrays where the input signal is equally divided between them using a 3-dB power divider. The sub-arrays are composed of directional couplers, amplifying stages, power combiners and phase shifters as shown in Fig. 4.14. The non-feeding end of each serially fed sub-array is connected to a reflective phase shifter. The sub-array has been designed according to the approach previously discussed.

4.4   Fabrication and Measurement Results

An eight-element phased array at 2 GHz based on the proposed method is design and fabricated (Fig. 4.15). The phased array is fabricated on Rogers RO4003C with a

dielectric constant of 3.55 and a thickness of 20 mils. The 3-dB hybrid couplers are designed and implemented on the same substrate. The surface-mount power combiners SP-2U2+ from Mini-circuits are used to combine the power at each antenna element. The ERA2+ amplifiers from Mini-circuits are used to implement the fixed-gain stages while HP MGA-64135 amplifiers are used as the variable gain stages. The gain of this amplifier can be varied from 1 dB to 13 dB as its bias voltage is tuned from 8.5 to 13 volts. The varactor diodes used in the design of phase shifter are MA46H120 from MA/COM with a tunability of 4:1 and a quality factor of 50 at the design frequency. The varactor capacitance can be tuned from 0.3 pF to 1.2 pF by varying its bias voltage from -0.5 volts to -15 volts. The lumped inductors used in the design of the phase shifting circuits are 0603CS-1N8XJL, 0603CS-4N7XJL and 0603CS-6N8XJL from Coilcraft with inductance values of 1.7 nH, 4.7 nH and 7.1 nH and quality factors of 55, 60 and 80 respectively. Each phase shifter is tuned separately with a single bias voltage ranging between 0.5 to 15 volts. The S-parameters at each of the eight output ports are measured at various bias voltages and subsequently the corresponding array factors are calculated. The plot of the array factors shows a good agreement with the simulated results (Fig. 4.16). A Scan angle of 25 degrees is achieved while the side-lobes are approximately 10 dB below the main beam.
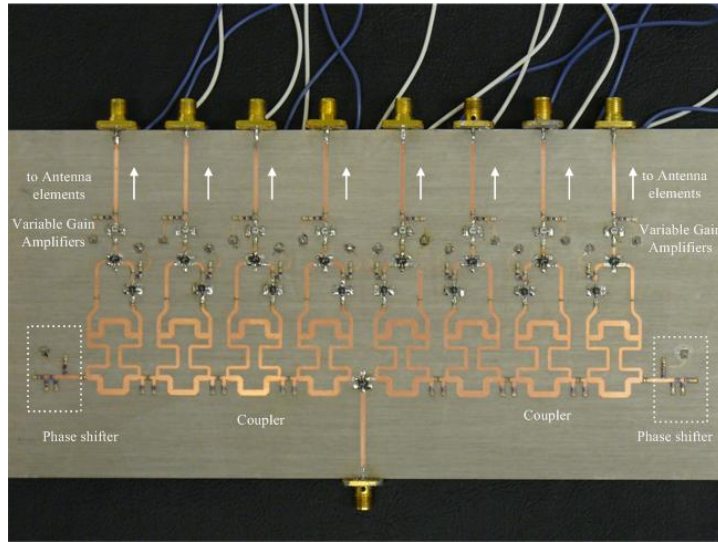
Fig. 4.15. Photograph of the symmetrical phased array
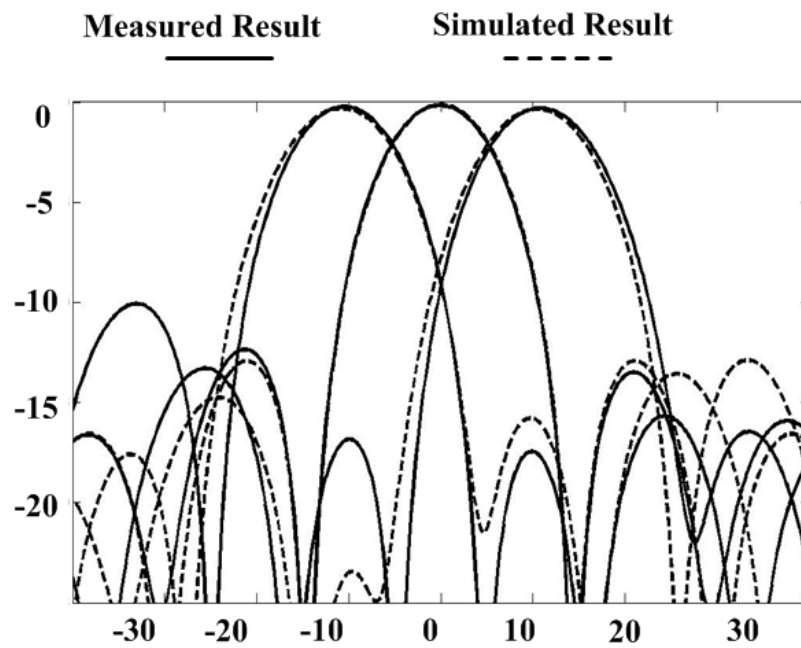
Fig. 4.16. The normalized array factor based on measured S-parameters compared to the simulation.

4.5   Chapter Conclusion

A new approach to the design of low complexity phased arrays is presented. In this approach, phase progression in the entire array is controlled by using a single phase shifters.   This approach is a general method that can be applied to any type of phased array including passive, active or series, parallel in both of receive and transmit mode. A new phased array based on this approach is designed. The proposed phased array is composed of couplers, amplifying stages, power combiners and two phase shifters. The phase shifters are simple and compact consisting of varactor diodes and lumped inductors. The array scan angle can be controlled with a single bias voltage. In order to validate the design, an eight-element phased array at 2 GHz is fabricated and measured. Based on the measured S-parameters for the eight element array, the corresponding array factor is calculated. A scan angle of 25 degrees is achieved demonstrating a very good agreement with the simulated results.

Chapter 5

Conclusion and Future Work

In conclusion, this thesis presents several new approaches to the design of phased arrays with reduced complexity. As mentioned before, phased array antenna systems have traditionally been in use for military applications in the past several decades. However, there has also been recent growth in civilian radar-based sensors and advanced communication systems that have drawn an increasing interest in utilizing phased array technologies for commercial applications. Phased array, capable of providing a directional beam that can be electronically steered, can significantly enhance the performance of sensors and communications systems. The spatial selectivity of phased arrays can increase the channel capacity and data rate without requiring extra bandwidth. The directional beam of a phased array also allows for a more efficient power management. In addition, the spatial filtering nature of the phased array systems alleviate the problem of multipath fading and co-channel interference by suppressing signals emanating from undesirable directions. Despite the broad range of potential phased array applications, phased array technology has not been widely deployed in the commercial arena. The high cost and complexity of phased arrays is the primary impediment to their

122

deployment in any large-scale commercial application. Thus, any substantial reduction in the cost and complexity of phased array systems will facilitate their much wider use. This thesis presents several new approaches to the design of phased arrays which can significantly reduce their complexity.

5.1   Thesis Summary

In the Chapter 2, a new method to design phased arrays based on the extended resonance technique is presented. In this method, power dividing and phase shifting tasks are performed using the same circuitry. Unlike the conventional phased arrays, this technique eliminates the need for a separate phase shifter per each antenna element hence reducing their complexity. In the design of the phased array, extended resonance technique is utilized with heterodyne mixing to achieve uniform power distribution at the LO/IF paths and to perform phase-shifting at the IF-stage. A new extended resonance circuit topology has been employed in the IF stage to enhance the scan range of the phased array. In addition to the design description of the IF-stage, comprehensive analysis of the maximum achievable phase shift in the new extended resonance circuit is presented. Furthermore, a modular approach to realize scalable phased array design is introduced.   The design complexity associated with large phased arrays can be significantly reduced by using the scalable phased array design introduced here. Finally, a complete modular 7-element 24 GHz has been demonstrated.

Because of the cumulative loss of ladder networks, extended resonance technique can be used to design phased array modules with 8-12 array elements. Increasing the size of the phased array beyond this limit can be realized based on the modular approach

described in chapter 2. The modular approach allows placing several circuit modules in tandem to expand the size of the array up to 80-120 elements. Furthermore, the extended resonance phased arrays can achieve a scan range as wide as +/-90 degrees. Therefore, in principle, extended resonance technique can be used to design phased arrays with a broad scan range. The extended resonance phased array can achieve a bandwidth of several percents in order to minimize the effect of beam squint. Therefore, it would be more appropriate to utilize extended resonance phased array for applications requiring a relatively narrow bandwidth.

In Chapter 3, a new bi-directional phased array design is presented. This design takes advantage of a bi-directional series feed network to reduce the phase tuning requirement in a phased array. As the result, complexity of the phase shifters required in the array can be reduced resulting in overall phased array cost and complexity reduction. A general design procedure for a bidirectional n-element phased array feed network is presented. Furthermore, a compact phase shifter is designed and utilized in the phased array. The overall architecture allows one to steer the radiation beam by a single control voltage obviating the need for complex bias circuits. As a proof-of-principle, an eight-element bi-directionally fed phased array at 2.4 GHz is designed, fabricated and its measurement results are reported.

The bi-directional series-fed phased array can be designed to incorporate 10-20 array elements. Increasing the size of the phased array beyond this range would be possible if phase shifters with low loss were available. The bi-directional phased array allows scan ranges as wide as +/-90 degrees. This approach is desirable to achieve a wide

scan range phase arrays employing low complexity phase shifters. The beam squint characteristic of the bi-directional phased array depends on the type of the phase shifter used in the array.

In Chapter 3, a new approach to the design phased arrays with low complexity is presented. Unlike the conventional design of phased arrays requiring a separate phase shifter for each antenna element, in the proposed design, the phase progression across the antenna elements can be controlled by using only a single phase shifter. As a result, the cost and complexity of the phased arrays can be significantly reduced based on this design. The proposed phased array is composed of couplers, amplifying stages, power dividers and two phase shifters. The phase shifters are placed at the two opposite ends of a serially fed array. Implementation and measurement results for an eight-element phased array designed based on this approach to operate at 2 GHz are presented.

Considering the dependence of achievable scan range on the number of antenna elements, the approach above can be used to design phased array modules having of 5-10 elements. Increasing the size of the phased array beyond this limit can be realized based on the modular approach described in chapter 2. The modular approach allows for placing several circuit modules in tandem to expand the size of the array up to 20-40 elements. The frequency performance of the proposed phased array depends on the type of the feed network used in the array. Parallel feed network can be used to realize phased arrays based on this approach to achieve a wide bandwidth performance.

In the first chapter, different techniques to reduce the complexity of phased arrays by reducing the number of required phase shifters were discussed. Extended resonance

125

technique does not need separate power dividing and phase shifting circuits as compared to sub-arrayed antenna approaches. Furthermore, it can be used at RF stage, eliminating the need for LO signal distribution circuits and the accompanying large number of mixers. Like any other series-fed arrays, the extended resonance phased array may show a higher beam squint compared to the other approaches discussed here. Since the losses of passive elements are cumulative in a ladder network and, the performance of the arrays designed based on these approaches are more prone to losses as the number of antenna elements increases. The modular approach presented in the second chapter can be exploited to alleviate this problem. The novel phased array design approach described in chapter 4 uses a substantially lower number of phase shifters while it doesn't suffer from increase of side-lobe levels and emergence of grating lobes that are usually seen in sub-arrayed antenna arrays.

5.2   Future Work

5.2.1   Extended Resonance Phased Array

Extended resonance can significantly reduce the complexity of phased arrays by achieving phase shifting and power division in a single network. Extended resonance can be utilized at RF stage to realize a passive phased array. Passive phased arrays have advantage of high dynamic range, better power handling and higher linearity. In this phased array, extended resonance will be used to directly phase shift and combine the signals from antenna elements. In this case, there will be no need for several mixers and active elements. In order to accomplish this at mm-wave, varactors will high quality factor are required. MEMS varactors have shown to achieve high quality factors at this

frequency regime. Furthermore, as shown in chapter 2, increasing the capacitance value of varactors can increase the maximum achievable inter-element phase shift in extended resonance circuit. MEMS varactors can usually provide higher capacitance values compared to the other conventional varactor technologies. Therefore using MEMS varactors allows extended resonance to operate at RF stage resulting in entirely passive phased array.

A modular approach has been presented in chapter 2 to realize a scalable extended resonance phased array. However, the presented approach has been used for transmit phased array. Extended resonance circuit can be modified to apply the modular approach to receive phased array as well. The modular approach can significantly help to achieve large size phased arrays as the number of antenna elements increases; the loss in the network accumulates and it can negatively affect the uniform power distribution across the array.

5.2.2 Bi-directional Series-Fed Phased Array

Similar to any series-fed phased array, the loss of phase shifters and couplers can accumulate across the bi-directional array presented in chapter 3. The bi-directional feeding has already shown to reduce the number of tuning elements in the required phase shifter. Therefore, the phase shifters required in this phased array demonstrate relatively lower loss due to the reduced number of tuning elements. This allows the bidirectional feeding method to be applied to phased arrays implemented using integrated circuits where the loss of lumped element is relatively higher compared to the discrete elements. In integrated circuit, the lumped elements especially inductors occupy the major die area,

therefore reducing the number of lumped elements can substantially reduce the die size and thus the overall cost of the system. The bidirectional feeding approach also improve the performance of the phased array by reducing the lumped elements in the integrated phased arrays as quality of lumped element is usually a major limitation in the design of tunable integrated circuits.

5.2.3 Phased Array Using a Single Phase Shifter

In order to take advantage of the unique capabilities that phased array technology is offering for the recent commercial applications, certain strict requirements must be met. The new generation of phased arrays must be small, power efficient and inexpensive. Such phased arrays can then be integrated into the existing electronic appliances such as the iPhone and laptop computers. Recent advances in silicon based device performance accompanied with the high density of circuit integration have provided a unique opportunity to drastically lower the cost of phased arrays by implementing the entire phased array on a single chip. Furthermore, integration of all the required circuit modules on a silicon chip obviates the need for any external interconnects resulting in a significant performance improvement.

Ideally, a tunable true time delay that provides frequency independent operation is needed for each array element to prevent beam squint and bandwidth reduction. However, integration of high performance broadband and low loss tunable true time delays for each antenna element again results in excessively high power consumption and large die area requirement. Furthermore, each of the tunable time delays usually requires several independently controlled bias voltages. Thus, the design of true time delay based

phased arrays with a large number of array elements is very challenging due to the exceedingly large number of control voltages and their associated complex circuitry. On the other hand, for instance, in the next generation of gigabit rate commercial communication systems at 60 GHz, transmit power levels of up to 39 dBm equivalent isotropic radiated power (EIRP) are allowed. Considering the maximum power rating of power amplifiers at millimeter wave region, tens of array elements are required to generate such transmit powers levels. In order to realize larger phased arrays, the current integrated arrays employ compact but narrowband RF phase shifting architectures (narrow-bandwidth approximation of the true time delay). At the same time, the unlicensed band at 60 GHz is offering bandwidths as high as 7 GHz. Clearly, the full potential of this frequency band for the development of the next generation personal communication systems providing the highest possible data rates will not be fully realized unless the available bandwidth is efficiently exploited.

The phased array design approach presented in chapter 3 allows using a single phase shifter in the entire phased array; therefore, true tunable time delay can be used in this phase array to achieve high bandwidth. As result, phased arrays integrated on a single chip can be realized by this method to achieve performance that has not been possible due to large number of phase shifters required in conventional phased arrays. The integrated phased arrays with high performance such as wide operating bandwidth play key role for the emerging 60 GHz short range wireless systems.

BIBLIOGRAPHY

BIBLIOGRAPHY

[1]   G. Marconi, "Directive Antenna," *Proc. Royal Soc,* vol. 77A, 1906.

[2]   Wikipedia. *Karl Ferdinand Braun*. Available:
        http://en.wikipedia.org/wiki/Karl_Ferdinand_Braun

[3]   C. W. R. a. E. W. K. H. H. Beverage, "The wave antenna," *J. Am. Inst. Electr. Eng.,* vol. XLII, p. 12, March 1923.

[4]   R. J. Mailloux, "Electronically scanned arrays," *Synthesis Lectures on Antennas,* vol. 2, pp. 1-82, 2007.

[5]   H. T. Friis and C. B. Feldman, "A Multiple Unit Steerable Antenna for Short-Wave Reception," *Proceedings of the Institute of Radio Engineers,* vol. 25, pp. 841-917, 1937.

[6]   A. G. Fox, "An Adjustable Wave-Guide Phase Changer," *Proceedings of the IRE,* vol. 35, pp. 1489-1498, 1947.

[7]   *The Nobel Prize in Physics 1968*. Available:
        http://nobelprize.org/nobel_prizes/physics/laureates/1968/alvarez-bio.html

[8]   Wikipedia. *Phased Array*. Available: http://en.wikipedia.org/wiki/Phased_array

[9]   E. Brookner, "Phased-array radars," *Scientific American,* vol. 252, pp. 94-102, 1985.

[10]   J. Wenger, "Automotive radar - status and perspectives," in *Compound Semiconductor Integrated Circuit Symposium, 2005. CSIC '05. IEEE*, 2005, p. 4 pp.

[11]   I. Gresham, A. Jenkins, R. Egri, C. Eswarappa, F. Kolak, R. Wohlert, J. Bennett, and J. P. Lanteri, "Ultra wide band 24GHz automotive radar front-end," in *Microwave Symposium Digest, 2003 IEEE MTT-S International*, 2003, pp. 369-372 vol.1.

[12]   R. Schneider and J. Wenger, "System aspects for future automotive radar," in *Microwave Symposium Digest, 1999 IEEE MTT-S International*, 1999, pp. 293-296 vol.1.

[13]   W. D. Jones, "Keeping cars from crashing," *IEEE Spectrum,* p. 46, Sep 2001.

[14] A. Valdes-Garcia, S. Nicolson, L. Jie-Wei, A. Natarajan, C. Ping-Yu, S. Reynolds, J. H. C. Zhan, and B. Floyd, "A SiGe BiCMOS 16-element phased-array transmitter for 60GHz communications," in *Solid-State Circuits Conference Digest of Technical Papers (ISSCC), 2010 IEEE International*, 2010, pp. 218-219.

[15] S. K. Reynolds, A. S. Natarajan, T. Ming-Da, S. Nicolson, Z. Jing-Hong Conan, L. Duixian, D. G. Kam, O. Huang, A. Valdes-Garcia, and B. A. Floyd, "A 16-element phased-array receiver IC for 60-GHz communications in SiGe BiCMOS," in *Radio Frequency Integrated Circuits Symposium (RFIC), 2010 IEEE*, 2010, pp. 461-464.

[16] S. K. Reynolds, B. A. Floyd, U. R. Pfeiffer, T. Beukema, J. Grzyb, C. Haymes, B. Gaucher, and M. Soyuer, "A Silicon 60-GHz Receiver and Transmitter Chipset for Broadband Communications," *Solid-State Circuits, IEEE Journal of,* vol. 41, pp. 2820-2831, 2006.

[17] E. Cohen, C. G. Jakobson, S. Ravid, and D. Ritter, "A Bidirectional TX/RX Four-Element Phased Array at 60 GHz With RF-IF Conversion Block in 90-nm CMOS Process," *Microwave Theory and Techniques, IEEE Transactions on,* vol. 58, pp. 1438-1446, 2010.

[18] N. Guo, R. C. Qiu, S. S. Mo, and K. Takahashi, "60-GHz millimeter-wave radio: principle, technology, and new Results," *EURASIP Journal on Wireless Communications and Networking,* vol. 2007, pp. 48-48, 2007.

[19] C. Alakija and S. P. Stapleton, "A mobile base station phased array antenna," in *Wireless Communications, 1992. Conference Proceedings., 1992 IEEE International Conference on Selected Topics in*, 1992, pp. 118-121.

[20] P. V. Brennan, "Low cost phased array antenna for land-mobile satcom applications," *Microwaves, Antennas and Propagation, IEE Proceedings H,* vol. 138, pp. 131-136, 1991.

[21] P. F. Turner, "Regional Hyperthermia with an Annular Phased Array," *Biomedical Engineering, IEEE Transactions on,* vol. BME-31, pp. 106-114, 1984.

[22] M. O'Donnell, "Efficient parallel receive beam forming for phased array imaging using phase rotation [medical US application]," in *Ultrasonics Symposium, 1990. Proceedings., IEEE 1990*, 1990, pp. 1495-1498 vol.3.

[23] J. Souquet, P. Hanrath, L. Zitelli, P. Kremer, B. A. Langenstein, and M. Schluter, "Transesophageal Phased Array for Imaging the Heart," *Biomedical Engineering, IEEE Transactions on,* vol. BME-29, pp. 707-712, 1982.

[24] L. Wang, H. Hricak, M. W. Kattan, L. H. Schwartz, S. C. Eberhardt, H. N. Chen, and P. T. Scardino, "Combined endorectal and phased-array MRI in the prediction of pelvic lymph node metastasis in prostate cancer," *American Journal of Roentgenology,* vol. 186, p. 743, 2006.

[25] A. Villers, P. Puech, D. Mouton, X. Leroy, C. Ballereau, and L. Lemaitre, "Dynamic contrast enhanced, pelvic phased array magnetic resonance imaging of localized prostate cancer for predicting tumor volume: correlation with radical prostatectomy findings," *The Journal of urology,* vol. 176, pp. 2432-2437, 2006.

[26] L. Qian, L. Qingming, and B. Chance, "2D phased array fluorescence wireless localizer in breast cancer detection," in *Computer Architectures for Machine Perception, 2003 IEEE International Workshop on*, 2004, pp. 71-73.

[27] D. Parker and D. C. Zimmermann, "Phased arrays - part 1: theory and architectures," *Microwave Theory and Techniques, IEEE Transactions on,* vol. 50, pp. 678-687, 2002.

[28] J. H. Winters, "Smart antennas for wireless systems," *Personal Communications, IEEE,* vol. 5, pp. 23-27, 1998.

[29] Y. Lo and S. Lee, *Antenna Handbook: Applications*: Kluwer Academic Publishers, 1993.

[30] R. C. Hansen, *Phased array antennas*: Wiley-Interscience, 2009.

[31] R. C. Johnson and H. Jasik, "Antenna engineering handbook," 1984.

[32] R. J. Mailloux and I. Books, *Phased array antenna handbook*: Artech House, 2005.

[33] D. M. Pozar and D. H. Schaubert, "Comparison of three series fed microstrip array geometries," in *Antennas and Propagation Society International Symposium, 1993. AP-S. Digest*, 1993, pp. 728-731 vol.2.

[34] M. A. Y. Abdalla, K. Phang, and G. V. Eleftheriades, "A Steerable Series-fed Phased Array Architecture Using Tunable PRI/NRI Phase Shifters," in *Antenna Technology: Small Antennas and Novel Metamaterials, 2008. iWAT 2008. International Workshop on*, 2008, pp. 83-86.

[35] E. Cohen, C. Jakobson, S. Ravid, and D. Ritter, "A bidirectional TX/RX four element phased-array at 60GHz with RF-IF conversion block in 90nm CMOS process," in *Radio Frequency Integrated Circuits Symposium, 2009. RFIC 2009. IEEE*, 2009, pp. 207-210.

[36] K. Jeong-Geun, K. Dong-Woo, M. Byung-Wook, and G. M. Rebeiz, "A single-chip 36-38 GHz 4-element transmit/receive phased-array with 5-bit amplitude and phase control," in *Microwave Symposium Digest, 2009. MTT '09. IEEE MTT-S International*, 2009, pp. 561-564.

[37] K. Kwang-Jin and G. M. Rebeiz, "0.13um CMOS Phase Shifters for X-, K-, and K-Band Phased Arrays," *Solid-State Circuits, IEEE Journal of,* vol. 42, pp. 2535-2546, 2007.

[38] A. Natarajan, S. K. Reynolds, T. Ming-Da, S. T. Nicolson, J. H. C. Zhan, K. Dong Gun, L. Duixian, Y. L. O. Huang, A. Valdes-Garcia, and B. A. Floyd, "A Fully-Integrated 16-Element Phased-Array Receiver in SiGe BiCMOS for 60-GHz Communications," *Solid-State Circuits, IEEE Journal of,* vol. 46, pp. 1059-1075, 2011.

[39] A. M. Niknejad and H. Hashemi, *mm-Wave silicon technology: 60GHz and beyond*: Springer Verlag, 2008.

[40] K. Dong-Woo, L. Hui Dong, K. Chung-Hwan, and H. Songcheol, "Ku-band MMIC phase shifter using a parallel resonator with 0.18-/spl mu/m CMOS technology," *Microwave Theory and Techniques, IEEE Transactions on,* vol. 54, pp. 294-301, 2006.

[41] H. Zarei, C. T. Charles, and D. J. Allstot, "Reflective-Type Phase Shifters for Multiple-Antenna Transceivers," *Circuits and Systems I: Regular Papers, IEEE Transactions on,* vol. 54, pp. 1647-1656, 2007.

[42] M. Byung-Wook and G. M. Rebeiz, "Single-Ended and Differential Ka-Band BiCMOS Phased Array Front-Ends," *Solid-State Circuits, IEEE Journal of,* vol. 43, pp. 2239-2250, 2008.

[43] Y. Tiku and G. M. Rebeiz, "A 22-24 GHz 4-Element CMOS Phased Array With On-Chip Coupling Characterization," *Solid-State Circuits, IEEE Journal of,* vol. 43, pp. 2134-2143, 2008.

[44] W. Chao-Shiun, H. Juin-Wei, C. Kun-Da, and W. Chorng-Kuang, "A 60-GHz Phased Array Receiver Front-End in 0.13-um CMOS Technology," *Circuits and Systems I: Regular Papers, IEEE Transactions on,* vol. 56, pp. 2341-2352, 2009.

[45] K. Scheir, S. Bronckers, J. Borremans, P. Wambacq, and Y. Rolain, "A 52 GHz Phased-Array Receiver Front-End in 90 nm Digital CMOS," *Solid-State Circuits, IEEE Journal of,* vol. 43, pp. 2651-2659, 2008.

[46] A. Natarajan, A. Komijani, and A. Hajimiri, "A fully integrated 24-GHz phased-array transmitter in CMOS," *Solid-State Circuits, IEEE Journal of,* vol. 40, pp. 2502-2514, 2005.

[47]   D. Ehyaie and A. Mortazawi, "A 24 GHz modular phased array based on extended resonance technique," in *Phased Array Systems and Technology (ARRAY), 2010 IEEE International Symposium on*, 2010, pp. 814-818.

[48]   D. Ehyaie and A. Mortazawi, "A 24-GHz Modular Transmit Phased Array," *Microwave Theory and Techniques, IEEE Transactions on,* vol. 59, pp. 1665-1672, 2011.

[49]   J. D. Fredrick, W. Yuanxun, and T. Itoh, "A smart antenna receiver array using a single RF channel and digital beamforming," *Microwave Theory and Techniques, IEEE Transactions on,* vol. 50, pp. 3052-3058, 2002.

[50]   I. Chiba, R. Miura, T. Tanaka, and Y. Karasawa, "Digital beam forming (DBF) antenna system for mobile communications," *Aerospace and Electronic Systems Magazine, IEEE,* vol. 12, pp. 31-41, 1997.

[51]   B. C. Kane, L. A. Geis, M. A. Wyatt, D. G. Copeland, and J. A. Mogensen, "Smart Phased Array SoCs: A Novel Application for Advanced SiGe HBT BiCMOS Technology," *Proceedings of the IEEE,* vol. 93, pp. 1656-1668, 2005.

[52]   A. Tombak and A. Mortazawi, "A novel low-cost beam-steering technique based on the extended-resonance power-dividing method," *Microwave Theory and Techniques, IEEE Transactions on,* vol. 52, pp. 664-670, 2004.

[53]   J. T. Nemit, "NETWORK APPROACH FOR REDUCING THE," ed: Google Patents, 1974.

[54]   A. Abbaspour-Tamijani and K. Sarabandi, "An affordable millimeter-wave beam-steerable antenna using interleaved planar subarrays," *Antennas and Propagation, IEEE Transactions on,* vol. 51, pp. 2193-2202, 2003.

[55]   W. T. Patton, "Limited scan arrays," *Proceedings of Phased Array Antenna Symposium,* pp. 332-343, 1972.

[56]   S. P. Skobelev, "Methods of constructing optimum phased-array antennas for limited field of view," *Antennas and Propagation Magazine, IEEE,* vol. 40, pp. 39-50, 1998.

[57]   R. Mailloux, L. Zahn, and A. Martinez, III, "Grating lobe control in limited scan arrays," *Antennas and Propagation, IEEE Transactions on,* vol. 27, pp. 79-85, 1979.

[58]   J. Howell, "Limited scan antennas," in *Antennas and Propagation Society International Symposium, 1974*, 1974, pp. 117-120.

[59] S. Sugiura and H. Iizuka, "Reactively Steered Ring Antenna Array for Automotive Application," *Antennas and Propagation, IEEE Transactions on,* vol. 55, pp. 1902-1908, 2007.

[60] S. Chen, A. Hirata, T. Ohira, and N. C. Karmakar, "Fast beamforming of electronically steerable parasitic array radiator antennas: theory and experiment," *Antennas and Propagation, IEEE Transactions on,* vol. 52, pp. 1819-1832, 2004.

[61] R. Harrington, "Reactively controlled directive arrays," *Antennas and Propagation, IEEE Transactions on,* vol. 26, pp. 390-395, 1978.

[62] K. Aamo, "Frequency controlled antenna beam steering," in *Microwave Symposium Digest, 1994., IEEE MTT-S International*, 1994, pp. 1549-1552 vol.3.

[63] M. Kim, J. B. Hacker, A. L. Sailer, and J. H. Hong, "A heterodyne-scan phased-array antenna," *Microwave and Guided Wave Letters, IEEE,* vol. 9, pp. 535-537, 1999.

[64] T. Nishio, X. Hao, W. Yuanxun, and T. Itoh, "A frequency-controlled active phased array," *Microwave and Wireless Components Letters, IEEE,* vol. 14, pp. 115-117, 2004.

[65] J. F. Buckwalter, A. Babakhani, A. Komijani, and A. Hajimiri, "An Integrated Subharmonic Coupled-Oscillator Scheme for a 60-GHz Phased-Array Transmitter," *Microwave Theory and Techniques, IEEE Transactions on,* vol. 54, pp. 4271-4280, 2006.

[66] K. D. Stephan, "Inter-Injection-Locked Oscillators for Power Combining and Phased Arrays," *Microwave Theory and Techniques, IEEE Transactions on,* vol. 34, pp. 1017-1025, 1986.

[67] R. A. York and T. Itoh, "Injection- and phase-locking techniques for beam control [antenna arrays]," *Microwave Theory and Techniques, IEEE Transactions on,* vol. 46, pp. 1920-1929, 1998.

[68] R. Adler, "A Study of Locking Phenomena in Oscillators," *Proceedings of the IRE,* vol. 34, pp. 351-357, 1946.

[69] A. L. Martin and A. Mortazawi, "A class-E power amplifier based on an extended resonance technique," *Microwave Theory and Techniques, IEEE Transactions on,* vol. 48, pp. 93-97, 2000.

[70] A. L. Martin, A. Mortazawi, and B. C. Deloach, Jr., "An eight-device extended-resonance power-combining amplifier," *Microwave Theory and Techniques, IEEE Transactions on,* vol. 46, pp. 844-850, 1998.

[71] A. L. Martin and A. Mortazawi, "A new lumped-elements power-combining amplifier based on an extended resonance technique," *Microwave Theory and Techniques, IEEE Transactions on,* vol. 48, pp. 1505-1515, 2000.

[72] A. Mortazawi and B. C. de Leach, Jr., "Spatial power combining oscillators based on an extended resonance technique," *Microwave Theory and Techniques, IEEE Transactions on,* vol. 42, pp. 2222-2228, 1994.

[73] A. Martin, A. Mortazawi, and B. C. De Loach, Jr., "A power amplifier based on an extended resonance technique," *Microwave and Guided Wave Letters, IEEE,* vol. 5, pp. 329-331, 1995.

[74] A. Tombak and A. Mortazawi, "An X-band low-cost phased array based on the extended resonance power dividing technique," in *Antennas and Propagation Society International Symposium, 2005 IEEE*, 2005, pp. 334-337 Vol. 1A.

[75] A. Tombak and A. Mortazawi, "A novel phased array based on the extended resonance power dividing technique," in *Microwave Symposium Digest, 2003 IEEE MTT-S International*, 2003, pp. 1849-1852 vol.3.

[76] A. Tombak and A. Mortazawi, "Design of novel low-cost phased arrays based on the extended resonance technique," in *Antennas and Propagation Society International Symposium, 2003. IEEE*, 2003, pp. 672-675 vol.4.

[77] S. W. Alland, "Antenna requirements and architecture tradeoffs for an automotive forward looking radar," in *Radar Conference, 1998. RADARCON 98. Proceedings of the 1998 IEEE*, 1998, pp. 367-372.

[78] C. A. Balanis, *Antenna theory*: Wiley New York, 1997.

[79] M. Tsuji, T. Nishikawa, K. Wakino, and T. Kitazawa, "Bi-directionally fed phased-array antenna downsized with variable impedance phase shifter for ISM band," *Microwave Theory and Techniques, IEEE Transactions on,* vol. 54, pp. 2962-2969, 2006.

[80] E. Ojefors, C. Shi, K. From, I. Skarin, P. Hallbjorner, and A. Rydberg, "Electrically Steerable Single-Layer Microstrip Traveling Wave Antenna With Varactor Diode Based Phase Shifters," *Antennas and Propagation, IEEE Transactions on,* vol. 55, pp. 2451-2460, 2007.

[81] C. Shi, E. Ojefors, P. Hallbjorner, and A. Rydberg, "Compact reflective microstrip phase shifter for traveling wave antenna applications," *Microwave and Wireless Components Letters, IEEE,* vol. 16, pp. 431-433, 2006.

[82] L. Sungjoon, C. Caloz, and T. Itoh, "Metamaterial-based electronically controlled transmission-line structure as a novel leaky-wave antenna with tunable radiation

angle and beamwidth," *Microwave Theory and Techniques, IEEE Transactions on,* vol. 52, pp. 2678-2690, 2004.

[83]   M. A. Y. Abdalla, K. Phang, and G. V. Eleftheriades, "A Planar Electronically Steerable Patch Array Using Tunable PRI/NRI Phase Shifters," *Microwave Theory and Techniques, IEEE Transactions on,* vol. 57, pp. 531-541, 2009.

[84]   E. Brookner, *Practical phased-array antenna systems*: Artech house, 1991.

[85]   D. M. Pozar and B. Kaufman, "Comparison of three methods for the measurement of printed antenna efficiency," *Antennas and Propagation, IEEE Transactions on,* vol. 36, pp. 136-139, 1988.

[86]   P. Hallbjorner, M. Bergstrom, M. Boman, P. Lindberg, E. Ojefors, and A. Rydberg, "Millimetre-wave switched beam antenna using multiple travelling-wave patch arrays," *Microwaves, Antennas and Propagation, IEE Proceedings -,* pp. 551-555, 2005.

[87]   A. Natarajan, B. Floyd, and A. Hajimiri, "A Bidirectional RF-Combining 60GHz Phased-Array Front-End," in *Solid-State Circuits Conference, 2007. ISSCC 2007. Digest of Technical Papers. IEEE International*, 2007, pp. 202-597.

[88]   F. Ellinger, U. Mayer, M. Wickert, N. Joram, J. Wagner, R. Eickhoff, I. Santamaria, C. Scheytt, and R. Kraemer, "Integrated Adjustable Phase Shifters," *Microwave Magazine, IEEE,* vol. 11, pp. 97-108, 2010.

[89]   N. S. Barker and G. M. Rebeiz, "Optimization of distributed MEMS transmission-line phase shifters-U-band and W-band designs," *Microwave Theory and Techniques, IEEE Transactions on,* vol. 48, pp. 1957-1966, 2000.

[90]   A. Abbaspour-Tamijani, L. Dussopt, and G. M. Rebeiz, "Miniature and tunable filters using MEMS capacitors," *Microwave Theory and Techniques, IEEE Transactions on,* vol. 51, pp. 1878-1885, 2003.

[91]   J. S. Hayden and G. M. Rebeiz, "Low-loss cascadable MEMS distributed X-band phase shifters," *Microwave and Guided Wave Letters, IEEE,* vol. 10, pp. 142-144, 2000.

[92]   E. G. Erker, A. S. Nagra, Y. Liu, P. Periaswamy, T. R. Taylor, J. Speck, and R. A. York, "Monolithic Ka-band phase shifter using voltage tunable BaSrTiO3 parallel plate capacitors," *Microwave and Guided Wave Letters, IEEE,* vol. 10, pp. 10-12, 2000.

[93]   B. Acikel, T. R. Taylor, P. J. Hansen, J. S. Speck, and R. A. York, "A new high performance phase shifter using BaxSr1-x TiO3 thin films," *Microwave and Wireless Components Letters, IEEE,* vol. 12, pp. 237-239, 2002.

[94]   D. Kuylenstierna, A. Vorobiev, P. Linnér, and S. Gevorgian, "Composite right/left handed transmission line phase shifter using ferroelectric varactors," *Microwave and Wireless Components Letters, IEEE,* vol. 16, pp. 167-169, 2006.

[95]   A. S. Nagra, J. Xu, E. Erker, and R. A. York, "Monolithic GaAs phase shifter circuit with low insertion loss and continuous 0-360 phase shift at 20 GHz," *Microwave and Guided Wave Letters, IEEE,* vol. 9, pp. 31-33, 1999.

[96]   A. S. Nagra and R. A. York, "Distributed analog phase shifters with low insertion loss," *Microwave Theory and Techniques, IEEE Transactions on,* vol. 47, pp. 1705-1711, 1999.

[97]   F. Ellinger, H. Jackel, and W. Bachtold, "Varactor-loaded transmission-line phase shifter at C-band using lumped elements," *Microwave Theory and Techniques, IEEE Transactions on,* vol. 51, pp. 1135-1140, 2003.

[98]   D. Ehyaie and A. Mortazawi, "A modular extended resonance transmit phased array with improved scan angle," 2009, pp. 1557-1560.